Bohmian Trajectories of the Two-Electron Helium Atom

by

Jeff Timko

A thesis
presented to the University of Waterloo
in fulfillment of the
thesis requirements for the degree of
Master of Mathematics
in
Applied Mathematics

Waterloo, Ontario, Canada, 2007

Author's Declaration

I hereby declare that I am the sole author of this thesis. This is a true copy of the thesis, including any required final revisions, as accepted by my examiners.

I understand that my thesis may be made electronically available to the public.

Abstract

We introduce the de Broglie-Bohm causal interpreation of quantum mechanics and compare it to the standard interpretation of quantum mechanics, the Copenhagen interpretation. We examine the possibility of experimentally distinguishing between the two theories, as well as the potential for the causal interpretation to more easily bridge the gap between the physics of the quantum and classical worlds. We then use the causal interpretation to construct a deterministic model of the helium atom in which the two electrons move along trajectories through space and time about a stationary nucleus. The dynamics are governed by the non-relativistic Schrödinger equation and the spin vectors of both electrons are assumed to be constant along their respective trajectories. We examine the Bohmian trajectories associated with (approximations to) eigenstates of the helium Hamiltonian as well as the trajectories associated with some non-eigenstates. We also compute an approximation to the ground state energy of the helium atom using a representation of the helium wavefunction in terms of hydrogenic eigenfunctions which is motivated by a perturbation approach.

Acknowledgements

This research has been made possible through the financial support of the University of Waterloo. I thank them for this opportunity. In addition, a special thanks to my supervisor, Dr. Edward R. Vrscay. Your continual encouragement and academic assistance was key to the completion of this work. Thank you to my family for your neverending support. I love you all very much. And thank you to my friends for the good times.

This is for Gramma Timko.

Contents

List of Tables

List of Figures

Chapter 1

Introduction

The purpose of this thesis is to investigate a deterministic model of non-relativistic quantum mechanics known as the *de Broglie-Bohm causal interpretation of quantum mechanics* (commonly referred to as *Bohmian mechanics*). We highlight the main differences between Bohmian mechanics and the standard interpretation of quantum mechanics, known as the *Copenhagen interpretation*. We also apply Bohmian mechanics to the two electrons in the helium atom, thereby constructing a deterministic model of the atom in which the electrons follow trajectories through space and time, something that is impossible according to the Copenhagen interpretation.

With the advent of quantum mechanics in 1925 [41], humanity entered a new era of science marked by paradox and uncertainty. We now had a mathematical theory that set out to describe the dynamics of microscopic matter, but it was formulated in terms of a quantity that was not obvious how to interpret – the wavefunction. Clearly the wavefunction should represent some physical property of the system under examination, but the formalism did not say what this property was. One could use the wavefunction to make probabilistic predictions and in this way the theory was shown to be consistent with experiment. However, it was still unclear as to precisely what the wavefunction was and whether it provided anything more than just probabilities. Up until this point in time, scientists had not come across such a situation. Never before in a physical theory had the mathematics preceded the interpretation in such a profound way.

Not long after the inception of this new theory, Max Born noticed that the norm of the wavefunction remained constant in time if the wavefunction evolved in time according to the Schrödinger equation. Thus, he interpreted

the wavefunction as giving a measure of the relative probability of finding the system at a particular point in configuration space. The constancy of the norm of the wavefunction then expressed the fact that there is always a probability equal to unity of finding the system at *some* point in configuration space. Although this interpretation is consistent with logic and experiment, it makes quantum mechanics a statistical theory and does not provide a way to predict the outcomes of individual experiments.

This inability to completely analyze a single distinct quantum event is made even more evident in Heisenberg's Uncertainty Principle which is a consequence of the non-commutative mathematics behind the theory. It says that there are certain pairs of measurable quantities associated with every system that are termed *complementary observables*. For a given pair of complementary observables simultaneous measurements can only be made to a certain precision. Thus, knowing the value of one quantity to a high precision automatically lowers the precision to which one can know its complementary partner. According to the standard interpretation of quantum mechanics the Uncertainty Principle does not present a restriction on what we are able to measure, but on what we are able to know. This limit is somehow built into the physics of the universe and its existence is only made apparent to us when we describe things on the quantum level (i.e., on length and time scales characteristic of quantum events). The Uncertainty Principle is seen by some to be so fundamental that it is sometimes taken as an axiom of the theory.

Thus, it seems that quantum mechanics not only lends itself to being a statistical theory because of the consistency of Born's probabilistic interpretation of the wavefunction, but it contains a seemingly built-in mechanism by which we can no longer analyze a single quantum particle or event completely. This is markedly different to classical mechanics in which one can theoretically measure and know any number of dynamical quantities of a system at any time. The question now arises as to what this tells us about the quantum world. If we can only measure certain quantities of a quantum system simultaneously, what are we to say about the quantities we cannot measure? Does the system even simultaneously possess quantities associated with complementary observables? It is at this point that philosophy becomes hopelessly fused with the interpretation. One's preconceived notions about what the quantum world "should" look like and what the purpose of physics is will shape one's interpretation in profound ways. In fact, from the early days of the theory some of the most well-recognized and influential physicists

disagreed very strongly on certain matters of interpretation. Schrödinger, on one hand, believed that there was an underlying reality that his theory attempted to describe. For him, material particles existed and moved throughout spacetime regardless of whether or not they were being observed.[1] Werner Heisenberg and Niels Bohr argued that there is no meaning or benefit to speaking about this underlying reality since it is not revealed to us outside measurement. In their view, we can only gain information about our world by interacting with it (i.e., by measuring it) so any concept that goes beyond this is ultimately worthless since it cannot be proven or disproven through experience.

This is a positivist viewpoint and is what is known as the *Copenhagen interpretation* of quantum mechanics (we will commonly refer to this as SQM, standing for *standard quantum mechanics*). The Copenhagen interpretation was fathered by Heisenberg and Bohr and emerged from the tumultuous first couple decades of quantum mechanics as essentially the *only* interpretation. It is the interpretation that is commonly taught in classrooms today and the viewpoint commonly held among experts in the field. It is the purpose of this thesis to discuss an alternative interpretation of quantum mechanics known as Bohmian mechanics (we will frequently refer to this as BM) and show how it can be applied to the specific system consisting of a single helium atom. This extends the Ph.D. thesis work of Carolyn Colijn, who used Bohmian mechanics to provide a similar picture of the hydrogen atom [11]. In the next section we will examine the mathematical structure of quantum mechanics and discuss the Copenhagen interpretation in more detail. Following this, in Chapter 2, we will introduce the mathematical and conceptual basis of Bohmian mechanics. We will discuss how it provides a more intuitive description of the quantum world and is able to address some of the difficulties associated with the Copenhagen interpretation.

[1]The term "observed" is ambiguous. Does observing a quantum system imply mere interaction with other systems of matter and energy (i.e., the interaction between system and measuring apparatus) or does it require a human or "intelligent" being to somehow register the outcome of the measurement? For our purposes we will consider an observation or measurement of a quantum system to be the former – a physical interaction with a measuring apparatus.

1.1 The Mathematical Structure of Quantum Mechanics and the Copenhagen Interpretation

Quantum mechanics is unlike any other physical theory in that the mathematics largely preceded the interpretation. When Schrödinger developed wave mechanics in 1925 [37, 38, 39, 40], he did so by trying to associate, in some reasonable way, concepts normally associated with waves (frequency, wavelength, etc.) with material particles [41] (see also [32] for a discussion on this). In doing this, he arrived at his substitution rules – that each measurable quantity (which we will refer to as an *observable* from here onwards) should be represented mathematically as an operator as opposed to a variable. In particular, the variable representing position is replaced by itself (i.e., the operator representing multiplication by x) and the variable representing momentum is replaced by the operator $-i\hbar\nabla$. Using these two substitutions, any observable which can be written classically as $F(x,p,t)$ is replaced by the operator $\hat{F}\left(x,-i\hbar\nabla,t\right)$.[2]

Schrödinger's original formulation of wave mechanics is quite lacking in mathematical rigor. It is based on the comparison of a free particle and a plane wave and from this comparison he derives the above substitution rules. It is then assumed that the substitution rules are fundamental equations which will give the proper dynamics of any system of particles (i.e., by making the substitutions $x \to x$ and $p \to -i\hbar\nabla$ in the classical equation for any observable, we get the corresponding "quantum observable"). There is no justification for this assumption, except that no experiment has yet refuted any prediction made by the Schrödinger equation. Within a few years of Schrödinger's original formulation the lack of mathematical rigor was addressed by von Neumann. He formulated quantum mechanics in terms of a set of postulates from which one could derive all of the mathematical machinery needed to make predictions. We will now present these postulates and discuss how they are interpreted in the Copenhagen interpretation.[3]

Postulate 1: The state of a quantum mechanical system is completely de-

[2]Note that $\hat{F}$ is a function of the operators x and $-i\hbar\nabla$ and the parameter t.

[3]These postulates are listed and discussed in many quantum mechanics texts. Some well-written examples are [32] and [7].

scribed by a single-valued, finite, continuous function that depends on the coordinates of each particle in the system as well as on time. This function is referred to as the wavefunction and is commonly written $\Psi(x,t)$ where x refers to the coordinates of all particles in the system. The wavefunction has the property that $\Psi^*(x,t)\Psi(x,t)d\tau = |\Psi(x,t)|^2 d\tau$ gives the probability that the system is in the volume element $(x, x+d\tau)$ of configuration space at time t.

This interpretation of the wavefunction in terms of probability is nothing more than Born's statistical interpretation. It is interesting to note that the wavefunction is said to give a **complete** description of the system, even though it represents statistical properties of the system. In May 1935, Einstein, Podolsky and Rosen, hereafter referred to as EPR, published a paper in which they argued that the wavefunction cannot give a complete description of reality [15]. Using a property of quantum theory called *entanglement*[4] they outlined a thought experiment which presented a conundrum. We will outline a simpler experiment proposed by Bohm [8] which highlights the same issues as EPR.

First we define two terms – "element of physical reality" and "complete physical theory". EPR defined an "element of physical reality" as any physical quantity of a system, whose value can be predicted with certainty without measuring it or disturbing it in any way.[5] They defined a "complete physical theory" as one which accounts for all elements of physical reality. Using these two definitions, EPR endeavor to show that conventional quantum mechanics is not a complete physical theory. Here is a simple thought experiment due to Bohm which outlines the basic argument (see also [14] for a good discussion on the EPR paradox).

[4]Entanglement refers to the way in which two systems become intimately connected after interacting with each other. After interaction, the properties of each system are related so that measurement of a property of one system dictates the value of that property possessed by the other system.

[5]Some readers may find this definition troubling as it does not account for many quantities one would like to associate with an "element of physical reality". As an example, consider the position of a car parked in a garage. One may need to measure this before knowing its value but that does not mean the car's position is not an element of physical reality. EPR define "element of physical reality" as they do to produce the conclusion they desire. They define what may more correctly be called "a subset of all elements of physical reality" which have the special property that their values can be determined without measurement.

Suppose we start with a system of total spin 0 which disassociates into two identical particles, each of spin $\frac{1}{2}$ which travel away from each other. If the spin of particle A is measured along some direction (call it the z-direction), the result will either be $\frac{\hbar}{2}$ or $-\frac{\hbar}{2}$. If the measurement $\frac{\hbar}{2}$ is made, we know from conservation of spin (i.e., angular momentum) that a measurement of the spin of particle B along the same direction **must** yield the value $-\frac{\hbar}{2}$. Thus, by definition, the spin of particle B along the z-direction is an element of physical reality. However, were we to measure the spin of particle A along some other arbitrary direction, $\hat{n}$, we would come to the conclusion that the spin of particle B along the direction $-\hat{n}$ is an element of physical reality. In this way, it is easily seen that the spin of particle B in any direction can be made an element of physical reality by measuring the spin of particle A along the appropriate direction. It is as if particle B "knows" in which direction it should point its spin regardless of what direction the spin of particle 1 is measured. According to the Copenhagen interpretation, the Uncertainty Relations imply that the x-component and z-component of the spin of particle B do no simultaneously exist because they are complementary observables. Thus, EPR concluded that one of two possibilities had to hold. Either particle B always possessed the knowledge of how to orient its spin or it was influenced by the measurement of particle A. If the first case holds, it is clear that the standard interpretation of quantum mechanics is not a complete physical theory according to the definition given by EPR. If the second case holds some sort of effect must be propagated instantaneously from particle A to particle B at the exact moment of measurement of particle A. Thus, locality is violated. EPR concluded that either measurement of one of the entangled particles had a non-local effect on the other particle, or there was some element of physical reality that quantum mechanics could not account for. These elements of physical reality became known as *hidden variables* and various formulations of quantum mechanics have been developed which have attempted to incorporate them. In fact, Bohmian mechanics is a hidden variable theory as we will see in the next section.

About five months after the EPR paper was published, Bohr issued a reply which was published in the same journal under the same title. He defended the completeness of quantum mechanics by appealing to his concept of complementarity. Complementarity is a term commonly used in reference to complementary observables, but Bohr's usage of the word implied more than this. Bohr's complementarity refers to the way in which matter has to be described using two mutually exclusive, yet necessary, constructs –

particles and waves. The ramifications of the mathematical structure of the theory, for instance the Uncertainty Principle, stem from the fact that we are attempting to use one theory to encompass two different descriptions of matter. In the world of experiment, it is the particular measuring apparatus that we use to measure a quantum system that determines which of these two mutually exclusive forms of matter we observe. For instance, in the double slit experiment, we observe the wave nature of matter by the interference of the portions of the wavefunction coming through each slit. Similarly, the particle nature of matter is made manifest when the wavefunction interacts with a photographic plate on the other side of the system and collapses to a point. Different measuring apparatus causes matter to manifest itself in different ways – either particle or wave, but never both at the same time.

Essential to Bohr's concept of complementarity is the recognition that all information we can glean about the world in which we live ultimately comes through our observation (or equivalently, measurement) of it. Any quantity or property that we naturally ascribe to a particle (such as spin or position, for instance) only reveals itself once we make a measurement specifically designed to reveal it. What is more, the value that is measured cannot be connected to some previously existing state of the particle since the measurement implies an interaction between particle and measuring apparatus. The result of a measurement, then, reveals only the final state of the system after the measurement interaction is complete.

Bohr and Heisenberg chose to interpret this fact as a limit on what is **knowable** about the quantum world and this is representative of the *positivist* philosophical underpinnings of the Copenhagen interpretation.[6] Since the only way of ascertaining any information about the properties of a quantum system is through its interaction with some measuring apparatus it is meaningless to think about the system possessing any of these properties outside of such an interaction. Thus, according to SQM it is meaningless to think of a particle traveling along a spacetime trajectory. A particle possesses a well-defined position or momentum (for instance) only when it interacts with a suitable measuring apparatus and a value for that particular property is read off or inferred from the display of the apparatus. This measured value, and hence the existence of the property itself, is a product of the interaction and cannot be spoken of outside it.

[6]This is in contrast to Schrödinger's or Einstein's *realist* philosophy that there is an underlying quantum reality that exists independent of observation.

Bohr thought of measurement as revealing a specific potentiality of the object being measured. Before the measurement is made, the object exists in a state of potentialities. The measurement consists of an interaction between apparatus and object which ultimately changes the state of the object into a state we associate with the value measured. It is not proper to speak of the object as being in this state, or even any other particular state, before the measurement. All one can say is that it existed in a mixture of potential states and the measurement served to leave it in one of them. It is important to understand that for Bohr, different measuring apparatus revealed different sets of potentialities. Thus, the set of potentialities that exist for an object depends on the particular experimental setup with which it is measured.

For instance, in the version of the EPR experiment described above one can measure the spin of particle A in any direction. According to EPR, this means that the spin of particle B in any (hence, every) direction is an element of physical reality. This is not the case according to Bohr, however. In his analysis, measuring particle A in a particular direction, say the z-direction, causes the set of potentialities of particle B to reduce to those pertaining to the value of its spin in the z-direction. Speaking of Bohr's views, Bohm [8] wrote, "... there is no legitimate way to think about the properties of particle B apart from the experimental context in which they are measured. The context needed to think about the z-component of the spin of atom B is therefore not compatible with that needed to think about its x-component. This signifies that even though we can predict the properties of atom B from those of atom A without disturbing atom B, there is no experimental situation with regard to atom B in which both of the above predictions could have meaning together". It is Bohr's idea of complementarity and the unanalysable connection between apparatus and object in a measuring process that brings him to this conclusion. We will see in the next chapter that BM provides a reasonable solution to the EPR paradox.

Postulate 2: The wavefunction evolves in time according to the time-dependent Schrödinger equation:

$$i\hbar\frac{\partial\Psi}{\partial t} = \hat{H}\Psi \tag{1.1}$$

where $\hat{H}$ is the operator representing the Hamiltonian of the physical system.

Schrödinger derived this equation in an attempt to relate quantities normally associated with a wave, i.e., frequency, wavelength, etc., with a particle of matter. See [32] for a good discussion on how the derivation goes.

Postulate 3: To every observable in classical mechanics, there corresponds a linear, Hermitean operator in quantum mechanics.

We have already come across two of these "quantum operators" – to the classical position observable corresponds the operator x (multiplication by the function x) and to the classical momentum observable corresponds the operator $-i\hbar\nabla$. The operators are required to be linear because the underlying structure of the theory is linear and they are required to be Hermitean because it is necessary for them to have strictly real eigenvalues. To any classical observable that can be written as a power series

$$\sum_{n,m} c_{nm} x^n p^m$$

corresponds the observable

$$\sum_{n,m} c_{nm} x^n \left(-i\hbar\nabla\right)^m \tag{1.2}$$

where the appropriate Hermitization procedure[7] has been employed before making the operator substitutions.

Postulate 4:

Part 1: A measurement of an observable, A, represented by the operator $\hat{A}$, corresponds mathematically to the operator acting on the wavefunction representing the system under study. The only possible outcomes of measurements of the observable associated with the operator $\hat{A}$ are the solutions, a, to the eigenvalue equation

[7]The Hermitization procedure is to take the mean between the two possible ways of writing each of the terms in the sum (1.2). To do this, write the function such that all factors involving p are grouped together and all factors involving x are grouped together. Then replace $p^n x^m$ by $\frac{1}{2}\left(p^n x^m + x^m p^n\right)$. This procedure ensures that the operator is Hermitean.

$$\hat{A}\Psi = a\Psi.$$

Part 2: If an observable is measured and found to have the value a then directly after the measurement the system is represented by the eigenfunction corresponding to the eigenvalue a.

Since the measurement of any physical quantity should necessarily yield a real quantity, we see the impetus for the requirement that each quantum operator have only real eigenvalues (thus, the requirement that each quantum operator be Hermitean). This postulate also underlies a very important feature of quantum mechanics – that observables need not have a continuous set of possible measurement outcomes. This is due to the fact that operators representing observables need not have continuous sets of eigenvalues. This is a great triumph of quantum mechanics because the observed discreteness of certain physical quantities (for example, the energy levels of the hydrogen atom) comes directly out of the mathematics.

It is important to note that before a measurement, a system need not be in an eigenstate of the operator representing the observable being measured. In fact, every wavefunction is expressible as a linear combination of any complete set of eigenfunctions. In addition, every operator representing a physical observable possesses a complete set of eigenfunctions. Thus, when making a measurement of some observable, the wavefunction can be represented as a linear combination of the eigenfunctions of the operator representing that observable,

$$\Psi(x,t) = \sum_i c_i \Phi_i(x) f(t),$$

where $f(t) = \exp \frac{-iEt}{\hbar}$ is determined by the Schrödinger equation. Note that $f(t)$ does not depend on the index i and can be separated from the sum. If the wavefunction has been normalized the probability of measuring the eigenvalue a_i is equal to $c_i c_i^* = |c_i|^2$.

From Part 2 of the postulate, immediately after this measurement has been made the wavefunction is equal to the eigenfunction corresponding to the eigenvalue a_i. There is nothing in the theory to describe how this change in the wavefunction takes place. According to the Copenhagen interpretation, the change is instantaneous and is not described by the continuous time-

evolution of the Schrödinger equation. It is commonly referred to as the "collapse of the wavefunction" and it must be assumed as a postulate in order to give a reasonable description of a measurement (this is Postulate 4.2). It can be proven that no such Hamiltonian exists that would give rise under the Schrödinger equation to a discontinuous change like that required by the collapse of the wavefunction. In fact, it is impossible to describe this process using a linear equation such as the Schrödinger equation.[8] Many attempts have been made to modify the Schrödinger equation so that the collapse would appear naturally, but to no avail.

To understand more clearly why the collapse of the wavefunction is necessary to describe the measurement process, consider the measurement of the spin of an electron along some arbitrary direction that we will call the z-axis. This can be done in the laboratory via a Stern-Gerlach device. We shall denote the wavefunction of the measuring apparatus (which includes anything from the microscopic system which interacts directly with the electron to the macroscopic devices which convey the measured values to the experimenter) before it has made a measurement by ϕ, after it has measured the electron to be spin up by ϕ_{up} and after it has measured the electron to be spin down by ϕ_{down}. First, suppose we know the electron is in the "spin up" state with wavefunction ψ_{up}. Then before the measurement the wavefunction of the combined electron/apparatus system is $\Psi(t=0) = \psi_{up}\phi$ and after measurement is $\Psi(t) = \psi_{up}\phi_{up}$. We could find a suitable Hamiltonian to bring about this transition so there is no problem here. Similarly, if we know the electron is in the "spin down" state with wavefunction ψ_{down}, then before measurement we have $\Psi(t=0) = \psi_{down}\phi$ and after measurement, $\Psi(t) = \psi_{down}\phi_{down}$. This also presents no problems, as we could find a suitable Hamiltonian to bring about this transition. However, in general we do not know what state the electron is in before measurement. Thus, we must represent its wavefunction as $\psi = c_1\psi_{up} + c_2\psi_{down}$ where c_1 and c_2 are constants. Then due to the linearity of the Schrödinger equation, after measurement the combined wavefunction is $\psi(t) = c_1\psi_{up}\phi_{up} + c_2\psi_{down}\phi_{down}$. This represents a state in which the measuring apparatus (including its macroscopic parts) is in both the "up state" and the "down state" at the same time. This is something that is **never** observed in real life (how can a needle on a machine point to two different values, for instance?) and it is the heart of the measurement problem. To reconcile this disagreement between theory and observation we

[8] More on this in Section 3.2.3.

need to enforce the instantaneous collapse of the wavefunction:

$$c_1\psi_{up}\phi_{up} + c_2\psi_{down}\phi_{down} \rightarrow \begin{cases} \psi_{up}\phi_{up} & \text{with probability } |c_1|^2 \\ \psi_{down}\phi_{down} & \text{with probability } |c_2|^2. \end{cases}$$

where $\rightarrow$ implies an instantaneous change upon measurement. This is easily extended to the case where the initial wavefunction is a linear combination of any number of terms. The result is that the wavefunction collapses to the eigenfunction ψ_n with probability $|c_n|^2$.

Postulate 5: If a system is described by a normalized wavefunction, Ψ, then the expected value of measurements of the observable A is given by

$$\langle A \rangle = \int_{\text{all configuration space}} \Psi^* \left(\hat{A}\Psi \right) \, d\tau$$

where $\hat{A}$ is the operator representation of A.

This formula is nothing more than the standard expected value used in statistics for a continuous range of data points. It illustrates very clearly the role of the wavefunction as a probability density. Note that if Ψ is represented in terms of the complete set of eigenfunctions of $\hat{A}$, i.e., $\Psi = \sum_i c_i\phi_i$ where $\hat{A}\phi_i = a_i\phi_i$ then $\hat{A}\psi = \sum_i c_i a_i \phi_i$. In addition, using the fact that the eigenfunctions are orthonormal, we see that $\langle A \rangle = \sum_i |c_i|^2 a_i$.

Chapter 2

Bohmian Mechanics

In 1952 David Bohm published two papers which appeared in the journal *Physical Review* [5, 6]. He presented an extension of de Broglie's pilot wave theory which de Broglie suggested in 1927 and presented at the Solvay Congress that same year. De Broglie proposed a deterministic interpretation of quantum mechanics in which actual particles travel through space and time and are "guided" by their wavefunction. The pilot wave theory was formulated only for a one-body system and during the Solvay Congress in 1927 Pauli criticized the theory based on the argument that it could not be applied consistently to a two-body scattering process. De Broglie could not provide a response to this criticism and abandoned his ideas. A quarter of a century later, Bohm in these two papers, rekindled the pilot wave program and extended it to the many-body case. After further development his determinisitic model of quantum mechanics came to be known as *Bohmian mechanics*. Under Bohmian mechanics measurement is observer-independent and the collapse of the wavefunction is unnecessary. In addition, Bohm's theory provides a response to the EPR paradox (see also [14] and [30], among others). We will now examine the mathematics behind the theory.

2.1 Mathematical Formulation

Bohmian mechanics begins with the wavefunction and Schrödinger's equation (eqn. (1.1)). By writing the wavefunction in polar form,

$$\Psi(x,t) = R(x,t)\exp\left(\frac{iS(x,t)}{\hbar}\right),$$

the Schrödinger equation gives two coupled equations, one for the amplitude, R,

$$\frac{\partial R^2}{\partial t} + \nabla \cdot \left(R^2 \frac{\nabla S}{m} \right) = 0 \tag{2.1}$$

and one for the phase, S,

$$-\frac{\partial S}{\partial t} = V + Q + \frac{1}{2m} \nabla S \tag{2.2}$$

where

$$Q = -\frac{\hbar^2}{2m} \frac{\nabla^2 R}{R}. \tag{2.3}$$

Eqn. (2.1) describes the conservation of the probability distribution of particle positions (cf. Postulate 1 in section 1.1).[1] It is common to all interpretations of quantum mechanics that are based on the Schrödinger equation. It has the form of a continuity equation

$$\frac{\partial R^2}{\partial t} = -\nabla \cdot \vec{j} \tag{2.4}$$

where

$$\vec{j} = R^2 \frac{\nabla S}{m} \tag{2.5}$$

is the *probability distribution current*. Eqn. (2.2) is the same as the classical Hamilton-Jacobi equation,

$$-\frac{\partial S}{\partial t} = V + \frac{1}{2m} \nabla S \tag{2.6}$$

except for the inclusion of Q. Eqn. (2.6) describes classical particles that move orthogonal to isosurfaces of S with momentum $\vec{p} = \nabla S$. Bohm's great insight was to treat Q on the same footing as the classical potential, V, i.e., as another potential term, which he called the *quantum potential*. He called eqn. (2.2) the *quantum Hamilton-Jacobi equation* and gave it the same interpretation as the classical Hamilton-Jacobi equation – it describes particles which travel along trajectories through space and time with momentum

[1] Note that $R^2 = |\Psi|^2$.

$$\vec{p_i} = \nabla_i S. \tag{2.7}$$

where $\vec{p_i}$ is the momentum of the i^{th} particle and ∇_i refers to the gradient with respect to the coordinates of particle i.

This is a markedly different view of the quantum world when compared to SQM. In SQM the idea of a particle existing outside measurement is, as we have seen, nonexistent. In BM, however, particle trajectories are a central part of the theory, irregardless of whether or not they are being measured. Note that these trajectories are deterministic – given the initial positions of the particles their momenta can be calculated via eqn. (2.7) and their trajectories determined.

At this point, one may ask where the uncertainty relations have gone since it seems that we can predict the position and momentum of a particle simultaneously with unlimited uncertainty. This is true, but only if we specify the inital positions of the particles exactly. In practice, the uncertainty relations prohibit us from doing this – the initial positions must be specified by a probability distribution which does not contradict the uncertainty relations. Thus, in BM the uncertainty relations still act but their range of influence is diminished – they only effect the specification of the initial conditions. It is natural to use the distribution $|\Psi|^2$ for the initial particle positions in BM. If this is done the guidance condition, (2.7), ensures that the probability distribution of the particle positions is given by (2.1) for all times. This is known as the *quantum equilibrium hypothesis*, (or for short the QEH), and it ensures that BM gives the same statistical predictions as SQM [42, 6, 8]. One note about eqn. (2.1) – recall that according to Postulate 1 the probability of measuring a particle to be within the volume element $(x, x + d\tau)$ at time t is given by $|\Psi(x,t)|^2 d\tau$. Since in BM we are dealing with particles that exist independently of measurement, $|\Psi(x,t)|^2 d\tau$ is the probability that the particle *is* within the volume element $(x, x+d\tau)$ at time t, regardless of whether it is being measured or not.

To summarize, BM is an alternative to SQM. Like SQM it is based on Schrödinger's equation which describes a wavefunction, Ψ, but unlike SQM it is supplemented by the concept of particle trajectories according to the guidance condition, (2.7). The statisical predictions made by BM are the same as those made by SQM if the initial particle positions are distributed according to $|\Psi|^2$ (by the QEH). In this way, BM is equivalent to SQM as far

as predicting the outcomes of experiments,[2] but it gives a radically different picture of the quantum world. While SQM rejects all reality outside of what can be scientifically observed, BM supposes the existence of real particles travelling along real trajectories through space and time independently of their being observed. SQM only gives us half the story – that the *amplitude* of the wavefunction can accurately be given its statistical meaning. BM gives us the second half – that the *phase* of the wavefunction can consistently be given meaning in terms of determining particle trajectories.

So far this may look like nothing more than a classical theory with a restriction on our ability to prepare a system with precise initial conditions. How does one recover the "weird" quantum phenomena observed in experiment? Further examination of the quantum potential reveals some interesting properties that are seen to be responsible for these non-classical effects.

First, notice that the quantum potential (eqn. (2.3)) contains R, the amplitude of the wavefunction, linearly in both the numerator and the denominator . For this reason, the quantum potential does not depend on the magnitude of R. Thus, the quantum potential can be very large in regions of space which are distant from where the particles in the system are likely to be. This is a complete departure from our normal understanding of wave motion where classically, the size of the effect of a wave is determined by its amplitude.[3] In the case of BM it is the **form** of the wavefunction that determines the strength of the quantum potential. The presence of the term $\nabla^2 R$ in the numerator implies that in regions where R has a large spatial variation, the quantum potential is large. Similarly, the presence of R in the denominator implies a large quantum potential in regions where R is small. Overall, the quantum potential tends to "push" particles into regions of space where Ψ is large. This is consistent with the probabilistic interpretation of Ψ (Postulate 1).

Secondly, notice that the quantum potential is a function of the spatial coordinates of **all** particles in the system. Thus, the quantum potential acting on one particle in the system can depend, in arbitrarily complex ways, on the coordinates of all other particles in the system. This property of the quantum potential is responsible for non-local interactions between particles and in this way, stumbling blocks characteristic of the Copenhagen interpretation, such

[2]There is debate over this statement as we will see in the next chapter.

[3]Consider a cork bobbing in a water wave. The farther the cork is from the peak of the wave, the smaller the effect of the wave on its motion.

as the measurement problem, can be explained in a very intuitive way. We will discuss the Bohmian response to this issue, as well as the EPR paradox in future sections. First, however, we need to incorporate the concept of particle spin into our model in order to give a proper account of the helium atom. This will be the subject of the next section.

2.2 The Inclusion of Spin

The quantum description of spin[4] begins with the Pauli equation for a spin-$\frac{1}{2}$ single particle

$$i\hbar\frac{\partial\Psi}{\partial t} = -\left[\left(\frac{\hbar^2}{2m}\right)\left[\nabla - \left(\frac{ie}{\hbar c}\right)\vec{A}\right]^2 + \mu\vec{B}\cdot\vec{\sigma} + eA_0 + V\right]\Psi \tag{2.8}$$

where the wavefunction is represented by the two-component spinor,

$$\Psi(x,t) = \begin{pmatrix}\psi_a(x,t)\\ \psi_b(x,t)\end{pmatrix}.$$

We will denote its Hermitean adjoint as $\Psi^\dagger$. The constants e, m and μ are the charge, mass and magnetic moment of the particle, A_0 and $\vec{A}$ are the scalar and vector electromagnetic potentials, respectively, $\vec{B} = \nabla\times\vec{A}$ is the magnetic field, $\vec{\sigma}$ is a vector whose components are the Pauli matrices and V is an arbitrary external potential. The Pauli matrices are given by

$$\sigma_x = \begin{pmatrix}0 & 1\\ 1 & 0\end{pmatrix}, \quad \sigma_y = \begin{pmatrix}0 & -i\\ i & 0\end{pmatrix} \quad \text{and} \quad \sigma_z = \begin{pmatrix}1 & 0\\ 0 & -1\end{pmatrix} \tag{2.9}$$

.

The generalization to multi-particle systems is straightforward and we will not discuss it [30].

The Pauli equation describes particles having a property called "spin". Spin is an "internal angular momentum" possessed by the particle and is a purely quantum effect. It is common in quantum mechanics to view spin in terms of the particle actually spinning along an axis. This is consistent with the mathematics since one can use the Pauli wavefunction, $\binom{\psi_a}{\psi_b}$,

[4]This discussion is adapted from [30].

to define such an axis which continuously changes in time via eqn. (2.8).[5] We will make use of this picture in describing particles with spin. Writing $\psi_a(x,t) = R_a(x,t)\exp\left(\frac{iS_a(x,t)}{\hbar}\right)$ and $\psi_b(x,t) = R_b(x,t)\exp\left(\frac{iS_b(x,t)}{\hbar}\right)$ separates eqn. (2.8) into two equations in the same way that writing the wavefunction in polar form separates the Schrödinger equation. One of these is the Pauli version of the quantum Hamilton-Jacobi equation (cf. eqn. (2.2)). It is unimportant to our discussion and we will not discuss it. The other is a continuity equation,

$$\frac{\partial R^2}{\partial t} + \nabla \cdot \vec{j} = 0, \tag{2.10}$$

where $R^2 = \Psi^\dagger\Psi = (|\psi_a|^2 + |\psi_b|^2)^{1/2}$ and

$$\vec{j} = \frac{\hbar}{2mi}\left[\Psi^\dagger\nabla\Psi - (\nabla\Psi^\dagger)\Psi\right] - \left(\frac{e}{mc}\right)\vec{A}\Psi^\dagger\Psi \tag{2.11}$$

is the *probability density current* associated with the Pauli equation. Making the association $\vec{j} = R^2\vec{v}$ (cf. the discussion concerning eqns. (2.4), (2.5) and (2.6)), the momentum field is given by

$$\vec{p} = \frac{\hbar}{2iR^2}\left[\Psi^\dagger\nabla\Psi - (\nabla\Psi^\dagger)\Psi\right] - \left(\frac{e}{c}\right)\vec{A}.$$

Given initial particle positions, $\vec{x}(0)$, this allows one to determine particle trajectories according to

$$\frac{d\vec{x}}{dt} = \frac{1}{m}\vec{p}(\vec{x},t)|_{\vec{x}(t)}.$$

However, Holland [30] points out that the probability current, (2.11) is not the only function satisfying eqn. (2.10). Another possibility is[6]

$$\begin{aligned}\vec{j} &= \frac{\hbar}{2mi}\left[\Psi^\dagger\nabla\Psi - (\nabla\Psi^\dagger)\Psi\right] - \left(\frac{e}{mc}\right)\vec{A}\Psi^\dagger\Psi + \frac{1}{m}\epsilon_{ijk}\frac{\partial(R^2 s_k)}{\partial x_j} \\ &= \frac{\hbar}{2mi}\left[\Psi^\dagger\nabla\Psi - (\nabla\Psi^\dagger)\Psi\right] - \left(\frac{e}{mc}\right)\vec{A}\Psi^\dagger\Psi + \frac{1}{m}\left(\nabla(R^2)\times\vec{s}\right)\end{aligned} \tag{2.12}$$

[5] See [30] for a discussion of how to do this.

[6] The first term in eqn. (2.12) is equivalent to $R^2\frac{\nabla S}{m}$. This fact will be useful when we analyze the hydrogen atom and helium atom in chapters 4 and 5.

which, of course, leads to the momentum field

$$\vec{p} = \frac{\hbar}{2iR^2}\left[\Psi^\dagger \nabla\Psi - (\nabla\Psi^\dagger)\Psi\right] - \left(\frac{e}{c}\right)\vec{A} + \frac{\nabla(R^2)\times\vec{s}}{R^2}. \tag{2.13}$$

In (2.12), ϵ_{ijk} is the antisymmetric Levita-Cevi symbol and s_k is the spin in the k^{th} direction, given by

$$s_k = \frac{\hbar}{2R^2}\Psi^\dagger\sigma_k\Psi.$$

The addition of the spin-dependent term, $\frac{1}{m}(\nabla(R^2)\times\vec{s})$, to the current (2.12) is motivated by examining the probability distribution current for the Dirac equation.[7] It contains the above term and is responsible for all spin-dependent properties of the trajectories. Thus, it seems reasonable to include it in the definition of the probability density current for particles with spin. We will use (2.12) in our discussion of particles with spin.

In addition, we will only be interested in particles whose spin vectors are constant along their trajectories. Such particles can be described by wavefunctions in which the space and time coordinates decouple from the spin coordinate, ξ, i.e.,

$$\Psi(x,\xi,t) = \psi(x,t)\phi(\xi). \tag{2.14}$$

For the case where the electromagnetic potentials are all zero, eqn. (2.8) reduces to two copies of Schrödinger's equation (one for ψ_a and one for ψ_b). Thus, it is acceptable to describe a particle having constant spin by the wavefunction (2.14) which obeys Schrödinger's equation. However, when we represent the wavefunction as a scalar function as opposed to a 2-component spinor , the components of the spin vector are not well-defined mathematically (c.f. section 5.3). However, we will ignore this fact until we explicitly calculate the spin vectors in appendix C. Treating the wavefunction as a scalar function and using $\vec{A} = \vec{0}$, the momentum field (2.13) reduces to

$$\vec{p} = \frac{\hbar}{2iR^2}\left[\Psi^*\nabla\Psi - (\nabla\Psi^*)\Psi\right] + \frac{\nabla(R^2)\times\vec{s}}{R^2}. \tag{2.15}$$

This is the approach we will adopt to account for electron spin in our study of the helium atom.

[7] See [30] for a discussion of a Bohmian analysis of the Dirac equation.

2.3 The EPR Paradox

As we have seen in section 1.1, according to the EPR experiment, there are two logical possibilities – either quantum mechanics is an incomplete theory or it must predict nonlocal interactions. If we venture outside the box of SQM we find that BM provides a straightforward, yet unexpected solution – quantum mechanics is *both* incomplete *and* nonlocal. The incompleteness of SQM arises because there is an element of physical reality it does not describe – the particle positions of BM. Similarly, BM is a nonlocal theory as we have seen in section 2.1. This would have been an unacceptable solution to Einstein who was absolutely against any notion of nonlocality since nonlocality was thought to automatically allow for superluminal signaling. Such a thing is clearly prohibited by his theory of relativity. The whole point of the EPR paper for Einstein was to show that SQM was not a complete theory and should not be treated as such. The idea that the solution to the EPR paradox would be an intrinsically nonlocal theory is one he clearly did not entertain. We will now examine the Bohmian description of the EPR experiment [8] described in section 1.1 and see whether such concerns are founded.

As in SQM, when the molecule disassociates conservation of spin implies that each particle has equal and opposite spin (this result can be derived analytically, see [8] for instance). However, the difference between BM and SQM is that in BM each particle follows a trajectory through space and time and according to the Bohmian version of the Pauli theory each atom has a well-defined spin vector at each point along its trajectory (see section 2.2). Thus, upon measurement of the spin of, say, particle A, the value of the spin of particle B is determined with certainty, as in SQM. However, the distinction, which is at the heart of the issue, is that in BM the spin of particle B was well-defined *before* and *independent of* the measurement of particle A. Although the spin of particle B is instantly inferred by the outcome of the measurement of the spin of particle A, the spin of particle B is not changed by this process – it is only the pre-existing value of its spin that is revealed to us. Since we glean information about particle B immediately upon measurement of particle A this is an example of a nonlocal interaction. However, since we cannot control the measured value of the spin of particle A, we have no way to control the inferred value of the spin of particle B. Thus, although measurement in this context leads to a non-local interaction, one cannot use measurement in this way to control the unmeasured particle

[6, 8] – i.e., no superluminal signaling. Consequently, in spite of the non-local character of the measurement process described above, the basic tenet of special relativity – the prohibition of superluminal signaling – is maintained. So perhaps Einstein would accept the Bohmian solution of the EPR paradox after all.

2.4 Measurement

We have seen how in the Copenhagen interpretation measurement is treated as a special process in which the wavefunction is required to undergo a discontinuous change that cannot be described by the Schrödinger equation (the collapse of the wavefunction). It is also difficult to even define what a measurement is. Some, for instance, require some sort of intelligent observer (i.e., a human) to register the result of a measurement in order to induce the collapse of the wavefunction. Thus, until this occurs, a measurement has not been made. Von Neumann [44] , on the other hand, described a quantum measurement as having a quantum part, which was described according to quantum mechanics and a classical part which was described in terms of classical mechanics. In between these, he introduced a "cut", which served to separate the quantum world from the classical one. The problem here is that the location of the "cut" is quite arbitrary. How much of the measuring apparatus should be contained within the quantum description of the measurement? This is essentially left up to whomever is trying to describe the process and hence, von Neumann's version of quantum measurement is highly subjective.

BM, on the other hand, does not suffer from any of these problems. In fact, measurement is treated as nothing more than a regular interaction between quantum systems and as we will see, there is no need for a collapse of the wavefunction [8] . The tendency for the measurement of some observable to yield a distinct eigenstate, even though the system began as a linear combination of eigenstates, emerges naturally in Bohm's description. In addition, there is no need for the kind of "cut" between quantum and classical systems introduced by von Neumann. We will now examine the Bohmian description of a general measurement process.

Bohm's measurement process begins in the same way as in von Neumann's description. We represent the initial wavefunction of the system being measured as

$$\psi_{initial}(x,0) = \sum_n c_n \psi_n(x)$$

where the $\psi_n(x)$ are the eigenfunctions of the operator $\hat{O}$ that we wish to measure.[8] Similarly, we represent the wavefunction of the measuring apparatus as $\phi_{initial}(y)$, a wavepacket that suitably describes the classical device from which we receive the results of the measurement (for instance, the position of a pointer or dial on our apparatus). Thus, before interaction, the wavefunction of the combined system is

$$\Psi_{initial}(x,y,0) = \phi_{initial}(y)\psi_{initial}(x,0)$$

As von Neumann did, we use as an interaction Hamiltonian

$$\hat{H}_{int} = i\hbar L\hat{O}\frac{\partial}{\partial y}$$

where L is a suitable constant and we assume the interaction is strong enough so that during the time it acts, the changes to the system are due solely to the interaction (i.e., we can neglect all other terms in the Hamiltonian during the period of interaction). Thus, Schrödinger's equation during the interaction is

$$i\hbar\frac{\partial \Psi_{initial}}{\partial t} = i\hbar L\hat{O}\frac{\partial \Psi_{initial}}{\partial y}$$

which after a time t has solution

$$\Psi(x,y,t) = \sum_n c_n \psi_n(x)\phi_{initial}(y - LO_n t) \tag{2.16}$$

where $\{O_n\}$ are the eigenvalues of $\hat{O}$. If the interaction takes time Δt then after the interaction is over the combined wavefunction is

$$\Psi_{final}(x,y,\Delta t) = \sum_n c_n \psi_n(x)\phi_{initial}(y - LO_n\Delta t).$$

If the interaction is such that $L\Delta O_n \Delta t \gg 1$ where ΔO_n is the change in O_n for successive values of n, then after the interaction the combined wave-

[8] We use x to represent the spatial coordinates of all the particles in the system represented by ψ.

function will have split into n *non-overlapping* wavepackets, $\psi_n(x)\phi_{initial}(y - LO_n t)$. Thus, for each distinct apparatus wavepacket, $\phi_{initial}(y - LO_n t)$, there corresponds an eigenfunction $\psi_n(x)$. In this way, a correlation is set up between eigenfunctions of the operator being measured and different states of the measuring apparatus. If the combined system is now observed with another apparatus (which could be another machine, or even the human eye), the appropriate value of y will be measured on the first apparatus and the corresponding eigenfunction can now be associated with the state of the measured system. Naturally, the probability of obtaining the n^{th} value of y is $|c_n|^2$. In this way, von Neumann explains the collapse of the wavefunction.

According to BM, however, particles exist independently of measurement and follow trajectories through space and time. Thus, after the interaction is over, the apparatus particles, y, have definitely entered one of the non-overlapping wavepackets and from this moment on, are confined to remain there because it is impossible for the particles to be in a region of space where the wavefunction is zero (hence, no probability of a particle moving from one packet to another). In this way, the apparatus makes a distinct measurement in each run of the experiment, and due to the correlation between eigenfunctions and apparatus wavepackets, a particular state can be ascribed to the measured system in each case as well.

Notice that the entire measurement process has been described in a completely continuous fashion with the wavefunction evolving in time according to the Schrödinger equation throughout. The collapse of the wavefunction is then seen to arise from the separating of each component wavepacket and the fact that the apparatus particles and measured particles necessarily **must** enter only one of them. The wavefunction does not "collapse" in the sense that it "jumps" from being a linear combination of eigenfunctions at one moment to a particular eigenfunction the next. Instead, the interaction causes all wavepackets not entered by the particles to become essentially inactive after the interaction is complete. Since these parts of the total wavefunction no longer have any effect on the measured system or apparatus, it is completely reasonable to drop them and treat the wavefunction as though it is only made up of the packet in which the particles have entered – hence the collapse of the wavefunction.

From eqn. (2.16) it is apparent that during the interaction, the component wavefunctions will overlap and interface with each other. Because of this the amplitude of the total wavefunction can be a rapidly-varying function of x, y and t and the quantum potential can be responsible for very

complex and chaotic motions of all the particles involved in the interaction. For this reason, the results of the measurement depend very strongly on the initial conditions. Minute changes in initial conditions can produce changes in the resulting trajectories so that the system may end up in a completely different packet after the interaction is complete. This extreme dependence on initial conditions leads to the existence of bifurcation points associated with each measurement. A particle with initial conditions on one side of a bifurcation point will end up in one final wavepacket and a particle with initial conditions on the other side will end up in another.

Thus, BM is able to explain quantum measurement without invoking the collapse of the wavefunction. What one would refer to as this collapse in SQM, is seen to arise from the separation of the wavepackets representing individual measurement outcomes. It is not that the wavefunction has "collapsed", but that those packets into which the system particles do not enter become ineffective, and hence, can be dropped from the total wavefunction. Thus, under BM the Schrödinger equation is sufficient to give an accurate and reasonable description of the measurement process. It does not need to be modified to solve the measurement problem as some have sought to do.

Chapter 3

A Discussion of Some Relevant Literature

It is important to realize that BM is not the only alternative to SQM. In fact, many formulations of quantum mechanics have been developed over the past eighty years. Many of these, like BM, are attempts to provide a better explanation for troublesome quantum phenomena such as the measurement problem or the existence of quantum interference. Carolyn Colijn outlines many of these interpretations in her Ph.D. thesis [11] so in the interest of avoiding unnecessary repetition we direct the reader there for a description of alternate formulations of quantum mechanics.

We will instead investigate two questions particular to BM itself. One obvious question is whether it is possible to experimentally distinguish between SQM and BM. As we have seen in the previous chapter, the QEH ensures that the statistical predictions of BM and SQM are always equivalent but this does not necessarily eliminate the existence of such an experiment. In fact, certain experiments have been proposed in the literature which claim to differentiate between the two theories and we will examine these arguments in detail.

Another question one could ask is whether BM provides an explanation for the classical world. It is clear that the classical world to which we are accustomed operates very differently from the world of the quantum (at least as far as we can tell from our limited "classical" perspective). In fact, it has been a long-standing problem in physics to derive classical mechanics from quantum mechanics. We will investigate some attempts made in the literature to predict classical behaviour using BM. Before continuing, we wish

to point out to the reader that this chapter contains no results pertaining to the author's research. One may skip this chapter without loss of coherence.

3.1 Can An Experiment Differentiate Between BM and SQM

As was shown in the previous chapter the statistical predictions of SQM and BM are equivalent due to eqn. (2.1) and the QEH. Thus, it would seem that BM cannot differentiate itself from SQM at the experimental level. In fact, when Bohm originally presented his interpretation of quantum mechanics he himself made remarks to the same effect [5].

However, within the past twenty years a number of experiments have been proposed which claim to predict different results for BM and SQM. Some of these are purely thought experiments while others could be performed in the laboratory. To date, no experiment has been performed which has refuted the predictions of one or both of BM or SQM. We will now examine some of these proposals.

3.1.1 The Experiments Proposed By Golshani and Akhavan

Golshani and Akhavan, hereafter referred to as GA, have proposed three related experiments for which they claim BM gives different predictions than SQM [24, 25, 26, 27]. One of these experiments predicts differences only at the level of individual trials of the experiment but gives the same statistical results. Thus, it cannot be used in practice to differentiate between the two theories. However, the other two predict different results both at the individual and statistical levels. GA conclude that these last two experiments provide a feasible way to test between SQM and BM in the laboratory. All three experiments are variations of the standard double-slit experiment. We will review the experimental setups and discuss the results.

First Experiment – A Single Double Slit System With Unentangled Particles

The first proposal [25] involves a single source which emits pairs of identical non-relativistic particles (bosons or fermions) at a double slit apparatus. It is assumed that the particles are emitted one pair at a time so that at most one pair traverses through the slit system at a given instant. It is also assumed that the detecting screen will only detect simultaneous impacts of two particles so that single particle interference is avoided. The incident wavefunction is assumed to be a plane wave in the x-direction given by

$$\Psi_{in}(x_1, y_1; x_2, y_2; t) = C \exp\left[k_x(x_1 + x_2) + k_y(y_1 + y_2)\right] \exp\left(\frac{-iEt}{\hbar}\right)$$

where C is a constant and $E = E_1 + E_2 = \frac{\hbar^2(k_x^2+k_y^2)}{m}$ is the total energy of the system (E_i refers to the energy of particle i). The source is assumed to be far enough from the slit apparatus along the x-axis that $k_y \approx 0$. As in normal treatments of double slit experiments, the slits are assumed to have soft edges to avoid the mathematical complexities of Fresnel diffraction. Consequently, the waves emerging from the slits can be represented by Gaussian waves in the y-direction and plane waves in the x-direction. Taking time $t = 0$ to be the time at which the waves emerge from the slits the initial wavepackets have the form

$$\Psi_A(x, y, 0) = C(2\pi\sigma_0^2)^{-\frac{1}{4}} \exp\left(-\frac{(y - Y)^2}{4\sigma_0^2}\right) \exp\left(i\left[k_x x + k_y(y - Y)\right]\right)$$

$$\Psi_B(x, y, 0) = C(2\pi\sigma_0^2)^{-\frac{1}{4}} \exp\left(-\frac{(y + Y)^2}{4\sigma_0^2}\right) \exp\left(i\left[k_x x - k_y(y + Y)\right]\right)$$

where σ_0 is the half-width of each slit and the subscripts A and B refer to the top and bottom slits, respectively.

Each of these wavepackets evolves in time according to

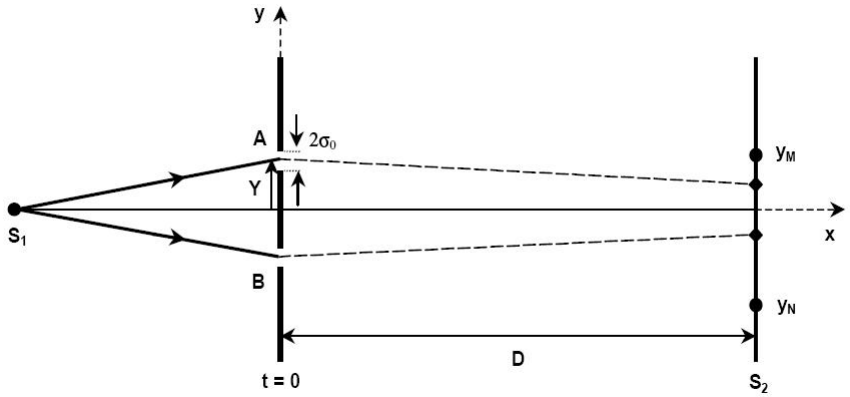

Figure 3.1: A two-slit experiment in which two identical entangled particles are emitted from the source S_1. They pass through the slits A and B and are detected on the screen S_2, simultaneously. The dashed lines are not real trajectories (taken from [25]).

$$\Psi_A(x,y,t) = C(2\pi\sigma_t^2)^{-\frac{1}{4}} \exp\left(-\frac{(y-Y-u_y t)^2}{4\sigma_0\sigma_t}\right) \times \exp\left(i\left[k_x x + k_y(y-Y-u_y t/2) - E_x t/\hbar\right]\right) \tag{3.2a}$$

$$\Psi_B(x,y,t) = C(2\pi\sigma_t^2)^{-\frac{1}{4}} \exp\left(-\frac{(y+Y+u_y t)^2}{4\sigma_0\sigma_t}\right) \times \exp\left(i\left[k_x x - k_y(y+Y+u_y t/2) - E_x t/\hbar\right]\right), \tag{3.2b}$$

where $\sigma_t = \sigma_0\left(1 + \frac{i\hbar t}{2m\sigma_0^2}\right)$ is the half-width of each wavepacket at time t, $u_y = \hbar k_y/m$ is the group velocity of each packet in the y-direction, $E_x = mu_x^2/2$ is the energy of each particle associated with its motion in the x-direction and u_x is the group velocity of each packet in the x-direction.

Thus, taking into account the required symmetry of the wavefunction (antisymmetric for fermions and symmetric for bosons), the total wavefunction of the two-particle system at time t is

$$\Psi(x_1,y_1;x_2,y_2;t) = N[\Psi_A(x_1,y_1,t)\Psi_B(x_2,y_2,t) \pm \Psi_A(x_2,y_2,t)\Psi_B(x_1,y_1,t)] \times [\Psi_A(x_1,y_1,t)\Psi_A(x_2,y_2,t) + \Psi_B(x_2,y_2,t)\Psi_B(x_1,y_1,t)], \tag{3.3}$$

where $N = \left[2\left(1+\exp\left(\frac{-Y^2}{2\sigma_0^2}\right)\right)\right]^{-1}$ is a normalization constant, the "+" is for bosons and the "−" is for fermions.

According to SQM the probability of simultaneously detecting one particle at $(x_1,y_1) = (D,Q_1)$ and the other particle at $(x_2,y_2) = (D,Q_2)$ (two different points on the detecting screen) at time t is

$$P_{12}(Q_1,Q_2,t) = \int_{Q_1}^{Q_1+\Delta} dy_1 \int_{Q_2}^{Q_2+\Delta} dy_2 |\Psi(x_1,y_1;x_2,y_2;t)|^2, \tag{3.4}$$

where D is the distance from the slits to the screen along the x-direction and Δ is a measure of the size of the detectors and is assumed to be small.

According to BM each particle follows a path according to the guidance condition

$$\frac{dx_i}{dt} = \frac{\hbar}{m_i} Im\left(\frac{\nabla_i \Psi(\vec{x}\ t)}{\Psi(\vec{x}\ t)}\right).$$

GA examine the y-coordinate of the center of mass of the two particles, given by $y = (y_1+y_2)/2$, and conclude that under certain circumstances BM will give measurably different results than SQM. Using eqn. (3.3),

$$\begin{aligned}\frac{dy_1}{dt} = N\frac{\hbar}{m} Im\Bigg\{\frac{1}{\Psi}\Bigg[&\left(-\frac{2(y_1-Y-u_y t)}{4\sigma_0\sigma_t} + ik_y\right)\Psi_{A_1}\Psi_{B_2} \\ &+ \left(-\frac{2(y_1+Y+u_y t)}{4\sigma_0\sigma_t} - ik_y\right)\Psi_{A_2}\Psi_{B_1} \\ &+ \left(-\frac{2(y_1-Y-u_y t)}{4\sigma_0\sigma_t} + ik_y\right)\Psi_{A_1}\Psi_{A_2} \\ &+ \left(-\frac{2(y_1+Y+u_y t)}{4\sigma_0\sigma_t} - ik_y\right)\Psi_{B_1}\Psi_{B_2}\Bigg]\Bigg\}\end{aligned} \tag{3.5a}$$

and

$$\frac{dy_2}{dt} = N\frac{\hbar}{m}Im\Bigg\{\frac{1}{\Psi}\Bigg[\left(-\frac{2(y_2+Y+u_yt)}{4\sigma_0\sigma_t} - ik_y\right)\Psi_{A_1}\Psi_{B_2} + \left(-\frac{2(y_2-Y-u_yt)}{4\sigma_0\sigma_t} + ik_y\right)\Psi_{A_2}\Psi_{B_1} + \left(-\frac{2(y_2-Y-u_yt)}{4\sigma_0\sigma_t} + ik_y\right)\Psi_{A_1}\Psi_{A_2} + \left(-\frac{2(y_2+Y+u_yt)}{4\sigma_0\sigma_t} - ik_y\right)\Psi_{B_1}\Psi_{B_2}\Bigg]\Bigg\} \tag{3.5b}$$

and according to eqns. (3.2a) and (3.2b),

$$\Psi_A(x_i, y_i, t) = \Psi_B(x_i, -y_i, t) \qquad \text{for } i = 1, 2. \tag{3.6}$$

Eqn. (3.6) represents the symmetry of $\Psi(x_1, y_1; x_2, y_2; t)$ with respect to reflection in the x-axis. Using this symmetry along with eqns. (3.5a) and (3.5b) GA arrive at the following expression for the motion of the y-coordinate of the center of mass of the two-particle system:

$$\begin{aligned}\frac{dy}{dt} &= \frac{1}{2}\left(\frac{dy_1}{dt} + \frac{dy_2}{dt}\right) \\ &= \frac{(\hbar/2m\sigma_0^2)^2 ty}{[1+(\hbar/2m\sigma_0^2)^2t^2]} \\ &\quad + N\frac{\hbar}{2m}Im\left[\frac{1}{\Psi}\left(\frac{Y+u_yt}{\sigma_0\sigma_t} + 2ik_y\right)(\Psi_{A_1}\Psi_{A_2} - \Psi_{B_1}\Psi_{B_2})\right].\end{aligned} \tag{3.7}$$

This is an ODE for the center of mass coordinate, y. In order to solve it, GA make the approximations $k_y \approx 0$ and $Y \ll \sigma_0$. Under these approximations $\Psi_{A_1}\Psi_{A_2} - \Psi_{B_1}\Psi_{B_2} \approx 0$ and the second term of eqn. (3.7) becomes negligible. The equation for $\frac{dy}{dt}$ becomes[1]

[1]Note that had we omitted the last term in square brackets on the right-hand side of eqn. (3.3) the second term in eqn. (3.7) would be identically zero. Then we could replace the "≈" in eqn. (3.8) with an "=". This corresponds to the case of an entangled wavefunction as we will see in the next section.

$$\frac{dy}{dt} \approx \frac{(\hbar/2m\sigma_0^2)^2}{1+(\hbar/2m\sigma_0^2)^2t^2} yt. \tag{3.8}$$

Solving eqn. (3.8) gives the equation for the y-coordinate of the center of mass:

$$y(t) \approx y_0\sqrt{1+(\hbar/2m\sigma_0^2)^2t^2}, \tag{3.9}$$

where $y_0 = y(0)$. Thus, if the center of mass is on the x-axis at $t = 0$, i.e. $y_0 = 0$, then $y(t) = 0$ for all t and the simultaneous detection of each particle pair will occur symmetrically with respect to the x-axis. However, it is not necessary that $y_0 = 0$. In fact, according to the QEH y_0 should be distributed according to $|\Psi|^2_{t=0}$. Since the distance between neighboring maxima on the detection screen is given by $\delta y \approx \lambda D/2Y$, where λ is the deBroglie wavelength, GA argue that symmetrical detection will be obtained to good approximation if the deviation of the y-coordinate of the center of mass of a particle-pair system is small compared to δy, i.e.,

$$\Delta y \ll \delta y \approx \frac{\lambda D}{2Y} \approx \frac{\pi\hbar t}{Ym}. \tag{3.10}$$

Under the conditions $\hbar t/2m\sigma_0^2 \sim 1$ and $\Delta y_0 \sim \sigma_0$, (Δy_0 is the initial deviation of the y-coordinate of the center of mass of the system), GA obtain the requirement to ensure symmetrical detection:

$$Y \ll 2\pi\sigma_0.$$

This is consistent with the approximations $k_y \approx 0$ and $Y \ll \sigma_0$ used in deriving eqn. (3.9).

Thus, under the conditions described above and using the appropriate approximations it is seen that BM predicts symmetrical detection of each particle pair while according to eqn. (3.4), SQM allows for unsymmetrical detection. However, since eqn. (3.3) can be written in the factored form:

$$\begin{aligned}\Psi(x_1,y_1;x_2,y_2;t) = N[&\Psi_A(x_1,y_1,t)\Psi_B(x_1,y_1,t)] \\ &\times[\Psi_A(x_2,y_2,t)\Psi_B(x_2,y_2,t)],\end{aligned}$$

the two particles behave independently at the ensemble level. As a result, both SQM and BM predict the same interference pattern for an ensemble of

particle pairs.

Next, GA investigate the conditions $\langle y_0 \rangle \neq 0$ and $\hbar t/2m\sigma_0 \gg 1$. They begin with eqn. (3.9) for the motion of the y-coordinate of the center of mass (thus, maintaining the approximations $k_y \approx 0$ and $Y \ll \sigma_0$) except now they enforce a *selective detection* process in which only pairs of particles that reach the detection screen simultaneously **and** on opposite sides of the x-axis are counted. According to BM there will be a region on the detection screen of length

$$L \approx 2\langle y \rangle \approx \frac{\hbar t \langle y_0 \rangle}{m\sigma_0^2} \tag{3.11}$$

where almost no particles will be recorded if $\Delta y \ll L$ and $\hbar t/2m\sigma_0^2 \gg 1$ are satisfied. If the constraint due to the QEH, $\Delta y_0 \sim \sigma_0$, is satisfied the condition $\Delta y \ll L$ can be written

$$\sigma_0 \ll \langle y_0 \rangle. \tag{3.12}$$

Thus, if eqn. (3.12) is satisfied and the given selective detection procedure is employed then BM predicts a region on the screen of length L, given by eqn. (3.11), in which almost no particle detections will be made.

However, according to SQM, there are two possibilities. In one case the probability relation, eqn. (3.4) remains valid except for a drop in intensity due to the rejection of single-particle detections. Thus, SQM would not predict the nearly empty region on the screen given by eqn. (3.11). In the other case SQM is unable to make a prediction concerning selective detection. GA then conclude that if the experiment were performed under the given conditions, ensuring that all approximations used above are valid in the experimental setup, BM would either predict a different interference pattern than SQM or would offer a prediction where SQM was silent, thus providing an observable way to test between the two theories, even at the ensemble level.

Second Experiment – A Single Double-Slit System With Entangled Particles

The second experiment of GA [25] has exactly the same setup as the first except that the source is now assumed to emit entangled particle pairs. In this case eqns. (3.2a) and (3.2b) remain the same and eqn. (3.3) becomes

$$\Psi(x_1, y_1; x_2, y_2, t) = N[\Psi_A(x_1, y_1, t)\Psi_B(x_2, y_2, t) \pm \Psi_A(x_2, y_2, t)\Psi_B(x_1, y_1, t)] \tag{3.13}$$

where the "+" refers to bosons and the "−" refers to fermions. Clearly eqn. (3.4) still represents the probability according to SQM of simultaneous detection of a particle pair at positions $(x_1, y_1) = (D, Q_1)$ and $(x_2, y_2) = (D, Q_2)$. As for the previous experiment, GA establish a discrepancy between BM and SQM by considering the y-coordinate of the center of mass, $y(t)$. For the present case of entangled particles, eqn. (3.7) becomes

$$\frac{dy}{dt} = \frac{\hbar/2m\sigma_0^2)^2}{1 + (\hbar/2m\sigma_0^2)^2 t^2} yt$$

and eqn. (3.9) becomes the identity

$$y(t) = y_0\sqrt{1 + (\hbar/2m\sigma_0^2)^2 t^2}. \tag{3.14}$$

Thus, BM predicts that if the center of mass of the particle pair is initially on the x-axis, i.e., $y_0 = 0$, then $y(t) = 0$ for all t and each particle pair will be detected symmetrically. This is in contrast to eqn. (3.4) which allows for unsymmetric detection. In addition, eqn. (3.4) permits a non-zero probability of detecting both particles in a pair on the same side of the x-axis while BM forbids this as long as $y_0 = 0$.

GA also consider the case where $\langle y_0 \rangle = 0$ and $\Delta y_0 \neq 0$. As for the unentangled wavefunction, they consider approximate symmetrical detection to occur when eqn. (3.10) is satisfied. Under the conditions

$$\frac{\hbar t}{2m\sigma_0^2} \sim 1 \qquad \text{and} \qquad Y \sim \sigma_0 \tag{3.15}$$

and using eqn. (3.14) GA conclude that eqn. (3.10) is satisfied when

$$\Delta y_0 \ll \sigma_0. \tag{3.16}$$

Thus, under the conditions given by eqn. (3.15) approximate symmetrical detection occurs when a source is used for which $y_0 \ll \sigma_0$ for each particle pair.

Third Experiment – A Two Double Slit System With Entangled Wavefunction

GA's third proposal [26] involves a source which emits pairs of identical entangled particles. Each particle in a given pair then goes through its own double-slit apparatus and is registered on a detecting screen. To eliminate the cases where only one particle in a pair goes through a slit system, only simultaneous impacts of particle pairs, one on each screen, are registered. Thus, the final interference patterns on each screen are due entirely to entangled particle pairs. The wavefunction of the pair of particles after coming through the slits is given by

$$\begin{aligned}\Psi(x_1, y_1; x_2, y_2, t) = \bar{N}[&\Psi_A(x_1, y_1, t)\Psi_{B'}(x_2, y_2, t) \pm \Psi_A(x_2, y_2, t)\Psi_{B'}(x_1, y_1, t) \\ &+ \Psi_B(x_1, y_1, t)\Psi_{A'}(x_2, y_2, t) \pm \Psi_B(x_2, y_2, t)\Psi_{A'}(x_1, y_1, t)]\end{aligned} \tag{3.17}$$

where $\bar{N}$ is a constant whose value is unimportant here. $\Psi_A(x_i, y_i, t)$ and $\Psi_B(x_i, y_i, t)$ are the waves coming out of the double slit apparatus on the right and are given by eqns. (3.2a) and (3.2b) while $\Psi_{A'}(x_i, y_i, t)$ and $\Psi_{B'}(x_i, y_i, t)$ represent the waves coming out of the apparatus on the left. They have the same form as eqns. (3.2a) and (3.2b) except the x-coordinates in the exponentials must undergo the transformation $x \rightarrow (x - 2d)$ where d is the distance from the source to the planes containing of the slits.

The analysis of the Bohmian trajectories proceeds in the same way as for GA's second experiment. Making use of the following symmetries;

$$\Psi_A(x_i, y_i, t) = \Psi_B(x_i, -y_i, t) \qquad \text{and} \qquad \Psi_{A'}(x_i, y_i, t) = \Psi_{B'}(x_i, -y_i, t),$$

they arrive at eqn. (3.14) for the motion of the y-coordinate of the center of mass of the two-particle system. Thus, as in the second experiment GA obtain the result that BM predicts symmetrical detection for each particle pair while SQM allows for unsymmetrical detection if the condition $y_0 = 0$ is met[2]. In the case that $y_0 \neq 0$, GA maintain that approximate symmetrical

[2]Once again, the probability of joint detection of particle 1 at position $(x_1, y_1) = (D, Q_1)$ and particle 2 at position $(x_2, y_2) = (D, Q_2)$ is given by eqn. (3.4) according to SQM.

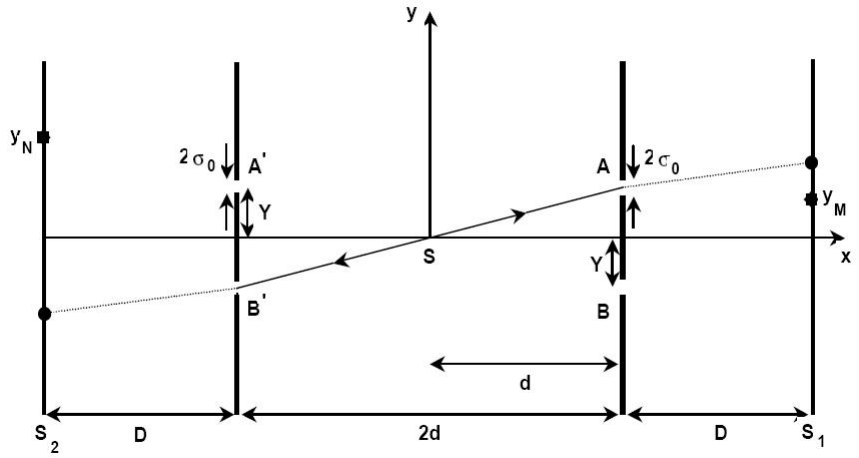

Figure 3.2: The two double-slit experiment setup. Two identical particles with zero initial momentum are emitted from the source S and pass through slits A and $B^{'}$ or B and $A^{'}$. They are detected simultaneously on the screens S_1 and S_2. The dotted lines do not correspond to real trajectories (taken from [26]).

detection of each particle pair can be achieved if conditions (3.15) are met and a source is used for which $y_0 \ll \sigma_0$ holds for each detected pair of particles. This is the same conclusion as was drawn for the second experiment.

GA also consider a variation of the experiment which they say predicts observably different results even at the ensemble level. They use a further form of "selective detection" which is motivated by the following. In the case where $y_0 \neq 0$ for each detected particle pair, BM predicts completely symmetrical detection of each particle pair. In addition, according to eqn. (3.14),

$$\dot{y}_i(x_1, y_1; x_2, y_2; t) = -\dot{y}_i(x_1, -y_1; x_2, y_2; t). \tag{3.18}$$

Evaluating (3.18) for $y_1 = 0$ and $y_2 = 0$ we see that $\dot{y}_i = 0$ for each particle along the x-axis and this is valid at all times, t, for both bosons and fermions. Thus, if both particles are simultaneously on the x-axis they cannot cross it or be tangent to it. The importance of this is that if $y_0 = 0$ then any particle traveling through a top slit will be detected on the top

half of the screen while any particle traveling through a bottom slit will be detected on the bottom half of the screen. It is important to see that this symmetry of motion is due to the assumed entanglement of each particle pair which in turn is due to the restriction that each pair is emitted from a common source with total momentum zero.

Using this symmetry GA conclude that according to BM if the particle going through the slit system on the right goes through the top slit then it must be registered on the top half of the screen. Also, the particle going through the slit system on the left must go through the bottom slit and be registered on the bottom half of the screen. GA then propose a "selective detection" in which only those particle pairs for which the particle going through the right slit system is detected on the top half of the screen are registered. Then BM predicts that *all* particles going through the left slit system *must* be detected on the bottom half of the screen. However, according to eqn. (3.4) SQM allows for detection on the top half of the screen. Thus, BM predicts observably different results than SQM.

To summarize, GA have proposed three related experiments based on the standard double-slit set-up. They claim that different results are predicted depending on whether one analyzes the experiments using BM or SQM. BM predicts symmetrical detection of each particle pair about the x-axis for each individual run of the experiments whereas SQM does not. This is of no help since both theories still predict the same interference patterns, but by employing certian "selective detection" techniques, GA propose that a differentiation can be made so that BM predicts different results than SQM even at the statistical level.

3.1.2 The Experiments Proposed By Ghose

In the same vein as GA, Partha Ghose, hereafter referred to as PG, has proposed two experiments [19, 20] which he maintains should serve to differentiate between BM and SQM. The first is quite similar to the proposals of GA and involves a pair of identical particles emitted at a double-slit system. The second is an appeal to the concept of *ergodicity* which is well-defined in classical mechanics but not so in quantum mechanics. PG attempts to provide a definition of an ergodic quantum system and describes a system for which SQM and BM predict different ergodic behaviour. We will examine each of these proposals in turn.

First Experiment – A Single Double-Slit System With Entangled Photons

The first experiment proposed by PG [19] is quite similar to those of GA. It involves a double-slit system which is traversed by identical non-relativistic bosons. Each particle is simultaneously diffracted by one of the slits in the apparatus and the slits are assumed to have a width d which is much larger than the de Broglie wavelength of the packets representing the particles. There is a region, R, in front of the slits in which the two diffracted packets will overlap and interfere with each other (see figure 3.3). R is assumed to be far enough from the slits that each packet can be well approximated by a plane wave (this corresponds to the case of Fraunhoffer diffraction). Taking the origin of the 2-dimensional plane in which the particles move as the center-point of the line joining the two slits, PG writes the wavefunction of the two-particle system as

$$\Psi(\vec{r_1}, \vec{r_2}, t) = \sqrt{N} g \left[e^{i(\vec{k_A}\cdot\vec{r_1} + \vec{k_B}\cdot\vec{r_2})} + e^{i(\vec{k_A}\cdot\vec{r_2} + \vec{k_B}\cdot\vec{r_1})} \right] e^{-iEt}$$

where N and g are constants whose values are unimportant for this discussion. The wavefunction has bosonic symmetry and due to this, is symmetric with respect to reflection in the y-axis.[3]

According to BM, the velocities of each particle are given by

$$\begin{aligned} \vec{v_i} &= \frac{1}{m} \nabla_i S(\vec{x}, t) \\ &= \frac{\hbar}{2m} (\vec{k_A} + \vec{k_B}) \qquad \text{where } i = 1, 2 \text{ refers to particle 1 and 2.} \end{aligned}$$

Due to the symmetry of the setup, $k_{A_x} + k_{B_x} = 0$ and consequently,

$$v_{1_x}(0) = v_{2_x}(0) = 0$$

and

$$v_{1_x}(t) + v_{2_x}(t) = 0 \qquad \text{for all } t.$$

Thus,

[3] Keep in mind that in figure 3.3 the vertical axis is the x-axis and the horizontal axis is the y-axis.

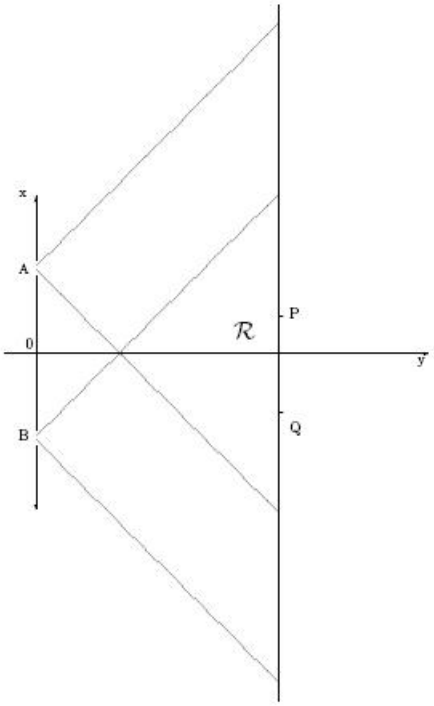

Figure 3.3: The double-slit experiment of PG. Two identical bosons each travel through one of the slits A and B. The wavepackets interfere in the region R (taken from [19]).

$$x_1(t) + x_2(t) = x_1(0) + x_2(0)$$

which is the same result as that obtained in the GA experiments – that if the initial positions of the particles are symmetric with respect to the y-axis (if $x_1(0) + x_2(0) = 0$) then they will remain that way for all time. Boson trajectories are therefore symmetric with respect to the y-axis and can never cross this axis.

Using this result, PG propose a way of differentiating between BM and SQM. According to SQM the probability of simultaneous detection of particle 1 at position (x_1, y_1) on the screen and particle 2 at position (x_2, y_2) on the screen is given by eqn. (3.4).

$$P_{12}(x(Q_1), x(Q_2)) = \int_{x(Q_1)}^{x(Q_1)+\Delta x(Q_1)} dr_1 \int_{x(Q_2)}^{x(Q_2)+\Delta x(Q_2)} dr_2 |\Psi|^2,$$

where $\Delta x(Q_1)$ and $\Delta x(Q_2)$ refer to the size of the detectors at $x(Q_1)$ and $x(Q_2)$ respectively (cf. eqn. (3.4)). If detectors are placed at positions symmetric with respect to the y-axis, then both BM and SQM predict complete joint detection of each particle pair but if they are placed asymmetrically then BM predicts no joint detections while SQM predicts a non-zero result. In this way an observable difference between the two theories is predicted.

Second Experiment – An Argument Based On Ergodicity

Ergodicity is a well-defined concept in classical mechanics. If the orbits of a dynamical system cover the entire phase space over an infinite time period, the system is said to be ergodic. If they do not, the system is said to be non-ergodic[4]. According to fundamental theorems in ergodic theory, the space averages and time averages of a system's dynamical variables exist and if the system is ergodic they will be equal. Similarly, if the system is non-ergodic they cannot be equal. The space average of a complex-valued function, F, defined on the phase-space manifold of the system, M, is defined as

$$\bar{F} \equiv \int_M F(q,p)\rho(q,p)\, dq\, dp, \qquad \text{where} \qquad \int \rho(q,p)\, dq\, dp = 1$$

and the time average of F over M is defined as

$$F^* \equiv \lim_{N\to\infty} \frac{1}{N} \sum_{n=0}^{N-1} F(\phi_t^n q),$$

where q and p represent the set of spatial coordinates and momenta coordinates, respectively, $\rho(q,p)\, dq\, dp$ is the invariant measure in phase space and $\phi_t : M \to M$ is a group of measure-preserving diffeomorphisms which depends on time.

The situation is a little different in SQM where particle trajectories, and consequently a phase space, do not exist. In this case the time average of

[4]In simpler terms, if a system's dynamics are periodic, it is non-ergodic.

a Hermitean operator, $\hat{F}$, for a system described by the state $\Psi(x_1, x_2, t)$ is defined as

$$F^* \equiv \lim_{T\to\infty} \frac{1}{T} \int_0^T dt \int dx_1\, dx_2 \Psi^*(x_1, x_2, t) \hat{F} \Psi(x_1, x_2, t). \tag{3.19}$$

Similarly, the space average of $\hat{F}$ for a system in the state $\Psi(x_1, x_2, t)$ is defined as

$$\bar{F} \equiv Tr(\hat{\rho}\hat{F}) \tag{3.20}$$

where $\hat{\rho}$ is the reduced density matrix corresponding to $\Psi(x_1, x_2, t)$. Using these definitions, the above theorems of classical ergodic theory also hold for quantum systems.

PG then appeals to a proof that all quantum systems according to SQM must be ergodic.[5] The details of the proof[6] are inconsequential for this discussion but using the result PG establishes a discrepancy between SQM and BM by providing two physical systems for which BM predicts non-ergodic behaviour.

The first is the quantum version of the classical system consisting of two identical simple pendulums each of length $L = 1$ and mass $m = 1$ connected by an unstretched weightless spring. Its wavefunction is described by the Schrödinger equation

$$i\hbar \frac{\partial \Psi(Q_1, Q_2, t)}{\partial t} = \left[\frac{\hbar^2}{2} \frac{\partial^2}{\partial Q_2^2} - \frac{\hbar^2}{2} \frac{\partial^2}{\partial Q_2^2} + \frac{1}{2}\omega_1^2 Q_1^2 + \frac{1}{2}\omega_2^2 Q_2^2 \right] \Psi(Q_1, Q_2, t). \tag{3.21}$$

Here we are using normal coordinates:

$$Q_1 = \frac{q_1 + q_2}{\sqrt{2}} \qquad \text{and} \qquad Q_2 = \frac{q_1 - q_2}{\sqrt{2}},$$

where q_1 and q_2 are the spatial coordinates of particle 1 and 2, respectively. Eqn. (3.21) has the solution

[5] See references 9 and 10 in [20].

[6] See [20] for a proof for special cases. PG refers the reader to [17], [34] ,[16] and [43] for details of the proof for the general case.

$$\Psi(Q_1, Q_2, t) = \psi_A(Q_1, t)\psi_B(Q_2, t)$$

where

$$\psi_A(Q_1, t) = \left(\frac{\omega_1}{\pi\hbar}\right)^{\frac{1}{4}} \exp\left\{-\left(\frac{\omega_1}{2\hbar}\right)(Q_1 - a_1\cos(\omega_1 t))^2 - \frac{i}{2}\left[\omega_1 t + \left(\frac{\omega_1}{\hbar}\right)\left(2Q_1 a_1 \sin(\omega_1 t) - \frac{1}{2}a_1^2 \sin(2\omega_1 t)\right)\right]\right\}$$

is a wavepacket initially centered at $Q_1 = a_1$ which oscillates around Q_1 and

$$\psi_B(Q_2, t) = \left(\frac{\omega_2}{\pi\hbar}\right)^{\frac{1}{4}} \exp\left\{-\left(\frac{\omega_2}{2\hbar}\right)(Q_2 - a_2\cos(\omega_2 t))^2 - \frac{i}{2}\left[\omega_2 t + \left(\frac{\omega_2}{\hbar}\right)\left(2Q_2 a_2 \sin(\omega_2 t) - \frac{1}{2}a_2^2 \sin(2\omega_2 t)\right)\right]\right\}$$

is a wavepacket initially centered at $Q_2 = a_2$ which oscillates around Q_2.

Calculating the momenta of each particle via the guidance conditions gives

$$p_1 = \frac{dQ_1}{dt} = \frac{\partial S(Q_1, Q_2, t)}{\partial Q_1} = -\omega_1 a_1 \sin(\omega_1 t)$$
$$p_2 = \frac{dQ_2}{dt} = \frac{\partial S(Q_1, Q_2, t)}{\partial Q_2} = -\omega_2 a_2 \sin(\omega_2 t)$$

which leads to the trajectories

$$Q_1(t) = Q_1(0) + a_1(\cos(\omega_1 t) - 1)$$
$$Q_2(t) = Q_2(0) - a_2(\cos(\omega_2 t) - 1) \tag{3.23}$$

where $Q_1(0)$ and $Q_2(0)$ are the initial normal coordinates. There are two possible motions resulting from (3.23):

1. $Q_1(t) = 0 \Rightarrow q_1(t) = q_2(t)$, i.e., the particles oscillate in phase both

with frequency ω_1,

or

2. $Q_2(t) = 0 \Rightarrow q_1(t) = -q_2(t)$, i.e., the particles oscillate out of phase with frequency ω_2.

In both cases the motion of the system is periodic and hence, BM predicts non-ergodic behaviour.

As a second example consider a source which emits two identical particles whose momenta are correlated (as in the original EPR paper). Each particle is described by a wavepacket and they are made to simultaneously pass through the slits of a double-slit apparatus, each through a different slit (as in the experiments of GA). The analysis of this experiment proceeds in exactly the same way as in the papers of GA except that PG uses spherical waves to describe the wavepackets emerging from the slits as opposed to the plane/Gaussian waves used in GA. Using the same coordinate system as GA, the wavefunction of the system in the region where the individual wavepackets do not overlap is given by

$$\Psi(r_{1A}, r_{2B}, t) = \frac{1}{2\pi} \frac{e^{ik(r_{1A}+r_{2B})}}{r_{1A} r_{2B}} e^{iEt/\hbar},$$

where $r_{1A} = \sqrt{x_1^2 + (y_1 - a)^2}$ and $r_{2B} = \sqrt{x_2^2 + (y_2 + a)^2}$ are the respective distances of each particle from the slit from which it originated. Note that $\Psi(r_{1A}, r_{2B}, t)$ is symmetric with respect to reflection in the x-axis as well as with respect to interchange of particle labels $1 \leftrightarrow 2$.

Solving the Bohmian equations of motion yields

$$\begin{aligned}
v_{1_x} &= \frac{1}{m} \frac{\partial S}{\partial r_{1A}} \frac{\partial r_{1A}}{\partial x_1} = \frac{\hbar k x_1}{m r_{1A}} \\
v_{2_x} &= \frac{1}{m} \frac{\partial S}{\partial r_{2B}} \frac{\partial r_{2B}}{\partial x_2} = \frac{\hbar k x_2}{m r_{2B}} \\
v_{1_y} &= \frac{1}{m} \frac{\partial S}{\partial r_{1A}} \frac{\partial r_{1A}}{\partial y_1} = \frac{\hbar k (y_1 - a)}{m r_{1A}} \\
v_{2_y} &= \frac{1}{m} \frac{\partial S}{\partial r_{2B}} \frac{\partial r_{2B}}{\partial y_2} = -\frac{\hbar k (y_2 + a)}{m r_{2B}}.
\end{aligned}$$

The spherical waves have the same speed of propagation. Therefore $r_{1A} =$

$r_{2B} = vt$ and we have

$$v_{1_x} - v_{2_x} = \frac{d(x_1 - x_2)}{dt} = \frac{1}{t}(x_1 - x_2) \tag{3.24}$$

and

$$v_{1_y} + v_{2_y} = \frac{d(y_1 + y_2)}{dt} = \frac{1}{t}(y_1 + y_2). \tag{3.25}$$

Using the initial conditions $x_1(t_0) - x_2(t_0) = \delta(0)$ and $y_1(t_0) + y_2(t_0) = \sigma_0$ eqns. (3.24) and (3.25) have the solutions

$$x_1(t) - x_2(t) = \delta(0)\frac{t}{t_0} \qquad \text{and} \qquad y_1(t) + y_2(t) = \sigma(0)\frac{t}{t_0}.$$

In the limits $\delta(0) \to 0$ and $\sigma(0) \to 0$,

$$x_1(t) = x_2(t) \qquad \text{and} \qquad y_1(t) = -y_2(t) \tag{3.26}$$

for all times t, i.e., the trajectories of the two particles approach complete symmetry about the x-axis.

Now let us consider the region where the two individual wavepackets overlap. Assuming the particles are bosons, the wavefunction in this region is given by

$$\Psi(r_1, r_2, t) = \frac{1}{N}\left[\frac{e^{ik(r_{1A}+r_{2B})}}{r_{1A}r_{2B}} + \frac{e^{ik(r_{1B}+r_{2A})}}{r_{1B}r_{2A}}\right] e^{iEt/\hbar}$$

where N is a normalization factor whose value is unimportant here, $r_{1B} = \sqrt{x_1^2 + (y_1 + a)^2}$ and $r_{2A} = \sqrt{x_2^2 + (y_2 - a)^2}$. This wavefunction is symmetric with respect to reflection in the x-axis and with respect to interchange of particle labels. Since $r_{1B} = r_{2A} = vt$, conditions (3.26) still hold and the Bohmian trajectories are symmetric about the x-axis for all time. Thus, in all regions beyond the slits the trajectories form two disjoint subsets (one subset for particles coming through the top slit and one for particles coming through the bottom slit) and thus the trajectories cannot fill the entire phase space and consequently, the system is non-ergodic.

In order to test this PG proposes doing this experiment using photons and setting up the detectors asymmetrically on the screen. If this is done, BM predicts no simultaneous joint detections of particles in the limits $\delta(0) \to 0$ and $\sigma(0) \to 0$ while SQM predicts non-zero probability of detection according

to eqn. (3.4).

3.1.3 The Response of Struyve and De Baere

After the publication of the papers by GA and PG, Struyve and De Baere (hereafter referred to as SD) published a response in which they contest the conclusions of both sets of authors [42]. We will examine their arguments as well as the responses of GA and PG to these arguments. We begin with SD's criticism of GA.

The Criticism of the Experiments of GA

All of the experiments of GA make use of one or more double-slit systems and their results are based on probabilities of joint detection of pairs of identical particles. The basic result is that under certain conditions, BM predicts symmetric trajectories of *every* particle pair while SQM does not. This provides an observable way to test between the two theories according to GA since coincidence counts of particle detectors placed asymmetrically on the screen are predicted to be different by each theory. SD disagree with this result. They argue that the conditions under which the conclusion holds are based on assumptions which contradict BM and thus, are nonsensical. Their appeal is based on the QEH which when applied to the experiments of GA require that the initial positions of each particle pair are distributed according to $|\Psi|^2$. In particular, the y-coordinates must be distributed as such and consequently, eqn. (3.16) is not consistent with the wavefunction, (3.13). According to SD, "$\ldots |\Psi|^2$ does not contain the constraint $y(0) = 0$, or put another way $|\Psi|^2$ does not restrict $y(0)$ from being different from zero." Since the initial particle coordinates are distributed in such a way, the center of mass coordinates must also be distributed in such a fashion. In particular, SD state that if the overlap of the individual wavepackets is negligible at time $t = 0$ (if σ_0 is small compared to Y), then $\Delta y_0 = \frac{\sigma_0}{\sqrt{2}}$.

In addition, SD note that in order to ensure the particles depart the slits symmetrically, the slits need to be small which corresponds to taking a small σ_0. However, according to eqns. (3.9) and (3.14) the smaller σ_0, the larger $y(t)$ becomes for all t, thus, the larger the probability of asymmetric detection according to BM.

The Response of GA

While GA accept the fact that according to the QEH, the initial positions of each particle must be distributed according to $|\Psi|^2$, they disagree that the center of mass coordinates must obey the same distribution [28]. To illuminate their point, they provide an in-depth analysis of their third experiment in which identical entangled particles are each sent through a different double-slit apparatus. First they examine the assumption that $\Delta y_0 \ll \sigma_0$. Before the particles reach the slits, the wavefunction of the system has the form

$$\begin{aligned}\Psi_0(x_1, x_2; y_1, y_2) &= \xi(x_1, x_2)\hbar \int_{-\infty}^{\infty} \exp\left[ik_y(y_1 - y_2)\right] dk_y \\ &= 2\pi\hbar\xi(x_1, x_2)\delta(y_1 - y_2), \end{aligned} \tag{3.27}$$

where $\xi(x_1, x_2)$ depends only on the x-components of the particles and whose form is unimportant to this discussion. The wavefunction (3.27) describes two particles whose total momentum in the y-direction is zero and whose center of mass has a y-component equal to zero. This entanglement is permitted by Heisenberg's Uncertainty Principle because

$$[(\hat{p}_{y_1} + \hat{p}_{y_2}), (\hat{y}_1 - \hat{y}_2)] = 0$$

Thus, the Hermitean operators $\hat{p}_{y_1} + \hat{p}_{y_2}$ and $\hat{y}_1 - \hat{y}_2$ commute and the system can exist in a state in which the corresponding dynamical quantities are both exactly specified.

Next, GA examine how the entanglement properties of the particle pair change when the particles go through the slits. According to GA's original paper [26] the individual wavepackets emerging from the slits maintain their plane wave form in the x-direction and obtain a Gaussian profile in the y-direction and the total wavefunction, $\Psi(x_1, x_2; y_1, y_2; t)$, is given by (3.17), (3.2a) and (3.2b). Note that

$$\begin{aligned}(\hat{p}_{1_y} + \hat{p}_{2_y})\Psi(x_1, x_2; y_1, y_2; t) &= -i\hbar \left(\frac{\partial}{\partial y_1} + \frac{\partial}{\partial y_2} \right) \Psi(x_1, x_2; y_1, y_2; t) \\ &= i\hbar \left(\frac{y_1(t) + y_2(t)}{2\sigma_0\sigma_t} \right) \Psi(x_1, x_2; y_1, y_2; t) \end{aligned} \tag{3.28}$$

which says that the system is in an eigenstate of the total momentum in the y-direction with eigenvalue $i\hbar\left(\frac{y_1(t)+y_2(t)}{2\sigma_0\sigma_t}\right)$. It is seen from (3.28) that momentum entanglement, in the form $p_{1_y} + p_{2_y} = 0$, leads to the position entanglement, $y_1 + y_2 = 0$. GA assume that the momentum entanglement is maintained in the Bohmian picture, an assumption which is supported by the symmetry of the setup. Since each double-slit apparatus is assumed to be identical, GA assume that the passage of each wavepacket through its respective slit is identical and hence, the momentum correlation is not changed. Thus, the y-component of the center of mass remains on the x-axis after passage through the slits, i.e., neither of the entanglement properties of the system are lost.

According to SQM asymmetrical joint detection is possible because the probability distribution at time t is $P(x_1, y_1, x_2, y_2, t) = |\Psi(x_1, y_1, x_2, y_2, t)|^2$ (cf. Postulate 1 in chapter 1). Therefore, the position entanglement does not exist for the particles at the screen in SQM, and consequently, neither does the momentum entanglement. GA concludes that in SQM the momentum entanglement is erased when the particles pass through the slits and the center of mass coordinates must then be distributed according to $|\Psi|^2$.

GA also point out that since the initial position of each particle is distributed according to the QEH, the final interference pattern on the screen will be consistent with the predictions of SQM. Thus, in spite of the fact that according to BM $P = |\Psi|^2$ is only true for particle pairs before they pass through the slits, we still obtain the same interference pattern after a large number of particles have been registered on the screen.

In summary, the rebuttal of GA is that SD have used the QEH incorrectly by insisting that $P = |\Psi|^2$ must be true for all times. They have shown that this assumption boils down to the statement that the momentum entanglement between the particles in a given pair (and consequently the position entanglement) is erased from the wavefunction when the particles pass through the slits. By arguing that this is not the case in BM – that the momentum entanglement of the system is not changed after passage through the slits – GA conclude that the y-component of the center of mass does, in fact, remain on the x-axis, and from this conclusion their entire argument follows.

The Criticism to the Ergodicity Argument of PG

SD refutes the ergodicity argument made by PG by rejecting the definition of the space average, eqn. (3.20). Instead, SD appeals to the definition of the "local expectation value" of the observable $\hat{F}$ given by Holland [30]:

$$F(x_1, x_2, t) = Re\left[\frac{\Psi^*(x_1, x_2, t)\hat{F}\Psi(x_1, x_2, t)}{\Psi^*(x_1, x_2, t)\Psi(x_1, x_2, t)}\right].$$

According to Holland, $F(x_1, x_2, t)$ can be interpreted as an actual property of the particle in the Bohmian picture. Using the local expectation value, the space average of $\hat{F}$ can naturally be defined by

$$\begin{aligned}\bar{F} &\equiv \int dx_1\, dx_2\, P(x_1, x_2, t)F(x_1, x_2, t) \\ &= \int dx_1\, dx_2\, \Psi^*(x_1, x_2, t)\hat{F}\Psi(x_1, x_2, t)\end{aligned}$$

where the fact that $\hat{F}$ is Hermitean has been used.

PG made the conclusion that the double-slit system is non-ergodic according to BM because the space average of the probability of joint detection, $\bar{P}_{12}$, is not equal to the time average of the probability of joint detection, P^*_{12}. Specifically, PG showed that

$$P^*_{12} = 0 \qquad \text{and} \qquad \bar{P}_{12} \neq 0 \tag{3.29}$$

where P^*_{12} is defined by eqn. (3.19) and $\bar{P}_{12}$ by eqn. (3.20).

Intrinsic to PG's conclusion that $P^*_{12} = 0$ is the assumption of symmetric trajectories. SD levy the same argument as they did against GA – that the conditions necessary to ensure symmetric trajectories are not consistent with the QEH. Thus, they argue that the conclusion $P^*_{12} = 0$ is unfounded, as is the entire argument that the system is non-ergodic under BM.

The Response of PG

PG responds to the above criticisms [21] in a similar fashion as GA. He considers an example using his proposed double-slit experiment (recall that the double-slit experiment proposed by PG is almost identical to one of the experiments proposed by GA) in which particle 1 is at a definite position

$X_1(t)$ and particle 2 is at the definite position $X_2(t)$ at time t. According to BM, all portions of the wavefunction where no particle actually *is* are considered to be empty and do not cause particle detectors to fire. Thus, only two trajectories out of the set of all possible trajectories will cause the detectors to fire in any run of the experiment. If the experiment is repeated N times at times $(t_1, t_2, \ldots, t_i, \ldots, t_N)$ then for each run the particles will be in positions $X_1(t_i)$ and $X_2(t_i)$ which are distributed according to $|\Psi|^2$. In the limit that $N \to \infty$, the collection of runs of the experiment approaches a Gibbs ensemble and the time average of the joint detection probability for detectors D_1 and D_2 is

$$\begin{aligned} P_{12}^* &= \lim_{N\to\infty} \frac{1}{N} \sum_{t_1}^{t_N} \frac{1}{\delta_0} \int_{D_1,D_2,t_i} \rho\big(x_1(t_i), x_2(t_i)\big)\delta\big(x_1(t_i) - X_1(t_i)\big) \\ &\qquad\qquad \times \delta\big(x_2(t_i) - X_2(t_i)\big)\, dy_1(t_i)\, dy_2(t_i) \\ &= \lim_{N\to\infty} \frac{1}{N} \sum_{t_1}^{t_N} \rho\big(X_1(t_i), X_2(t_i)\big) \\ &\neq \bar{P}_{12} \end{aligned}$$

where $\bar{P}_{12}$ is the space average of the joint detection probability. PG then points out that the above formula is true only if the guidance condition places no further restriction on the motion of the particles. This is not the case for the double slit experiment for which both GA and PG have shown that under certain conditions the guidance condition of BM predicts symmetric particle trajectories. In this case, each particle pair has the additional constraint $Y_1(t_i) + Y_2(t_i) = 0$ on the particle trajectories for each t_i. It is precisely this restriction on the motion that makes the system non-ergodic. Mathematically, the time average is now written

$$\begin{aligned} P_{12}^* &= \lim_{N\to\infty} \frac{1}{N} \sum_{t_1}^{t_N} \frac{1}{\delta_0} \int_{D_1,D_2,t_i} \rho\big(x_1(t_i), x_2(t_i)\big)\delta\big(x_1(t_i) - X_1(t_i)\big) \\ &\qquad\qquad \times \delta\big(x_2(t_i) - X_2(t_i)\big)\delta\big(Y_1(t_i) + Y_2(t_i)\big)\, dy_1(t_i)\, dy_2(t_i) \\ &\neq \bar{P}_{12}. \end{aligned}$$

Thus, we see that the time average is not equal to the space average

when the constraint of symmetric trajectories is taken into account and the system is non-ergodic. In the words of PG [21], "All this shows that QEH is applicable to the full ensemble but not to individual processes that make up this ensemble. There could be information regarding individual processes determined by Bohmian dynamics (through the guidance condition) that are hidden in the full ensemble. The symmetric trajectories in a double-slit experiment with single particles is a clear example of how the information that the trajectories are symmetrical about the line of symmetry and do not cross, is masked in the distribution function,[7] $\rho(x(t))$."

3.1.4 The Experiment Proposed By Gondran and Gondran

Recently Michel Gondran and Alexandre Gondran, hereafter referred to as GG, have proposed an experiment which relies on a completely different idea than the experiments of GA and PG [29]. In the wake of advances in nanotechnology, GG suggest using the non-zero size of material particles to differentiate between BM and SQM. Their experiment involves sending a beam of C_{60} molecules through a slit system consisting of two sets of slits, set A and set B. Set A is a single slit of width 50 nm and set B is a grating of 100 slits equidistantly spaced, each of width 0.5 nm with 0.5 nm between each of them. A detection screen is placed behind the slit system on which particle impacts are registered. The experimental set-up is given in figure 3.4. A 50 nm slit is realizable using modern technology but the grating of set B is not. As such, the following experiment is relegated to the mind for the time being, but it is expected that technology will eventually allow for such an experiment to be performed in the laboratory.

Since the size of the C_{60} molecule is larger that the size of each of the slits in grating B it is obvious that none of the particles should pass through it and be registered on the detection screen. However, under the influence of the Schrödinger equation the wavefunction of each molecule will be diffracted by the grating and will be non-zero on the detection screen after a certain amount of time, t, has passed. GG compare the interference patterns predicted by SQM to the trajectories predicted by BM and show that they are different, giving an observable way to test between the two theories. The patterns produced by SQM are given in figure 3.5.

[7] $\rho(x(t)) = |\Psi|^2$.

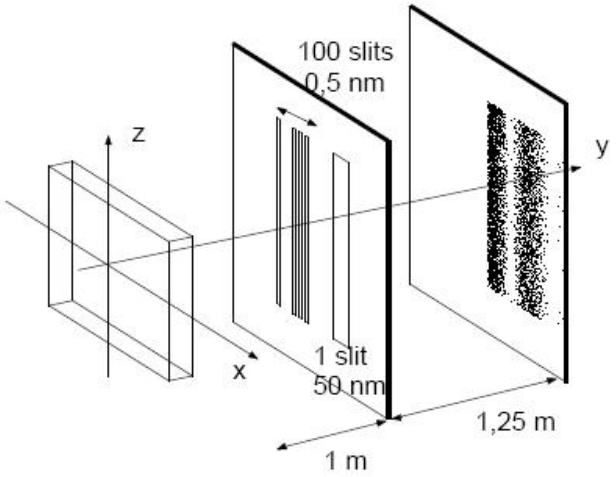

Figure 3.4: The experimental set-up (taken from [29]).

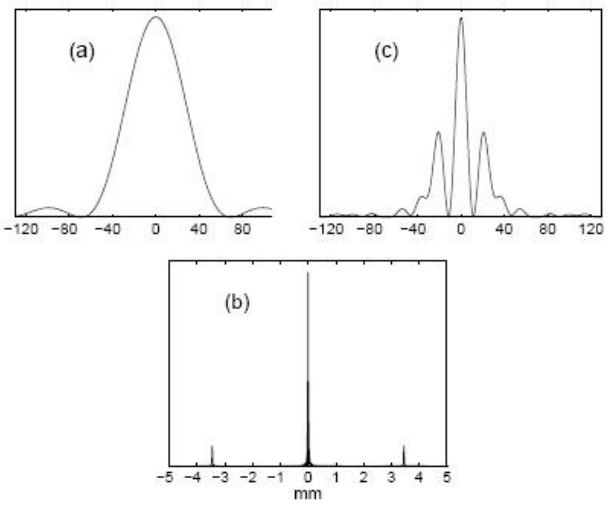

Figure 3.5: $|\Psi|^2$ on the detection screen respectively: (a) diffraction (slit A), (b) interference with asymmetrical slits (slit A and grating B), (c) magnification of the central peak of figure (b) (taken from [29]).

When the grating is closed and only slit A is open the interference pattern has one central peak whereas it has a smaller central peak and nearly-symmetric secondary peaks surrounding it when both sets of slits are open.[8]

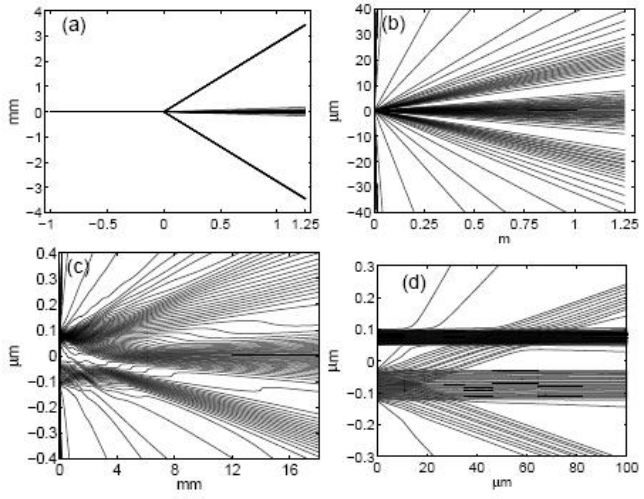

Figure 3.6: 100 Bohmian trajectories with randomly drawn initial positions: (a) global view, (b) central trajectories, (c) magnification of the first millimeters after the slits, (d) magnification of the first hundred micrometers after the slits (taken from [29]).

If the experiment is run with both A and B open figures 3.5(b) and 3.5(c) are predicted when the wavefunction is assumed to propagate through the grating. Figure 3.5(a) is predicted if it is assumed that the wavefunction does not propagate through the grating.[9]

[8]It appears from the figure that the interference patterns are symmetric which may be troubling to some readers since the slit system is asymmetric and is expected to produce an asymmetric total wavefunction. The wavefunction is in fact asymmetric after emerging from the slit system but slowly acquires a symmetric form as it propagates through space. By the time it reaches the detection screen it is nearly symmetric.

[9]It is unclear whether the wavefunction should be allowed to pass through grating B. On one hand, we know that the particle it represents (the C_{60} molecule) does not pass through due to its size. However, SQM treats every quantum particle as a mathematical point with no underlying size or structure. Thus, there is nothing in the mathematics of SQM to prevent the wavefunction from being diffracted by the grating. Because of this, we propose that according to SQM the wavefunction does, indeed, pass through grating B

Similarly, GG provide numerical simulations of the Bohmian trajectories for 100 C_{60} molecules (see figure 3.6). The particles went through either slit A or grating B (the particles were allowed to pass through grating B in spite of their size) and their initial positions were chosen randomly.[10][11] GG also ran the same simulations but did not allow the molecules to travel through the grating. The results are given in figure 3.7.

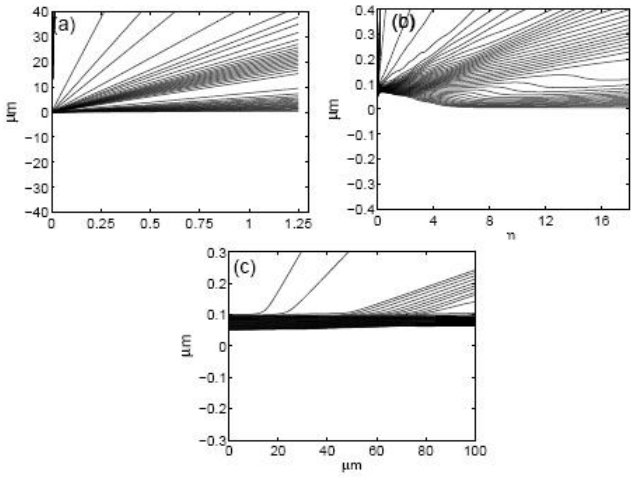

Figure 3.7: Bohmian trajectories through slit A only: (a) global view of trajectories, (b) magnification of the first millimeters, (c) magnification of the first hundred micrometers (taken from [29]).

It is seen that BM predicts an interference pattern with two peaks which is different from the predictions of SQM regardless of whether or not the wavefunction is allows to pass through the grating. In this way, GG have established an observable difference between the two theories. What is more, their experiment becomes increasingly realizable as our ability to manipulate the nanoworld improves.

in spite of the size of the particle. Consequently, SQM predicts the interference patterns of figures 3.5(b) and 3.5(c).

[10]It is not specified in what way the initial positions were chosen to be random. To be consistent with the QEH they should be distributed according to $|\Psi|^2_{t=0}$.

[11]Note the similarity between figure 3.5(c) and figure 3.6(b). This is expected on the grounds of the QEH – that BM and SQM predict the same statistical results for the same physical system. This is evidence that the simulations of GG are accurate.

3.2 Deriving the Classical World From BM

One of the first things an astute person will realize when learning quantum mechanics is that the quantum world looks nothing like the world in which we live. The waves which, according to the Copenhagen interpretation, represent every quantum system are, indeed, something we never notice in our everyday life. This is a big problem for quantum theory. If every object in the universe is ultimately made up of what we call "particles" and these "particles" are necessarily quantum systems which must be analyzed accordingly, then why do classical objects **never** exhibit any of the "waviness" of the particles of which they are made? Attempts have been made to bridge the gap between quantum and classical mechanics but this is somewhat of a malformed exercise to begin with because classical mechanics is a deterministic theory in which particles move along deterministic trajectories regardless of whether or not they are being measured[12]. On the other hand, according to SQM, particles do not follow trajectories through space and time and are not described by deterministic laws. They are described by probabilistic laws and the whole concept of a particle is not well-defined. Thus, it is difficult to see how one would even attempt to derive the deterministic world of classical mechanics from the probabilistic laws of SQM.

Problems such as these are nonexistent in BM. As we well know, the concept of the particle is central to BM. A Bohmian system is made up of particles which move through space and time along trajectories determined by the guidance condition, $\vec{p_i} = \nabla_i \Psi(\vec{x_1}, \ldots, \vec{x_i}, \ldots, \vec{x_N}, t)$, where $\vec{p_i}$ $(\vec{x_1}, \ldots, \vec{x_i}, \ldots, \vec{x_N}, t)$ is the momentum field of the i^{th} particle in the system described by the wavefunction, $\Psi(\vec{x_1}, \ldots, \vec{x_i}, \ldots, \vec{x_N}, t)$. Given a wavefunction, $\Psi(\vec{x_1}, \ldots, \vec{x_i}, \ldots, \vec{x_N}, t)$, the individual trajectory of particle i is completely determined by its initial position, $\vec{x_i} \mid_{t=0}$ for $1 \leq i \leq N$. Thus, the question of the classical limit becomes very straightforward to formulate in BM – when do the Bohmian trajectories of a classical object resemble those given by Newton's Laws? We will examine three papers in which this question is investigated. The first two give conditions which ensure that the

[12]Recall from Chapter 1 that the concept of measurement in quantum theory itself carries with it its own difficulties. We use the term here in a mainly Copenhagen sense, i.e. a particle is measured when it interacts with another system and from this interaction we are able to infer one or more of the dynamical properties of the particle. Questions such as whether the measurement reveals the pre-existing value of the property or not are unimportant for the present discussion so we will leave them unanswered.

center of mass of a macroscopic object obeys classical dynamics while the third is an attempt to join classical and quantum mechanics together into one overarching theory.

3.2.1 The COM Motion of Certain Macroscopic Quantum Systems

In a paper by Geiger, Obermair and Helm [18], hereafter referred to as GOH, the authors derive the conditions under which classical objects have the same trajectories under both Newtonian mechanics and BM. They characterize a classical object as being a collection of a large number (N $\sim 10^{23}$) of identical subsystems (i.e. atoms) each having center of mass coordinates $x_i(t)$ for $i \in \{1, \ldots, N\}$. The wavefunction is completely (anti)symmetric depending on whether the atoms are (fermionic) or bosonic and is given by

$$\begin{aligned}\Psi_{total}(x_1, \ldots, x_N, t) &= \sum_{\nu=1}^{N!} c_\nu \Psi(x_{\pi_\nu(1)}, \ldots, x_{\pi_\nu(N)}, t) \\ &\equiv \sum_{\nu=1}^{N!} c_\nu \Psi_\nu(x_1, \ldots, x_N, t)\end{aligned}$$

where $\{\pi_\nu | \nu \in \{1, \ldots, N!\}\}$ represents the set of all permutations of particle coordinates and $\{c_\nu\}$ is the set of corresponding coefficients which are chosen so as to preserve the appropriate symmetry of Ψ_{total}.

GOH then make two assumptions about the total system. They first assume that the motion of each subsystem is restricted to its own region of configuration space and that none of these regions overlap. This assumption is reasonable if the uncertainty in the center of mass position of each atom is much smaller than the distance between the center of mass coordinates of neighboring atoms. Mathematically, this means that every term in Ψ_{total}, each of which represents a particular permutation, is orthogonal to every other term, i.e. $\{\Psi_\nu\}$ is an orthogonal set and

$$\int dx_1 \ \ldots \ dx_N \, \Psi_\nu^*(x_1, \ldots, x_N, t) \Psi_{\bar{\nu}}(x_1, \ldots, x_N, t) = \delta_{\nu\bar{\nu}} \tag{3.30}$$

if each Ψ_ν is properly normalized. As a consequence, if the system particle[13] is represented by the term Ψ_μ at time t then it cannot be represented by a different term, Ψ_λ , $\lambda \neq \mu$, at a later time. Thus, all other terms in the wavefunction can be neglected when performing calculations (expectation values, etc.).

The second assumption GOH makes is that each term in Ψ_{total} is factorizable as follows:

$$\Psi_\mu(x_1, \ldots, x_N, t) = R_{\mu_1}(x_1, t) \cdots R_{\mu_N}(x_N, t) \exp\left[\frac{i}{\hbar} S_\mu(x_1, \ldots, x_N, t)\right]. \tag{3.31}$$

This condition is responsible for decoupling the trajectory of each subsystem from the quantum contribution of all of its partners. Indeed, from eqn. (3.31),

$$|\Psi(x_1, \ldots, x_N, t)| = |\Psi_1(x_1, t)| \cdots |\Psi_i(x_i, t)| \cdots |\Psi_N(x_N, t)| \tag{3.32}$$

and

$$Q(x_1, \ldots, x_N, t) = Q_1(x_1, t) + \cdots + Q_N(x_N, t). \tag{3.33}$$

Then from eqn. (3.33), the Bohmian trajectory of the center of mass of subsystem i is given by

$$m_i \ddot{x}_i = -\frac{\partial}{\partial x_i} V(x_1, \ldots, x_N, t)\Big|_{x(t)} - \frac{\partial}{\partial x_i} Q_i(x_i, t)\Big|_{x_i(t)}$$

and it is clearly seen that the center of mass motion of atom i is correlated to the other atoms only through the classical potential, $V(x_1, \ldots, x_N, t)$. Thus, the physical content of eqn. (3.31) is apparent – the quantum mechanical processes within each subsystem can only effect its own center of mass motion and not that of the others. In addition, if the system is composed of n different types of subsystem (i.e., different kinds of atoms) then eqn. (3.32) can be written

[13]By system particle we mean the point in configuration space which represents the collective positions of all particles in the system. For example, the system particle at time t is written $(x_1, \ldots, x_N)(t)$ and means that subsystem 1 is at position x_1 at time t, particle 2 is at position x_2 at time t and so on.

$$|\Psi(x_1,\ldots,x_N,t)| = \prod_{i=1}^{N} \left|\Psi^{a(i)}(x_i - \bar{x}_i(t),t)\right| \tag{3.34}$$

where each $a(i) \in \{1,\ldots,n\}$ refers to the set of subsystems of a certain type. Eqn. (3.34) is a consequence of the fact that the probability distributions, $|\Psi^{a(i)}(x,t)|^2$ of the Bohmian particles, x_i, around their mean values $\bar{x}_i$ are the same for identical subsystems (for each distinct value of $a(i)$).

GOH now consider the center of mass motion of the entire object. The center of mass is given by

$$x_{CM}(t) \equiv \frac{1}{M}\sum_{i=1}^{N} x_i(t) m_i \tag{3.35}$$

where M is the total mass of the object. Eqn. (3.35) is the average of the center of mass coordinates of the subsystems comprising the whole object. The Bohmian equation of motion for the COM coordinate given by eqn. (3.35) is

$$M\ddot{x}_{CM}(t) = -\sum_{i=1}^{N} \frac{\partial}{\partial x_i} V(x_1,\ldots,x_N,t)|_{x(t)} - \sum_{i=1}^{N} \frac{\partial}{\partial x_i} Q(x_1,\ldots,x_N,t)|_{x(t)}. \tag{3.36}$$

The classical contribution is a sum of external and internal forces:

$$-\sum_{i=1}^{N} \frac{\partial}{\partial x_i} V(x_1,\ldots,x_N,t)|_{x(t)} = \sum_{i,j,i\neq j}^{N} F_{ij} + \sum_{i=1}^{N} F_i^{ext} \equiv F^{ext}$$

where the sum of the internal forces, $\sum\limits_{i,j,i\neq j}^{N} F_{ij}$, cancels due to Newton's second law, $F_{ij} = -F_{ji}$.

Using eqn. (3.34) the quantum contribution becomes

$$-\sum_{i=1}^{N} \frac{\partial}{\partial x_i} Q(x_1,\ldots,x_N,t)|_{x(t)} = -\sum_{i=1}^{N} \frac{\partial}{\partial x_i} Q(x_i - \bar{x}_i(t),t)|_{x_i(t)}$$

where

$$Q(x_i - \bar{x}_i(t), t) \equiv -\frac{\hbar^2}{2m} \frac{\frac{\partial^2}{\partial x_i^2}|\Psi(x_i - \bar{x}_i(t), t)|}{|\Psi(x_i - \bar{x}_i(t), t)|}.$$

If N is large (as is the case for a classical object) and $n = 1$ (identical subsystems), the total quantum force on a single subsystem can be approximated by an integral. Using the QEH this integral is given by

$$\begin{aligned} F_Q^{CM} &\equiv -\frac{1}{N} \sum_{i=1}^{N} \frac{\partial}{\partial x_i} Q(x_i - \bar{x}_i(t), t)|_{x_i(t)} \\ &\approx -\int_{-\infty}^{\infty} du\, |\Psi(u - \bar{x}_i(t), t)|^2 \frac{\partial}{\partial u} Q(u - \bar{x}_i(t), t). \end{aligned}$$

This integral is shown to vanish [18] and the authors conclude that the effect of the quantum force on the center of mass of the classical object is smaller than $\frac{|F_{Q_{max}}|}{N}$ where $F_{Q_{max}}$ is the largest of the single-subsystem quantum forces in the object. Thus, the total quantum force on the object is bounded above as follows:

$$\left| \sum_{i=1}^{N} \frac{\partial}{\partial x_i} Q(x_1, \ldots, x_N, t) \right|_{x_1(t), \ldots, x_N(t)} \leq |F_{Q_{max}}|\,.$$

Since $|F_{Q_{max}}|$ is the largest force on a single subsystem, it is clearly not large enough to accelerate the classical object noticeably and the total force on the center of mass of the object is accurately approximated by

$$M\ddot{x}_{CM}(t) = F^{ext}$$

which is Newton's second law. The results also holds when $n \neq 1$ since the above argument remains true for each type of subsystem.

To summarize, GOH have shown that under the assumptions of locality, eqn. (3.30), and factorizability of the wavefunction, eqn. (3.31), the Bohmian motion of the center of mass of a classical object is essentially equal to its motion under Newton's second law. Note, however, that GOH examine only the motion of the center of mass of the object. The stability of matter is not explained by their analysis and is the subject of another discussion.

3.2.2 Another Derivation of the Classical World Using BM

In a paper by Allori, Dürr, Goldstein and Zanghi, hereafter referred to as ADGZ, the authors approach the problem of the classical limit in a different way [1]. They consider a classical object as being composed of N particles where $N \gg 1$ and examine the motion of the center of mass of the object (see eqns. (3.35) and (3.36)) as was done in GOH. Under the coordinate transformation, $(x_1, \ldots, x_N) \rightarrow (x, y_1, \ldots, y_{N-1})$ where x is the center of mass of the object, given by eqn. (3.35) and $\{y_i\}, i \in \{1, \ldots, (N-1)\}$ are a set of coordinates relative to x, the Schrödinger equation is

$$i\hbar \frac{\partial \Psi}{\partial t} = \left(H^{(x)} + H^{(y)} + H^{(x,y)}\right) \Psi$$

where $H^{(x)}$ is the free Hamiltonian for the center of mass coordinate, x, $H^{(y)}$ is the free Hamiltonian for the coordinates $\{y_i\}$ and $H^{(x,y)}$ describes the interaction between x and $\{y_i\}$. Thus,

$$H^{(x)} = \frac{\hbar^2}{2m}\nabla_x^2 + V(x), \qquad \text{where} \qquad V(x) \equiv \sum_{i=1}^{N} V_i(x)$$

and $H^{(y)}$ has a similar form. If each V_i varies slowly in relation to the size of the object, $H^{(x,y)}$ is small and can be neglected to first approximation. Then if $\Psi = \psi(x)\phi(y)$ at any time, t, the evolution of x decouples from the evolution of the $\{y_i\}$ and $\psi(x)$ evolves according to the single-particle Schrödinger equation

$$i\hbar \frac{\partial \psi}{\partial t} = \frac{\hbar^2}{2m}\nabla_x^2 \psi + V(x)\psi.$$

The center of mass follows the Bohmian trajectory given by

$$\frac{dx}{dt} = \frac{\hbar}{m} Im \left(\frac{\nabla_x \psi(x)}{\psi(x)}\right).$$

As in GOH, the classical limit is embodied in the condition that quantum effects play a negligible role in the dynamics of the center of mass of the object. When this is the case, eqn. (3.36) becomes

$$M\ddot{x}_{CM} \simeq F_{classical}.$$

ADGZ attack this problem in a very different manner than GOH. Instead of looking at the quantum contributions to the center of mass motion, they begin with the condition

$$\lambda \ll L \tag{3.37}$$

where λ is the de Broglie wavelength of the system and L is the scale of variation of the potential, V. ADGZ argue that this condition is both necessary and sufficient to ensure that the system behaves classically. Condition (3.37) is motivated by its similarity to how geometrical optics is obtained from wave optics. Also, (3.37) is regarded as equivalent to the condition

$$\hbar \ll A_0 \tag{3.38}$$

where A_0 is some characteristic action of the corresponding classical motion. (3.38) is commonly used as the condition to ensure classical behaviour. Hence, (3.37) seems reasonable and the goal is to find an expression for the scale of variation of the potential, L, in terms of known physical quantities.

The authors first examine the case where the wavefunction has a well-defined de Broglie wavelength. They consider a wavepacket of width σ and mean wave vector k. Such a wavepacket has a de Broglie wavelength of $\lambda = \frac{2\pi}{|k|}$. The mean particle position at time t is

$$\langle X \rangle = \int x |\Psi_t(x)|^2 \, dx$$

and

$$m \frac{d^2}{dt^2} \langle X \rangle = - \int \nabla_x V(x) |\Psi_t(x)|^2 \, dx.$$

Expanding the function $F(x) = -\nabla_x V(x)$ in a Taylor series around $\langle X \rangle$ gives

$$m \frac{d^2}{dt^2} \langle X \rangle = F(\langle X \rangle) + \frac{1}{2} \sum_{j,k} \Delta_{j,k} \frac{\partial^2 F}{\partial_{x_j} \partial_{x_k}} (\langle X \rangle) + \dots \tag{3.39}$$

where

$$\Delta_{j,k} = \langle X_j X_k \rangle - \langle X_j \rangle \langle X_k \rangle$$

is of order σ^2. Thus, neglecting terms of order higher than σ^2, in (3.39) the mean particle position will satisfy

$$m\frac{d^2}{dt^2}\langle X\rangle \approx F(\langle X\rangle)$$

when

$$\sigma^2\left|\frac{\partial^3 V}{\partial_{x_i}\partial_{x_j}\partial_{x_k}}\right| \ll \left|\frac{\partial V}{\partial_{x_i}}\right|,$$

i.e.,

$$\sigma \ll \sqrt{\left|\frac{V'}{V'''}\right|}, \tag{3.40}$$

where V' and V''' are suitable estimates on the first and third derivatives of V (for example, taking the supremums).

Since the minimum value of σ is of order λ, (3.40) can be written

$$\lambda \ll \sqrt{\left|\frac{V'}{V'''}\right|}. \tag{3.41}$$

This is a *necessary* condition to ensure classical behaviour of the system. In addition, eqn. (3.41) provides an expression for the scale of variation of the potential,

$$L = L(V) = \sqrt{\left|\frac{V'}{V'''}\right|}. \tag{3.42}$$

Now ADGZ proceed to argue that (3.37) with L defined by (3.42) is also a sufficient condition for classicality. For wavepackets such as the one examined above this is true because over a time period for which the spreading of the wavepacket can be neglected the large majority of the trajectories will remain close to their mean value. This is a consequence of the QEH. Thus, the majority of particle trajectories will be classical.

Next, ADGZ examine "local plane waves". Local plane waves have the property that their amplitude, $R(x)$, and local wave vector, $k(x) \equiv \nabla_x S(x)/\hbar$, vary slowly over distances of the order of the local de Broglie wavelength, $\lambda(x) \equiv h/|\nabla_x S(x)|$. Locally, they look like wavepackets and they can be

thought of as being composed of a sum of wavepackets.

Suppose we partition physical space into a union of disjoint sets, Δ_i in such a way that the value of the local wave vector, $k(x)$ is almost constant within each set. If we call these almost constant values k_i, then we have $k(x) \approx k_i$ for $x \in \Delta_i$. Let χ_{Δ_i} be the characteristic function on the set Δ_i (i.e., $\chi_{\Delta_i}(x) = 1$ if $x \in \Delta_i$ and $\chi_{\Delta_i}(x) = 0$ otherwise). Then we can expand the wavefunction as follows:

$$\psi(x) = \sum_i \chi_{\Delta_i}(x)\psi(x) = \sum_i \psi_i(x). \tag{3.43}$$

At any particular time, t, the system particle is in the support of one of the packets forming the sum in (3.43), say ψ_i. The minimum size of the packet depends on the size of the set Δ_i. Since $k(x)$ is almost constant in each Δ_i, Δ_i can be the size of many wavelengths down to a size of the order of λ_i.[14] Thus, the same argument used for wavepackets can be used here: the size of the packet, ψ_i, is taken to be of order $\lambda(x)$ and if eqn. (3.40) holds then we arrive at condition (3.41) for classical behaviour.

Now ADGZ investigate a general wavefunction. In this case the de Broglie wavelength may not be well-defined so an alternative is needed. Using the mean kinetic energy associated with a wavefunction, ψ,

$$E_{kin}(\psi) = \left\langle \psi, -\frac{\hbar^2}{2m}\nabla_x^2\psi \right\rangle, \tag{3.44}$$

an estimate of the wavelength is given by

$$\lambda = \lambda(x) = \frac{h}{\sqrt{2mE_{kin}(\psi)}}. \tag{3.45}$$

Now suppose that (3.41) is satisfied with λ as in (3.45). ADGZ show that under the evolution of the Schrödinger equation, ψ quickly becomes a local plane wave, and hence, evolves classically according to the previous discussion. They argue that if $\lambda \ll L(V)$, the kinetic energy dominates the potential energy so that the system approximately follows free Schrödinger evolution up until the time the potential significantly affects the motion. During this time the different wave vectors in ψ become spatially separated and a local plane wave is formed. Indeed, the free Schrödinger evolution is

[14] Here λ_i represents the almost-constant value of $\lambda(x)$ inside Δ_i.

given by

$$\psi_t(x) = \frac{1}{(2\pi)^{3/2}} \int \exp\left[it\left(\frac{kx}{t} - \frac{\hbar k^2}{2m}\right)\right] \hat{\psi}(k)\, dk$$

where $\hat{\psi}(k)$ is the Fourier transform of the initial wavefunction, $\psi_t(x)$. Using the stationary phase method, the long-time asymptotics of $\psi_t(x)$ is

$$\psi_t(x) \sim \left(\frac{im}{\hbar t}\right)^{\frac{3}{2}} \exp\left(i\frac{mx^2}{2\hbar t}\right)\hat{\psi}(k)$$

where $k = \frac{mx}{\hbar t}$. This is a local plane wave with local wave vector $k(x) = \frac{mx}{\hbar t}$.

The question now arises as to how quickly this local plane wave is produced. Consider a wavefunction composed of two overlapping wavepackets with the width, Δx, and with opposite momenta, p and $-p$. The time it takes for the packets to separate, τ, (i.e., the time for the formation of a local plane wave) is the time it takes for the packets to travel a distance of Δx. Using $\Delta x \Delta p \sim \hbar$ and $\Delta p \sim p$,

$$\tau \sim \frac{\Delta x}{p/m} \sim \frac{\hbar}{p^2/m} \sim \frac{\hbar}{\langle E \rangle} \tag{3.46}$$

where $\langle E \rangle$ is the mean energy of the particle. ADGZ then propose that (3.46) with $\langle E \rangle$ given by (3.44) could give a rough estimate of the time required for formation of a local plane wave for a general wavefunction. They point out that the time needed for the potential to produce significant effects is of order

$$T = \frac{L}{v} \qquad \text{where} \qquad v = \frac{h}{m\lambda}.$$

Thus, if $\lambda \ll L$ then $\tau \ll T$ and the local plane wave is formed on a time scale smaller than that required for the potential to have a significant effect on the dynamics. The time estimate, (3.46), although not necessarily very accurate, is at least consistent. In this way, ADGZ establish a condition, eqn. (3.41), to ensure the classical dynamics of the center of mass of a macroscopic object.

3.2.3 A Continuous Transition Between Quantum and Classical Mechanics

In a series of two papers, one by Partha Ghose [22] and the other by Ghose and Manoj Samal [23], hereafter referred to as GS, the authors attempt to join classical and quantum mechanics in one overarching theory. The usual approach is to try to derive classical mechanics as some sort of "classical limit" of the Schrödinger (or Pauli, etc.) equation. Many times this involves examining the condition $\hbar \to 0$, or in the case of BM one usually tries to find conditions which ensure quantum effects are negligible to the dynamics of a macroscopic object, (for instance, the two papers discussed above). In both cases, one starts with quantum mechanics and tries to turn it into classical mechanics. GS take a different approach and begin with the classical Hamilton-Jacobi equation

$$\frac{\partial S_{cl}(x,t)}{\partial t} + \frac{1}{2m}(\nabla S_{cl}(x,t))^2 + V(x) = 0 \tag{3.47}$$

and the equation of continuity

$$\frac{\partial R_{cl}^2(x,t)}{\partial t} + \nabla \cdot \left(R_{cl}^2(x,t)\frac{p}{m} \right) = 0 \tag{3.48}$$

where $S_{cl}(x,t)$ is the action function for a classical particle in a potential, $V(x)$, and $R_{cl}^2(x,t)$ is a position distribution function for the trajectories determined by $S_{cl}(x,t)$. The momentum of the particle is given by

$$p = m\frac{dx}{dt} \equiv \nabla S_{cl}(x,t). \tag{3.49}$$

GS then introduce the complex-valued wavefunction

$$\psi_{cl}(x,t) = R_{cl}(x,t)\exp\left(\frac{i}{\hbar}S_{cl}(x,t)\right). \tag{3.50}$$

In order that eqns.(3.47) and (3.48) remain valid with p defined by (3.49), $\psi_{cl}(x,t)$ must satisfy the equation

$$i\hbar\frac{\partial \psi_{cl}}{\partial t} = \left(\frac{\hbar^2}{2m}\nabla^2 + V(x)\right)\psi_{cl} - Q_{cl}\psi_{cl} \tag{3.51}$$

where

$$Q_{cl} = -\frac{\hbar^2}{2m}\frac{\nabla^2 R_{cl}}{R_{cl}}. \tag{3.52}$$

Eqn. (3.51) is the Schrödinger equation with the additional term, (3.52), on the right-hand side. It is very interesting that a particle can behave classically while being described by the wavefunction (3.50) and eqn. (3.51) since (3.51) contains the parameter $\hbar$. The last term in (3.51) is nonlinear in $|\psi_{cl}|$ and cancels all quantum effects exactly to produce classical particle trajectories.

Note the similarities between the above classical equations and the corresponding equations in BM. Specifically, one gets BM if the quantum potential term, $Q = \frac{\hbar^2}{2m}\frac{\nabla^2 R}{R^2}$ is added to eqn. (3.47) and all classical quantities (R_{cl}, S_{cl}, etc.) are replaced by their quantum counterparts, (R, S, etc.). Similarly, the classical wave equation, eqn. (3.51), is Schrödinger's equation with the additional term, $-Q_{cl}\psi_{cl}$, on the right-hand side. Making use of this observation, GS propose the following equation:

$$i\hbar\frac{\partial\psi}{\partial t} = \left(\frac{\hbar^2}{2m}\nabla^2 + V(x) - \lambda(t)Q_{cl}\right)\psi \tag{3.53}$$

with Q_{cl} defined by (3.52). $\lambda(t) = 1$ corresponds to classical mechanics and $\lambda(t) = 0$ corresponds to BM while $0 < \lambda < 1$ represents some sort of mixture of the two. GS refer to this mixture as a *mesoscopic* system. A prudent choice of the function $\lambda(t)$ then provides a model in which the system begins as a completely quantum system ($\lambda(0) = 0$) and can be continuously transformed into a completely classical system over a time period of Δt ($\lambda(\Delta t) = 1$).

To find a reasonable form for $\lambda(t)$ it is instructive to look at the conventional view on decoherence, environmental-induced decoherence, (EID). According to EID, a quantum system interacting with its environment is described by the Schrödinger equation

$$i\hbar\frac{\partial\psi}{\partial t} = \left(-\frac{\hbar^2}{2m}\nabla^2 + V(x) + W\right)\psi$$

where W is the operator representing the effects of the environment. If the environment interactions are complex, such as for a heat bath, the density matrix quickly becomes diagonal in the position representation. Specifically, for a heat bath of temperature T, the density matrix is governed by the equation

$$\frac{d\rho}{dt} = -\frac{i}{\hbar}[H,\rho] - \gamma(x-x')(\partial_x - \partial_{x'})\rho - \frac{\rho}{\tau_D}$$

where γ is the relaxation time and

$$\tau_D = h^2/2m\gamma k_B T(x-x') \tag{3.54}$$

is the decoherence time scale. Although the system decoheres in the position representation, it does not in other representations (for instance, in the momentum representation). Thus, the above theory of decoherence does not produce true decoherence and true classical behaviour. The reason for this is the linearity of the Schrödinger equation. A linear equation cannot describe the process of decoherence and it is precisely the non-linear term, (3.52), that is responsible for the decoherence of the system in eqn. (3.51).

Making use of eqn. (3.54) GS propose $\lambda(t) = 1 - e^{-bt}$ with $b = 1/\tau_D$ and τ_D given by eqn. (3.54) as a possible form for the function $\lambda(t)$.[15] Using this form of $\lambda(t)$, a macroscopic system in an high-temperature environment would very quickly decohere and behave classically. However, certain systems could exist in a mesoscopic state for long times under appropriate temperatures.

In this way, GS provide a model which describes both classical and quantum mechanics in a single wave equation. It also provides a straightforward way of looking at quantum decoherence and contains the tools for examining a new state of matter, the mesoscopic state, which is described by a mixture of classical and quantum dynamics. However, their theory only works within the context of BM where the concept of a particle trajectory is well-defined. In addition, the entire mathematical framework is based on the Hamilton-Jacobi equation which has a quantum counterpart only in BM.

To close this section, we provide trajectories for a quantum harmonic oscillator as predicted by eqn. (3.53). These are taken from [23] in which trajectories are provided for three systems – stationary states of the classical harmonic oscillator, a one-dimensional free wavepacket and the wavepacket solution of the quantum harmonic oscillator. The trajectories for the quantum oscillator are given in figure 3.8. They are seen to continuously change

[15] The authors point out that there are many continuous functions that satisfy $\lambda(0) = 1$ and $\lambda(t_0) = 0$ for some t_0. This is indicative of the fact that there are many ways a system can decohere. For instance, a different environment would likely cause a given system to decohere in a different way.

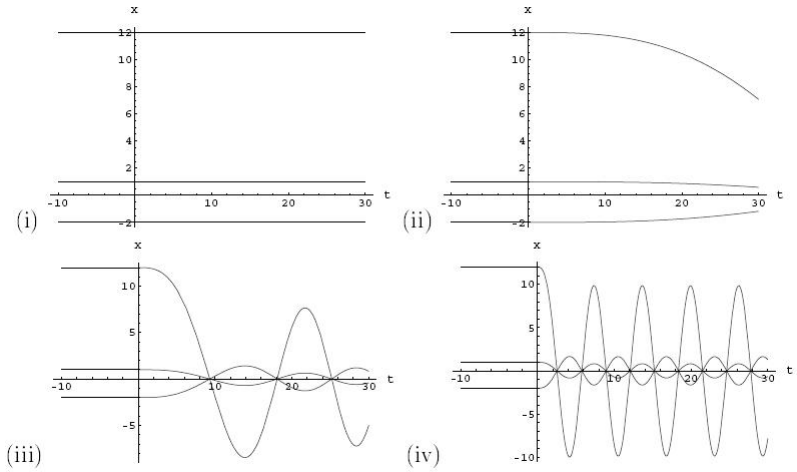

Figure 3.8: x vs. t for the quantum oscillator for (i) $b = 0$, (ii) $b = 0.0001$, (iii) $b = 0.01$ and (iv) $b = 0.7$ (taken from [23]).

from completely quantum mechanical to completely classical as λ is increased from 0 to 1. This gives a picture of a mesoscopic system in action – the trajectories are "between" classical and quantum while $0 < \lambda < 1$. The above plots are for four different values of the parameter b where $\lambda(t) = 1 - e^{-bt}$.

Chapter 4

A Warm-up – The Hydrogen Atom

The hydrogen atom is one of the standard examples of a system for which the wavefunction is easily solved and well-known. As such, it is a natural candidate to which to apply Bohmian mechanics and to determine particle trajectories. In recent years Colijn has done an in-depth Bohmian analysis of the hydrogen atom [11]. We will outline her procedure for examining the hydrogen atom evolving in time under the non-relativistic Schrödinger equation.[1] This will provide a good warm-up for the remaining chapters in which we investigate some Bohmian trajectories associated with the helium atom. We will see that *Colijn's* representation of the wavefunction of the hydrogen atom leads very naturally to a similar representation of the wavefunction of the helium atom.

4.1 The Model

This model is that used in [11]. As in standard treatments of the hydrogen atom, we take the nucleus to be infinitely heavy and stationary in space.[2] Thus, the model consists of a lone electron which is electrically attracted

[1] Colijn also analyzed the hydrogen atom using the Pauli equation and Dirac equation, but we will not be concerned with these procedures or results (see [13] for these results).

[2] This is a reasonable approximation since the mass of the nucleus is nearly 2000 times the mass of the electron. Thus, during the time in which the electron moves a reasonable distance the nucleus is nearly stationary due to conservation of linear momentum.

to a stationary proton. When this approximation is made, one neglects the parts of the wavefunction corresponding to the nucleus and approximates the wavefunction of the atom as the wavefunction of the electron. We situate the nucleus at the origin of our coordinate system and the general wavefunction of the electron is a linear combination of energy eigenstates:

$$\Psi_{hyd}(\vec{r},t) = \sum_{n=1}^{\infty} \sum_{l=0}^{l<n} \sum_{m=-l}^{m=l} c_{n,l,m}(t)\Phi_{n,l,m}(\vec{r}), \tag{4.1}$$

where $\Phi_{n,l,m}(\vec{r})$ is an energy eigenfunction with quantum numbers n (principle quantum number), l (orbital angular momentum quantum number) and m (spin angular momentum quantum number) and the $c_{n,l,m}(t)$ are constants that depend only on time. $\Phi_{n,l,m}(\vec{r})$ is a simultaneous eigenfunction of the Hamiltonian, $\hat{H}_{hyd}$ with eigenvalue $E_n^{(0)}$, the total angular momentum operator, $\hat{L}^2$ with eigenvalue $l(l+1)\hbar^2$ and the orbital angular momentum (or spin) operator in the z-direction, $\hat{L}_z$ with eigenvalue $m\hbar$. The Hamiltonian, $\hat{H}_{hyd}$ is given by

$$\hat{H}_{hyd} = -\frac{\hbar^2}{2m_e}\nabla^2 - \frac{Ze^2}{r},$$

where m_e is the mass of the electron, Z is the nuclear charge ($Z = 1$ for hydrogen), e is the electronic charge and r is the distance from the electron to the nucleus. The form of the operators $\hat{L}^2$ and $\hat{L}_z$ is unimportant. The eigenfunctions are most easily given in spherical coordinates as

$$\Phi_{n,l,m}(r,\theta,\phi) = R_{n,l}(r)Y_l^m(\theta,\phi), \tag{4.2}$$

where the $\{R_{n,l}\}$ are radial eigenfunctions and the $\{Y_l^m\}$ are angular eigenfunctions. We use θ to specify the polar angle and ϕ to specify the azimuthal angle (cf. figure 4.1). The radial eigenfunctions are given by

$$R_{n,l}(r) = -\left\{\left(\frac{2Z}{na_0}\right)^3 \frac{(n-l-1)!}{2n[(n+l)!]^3}\right\}^{\frac{1}{2}} e^{-\frac{\rho}{2}}\rho^l \mathcal{L}_{n+l}^{2l+1}(\rho), \tag{4.3}$$

where Z is the nuclear charge, $a_0 = \frac{4\pi\epsilon_0\hbar^2}{m_e e^2}$ is the Bohr radius, $\rho = \frac{2Zr}{na_0}$ and $\mathcal{L}_a^b$ is the associated Laguerre polynomial of degree a and order $0 \leq b \leq a$. The angular eigenfunctions are given by

$$Y_l^m(\theta,\phi) = (-1)^m \left[\frac{(2l+1)(l-m)!}{4\pi(l+m)!}\right]^{\frac{1}{2}} \mathcal{P}_l^m(cos\theta)e^{im\phi}, \tag{4.4}$$

where $\mathcal{P}_a^b$ is the associated Legendre polynomial of degree a and order $|b| \leq a$.

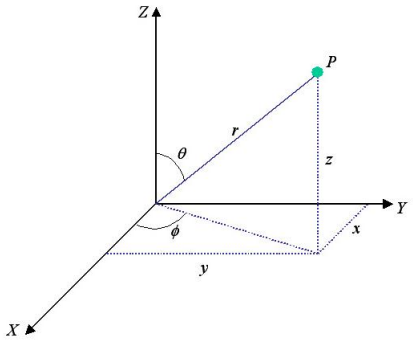

Figure 4.1: Our convention for spherical coordinates, (r, θ, ϕ).

Substituting the wavefunction, (4.1), into the Schrödinger equation yields

$$i\hbar\frac{\partial\Psi_{hyd}(\vec{r},t)}{\partial t} = \hat{H}_{hyd}\Psi_{hyd}(\vec{r},t),$$

where $\hat{H}_{hyd}$ is the Hamiltonian for the hydrogen atom. Evaluating the right-hand-side we see that

$$\begin{aligned}\hat{H}_{hyd}\Psi_{hyd} &= \hat{H}_{hyd}\sum_{n=1}^{\infty}\sum_{l=0}^{l<n}\sum_{m=-l}^{m=l} c_{n,l,m}(t)\Phi_{n,l,m}(\vec{r}) \\ &= \sum_{n=1}^{\infty}\sum_{l=0}^{l<n}\sum_{m=-l}^{m=l} E_n^{(0)}c_{n,l,m}(t)\Phi_{n,l,m}(\vec{r})\end{aligned}$$

because each $\Phi_{n,l,m}(\vec{r})$ is an eigenfunction of $\hat{H}_{hyd}$ with eigenvalue $E_n^{(0)}$.

Evaluating the left-hand-side we see that

$$\frac{\partial\Psi_{hyd}}{\partial t} = \sum_{n=1}^{\infty}\sum_{l=0}^{l<n}\sum_{m=-l}^{m=l}\Phi_{n,l,m}(\vec{r})\frac{\partial c_{n,l,m}(t)}{\partial t}$$

because the time-dependence of the wavefunction is contained entirely in the coefficients, $c_{n,l,m}(t)$. Thus, the Schrödinger equation can be simplified to

$$i\hbar \sum_{n=1}^{\infty} \sum_{l=0}^{l<n} \sum_{m=-l}^{m=l} \Phi_{n,l,m}(\vec{r}) \frac{\partial c_{n,l,m}(t)}{\partial t} = \sum_{n=1}^{\infty} \sum_{l=0}^{l<n} \sum_{m=-l}^{m=l} E_n^{(0)} c_{n,l,m}(t) \Phi_{n,l,m}(\vec{r}). \tag{4.5}$$

To solve for the $\{c_{n,l,m}(t)\}$ we make use of the orthonormality of the hydrogenic eigenfunctions, given by

$$\int_0^{\infty} \int_0^{2\pi} \int_0^{\pi} \Phi^*_{n',l',m'}(r,\theta,\phi) \Phi_{n,l,m}(r,\theta,\phi)\, dr\, d\theta\, d\phi = \delta_{n,n'} \delta_{l,l'} \delta_{m,m'}, \tag{4.6}$$

where $\delta_{a,b}$ is the Kronecker delta. Multiplying (4.5) by $\Phi^*_{n',l',m'}$, integrating over all space and using (4.6) gives

$$i\hbar \frac{\partial c_{n',l',m'}(t)}{\partial t} = E^{(0)}_{n'} c_{n',l',m'}(t) \tag{4.7}$$

and this is true for each $n^{'}$, $l^{'}$ and $m^{'}$. Eqn. (4.7) has solution

$$c_{n',l',m'}(t) = \exp\left(\frac{-iE^{(0)}_{n'}t}{\hbar}\right)$$

and using this the wavefunction becomes

$$\Psi_{hyd}(\vec{r},t) = \sum_{n=1}^{\infty} \sum_{l=0}^{l<n} \sum_{m=-l}^{m=l} \Phi_{n,l,m}(\vec{r}) \exp\left(\frac{-iE_n^{(0)}t}{\hbar}\right). \tag{4.8}$$

where $\Phi_{n,l,m}(\vec{r})$ is given by (4.2). (4.3) and (4.4). Thus, each $c_{n,l,m}(t)$ is independent of each of the others under the evolution of the Schrödinger equation. We will see in the next section that is not true for the wavefunction of the helium atom.

4.2 Results

Colijn first examines the Bohmian trajectories associated with eigenstates of $\hat{H}_{hyd}$. For all eigenstates with $m = 0$ the wavefunction is real because the

associated Laguerre polynomials and associated Legendre polynomials of all degrees and orders are real. Thus, the phase, S, is zero and consequently the first term in the guidance condition, eqn. (2.15), is zero (cf. footnote 6 in Chapter 2). This is a very interesting result for it says that by neglecting the effects of spin, the ground state electron in the hydrogen atom is stationary. Bohm knew of this when he first published his theory[3] and used the result as evidence that his theory was correct [5, 6]. According to him, it gave an explanation for why the electron in the hydrogen atom did not fall into the nucleus – the quantum potential acting on the electron is such as to completely balance the electrical attraction exerted by the nucleus, thus canceling the motion of the electron exactly.

Since $\nabla S = \vec{0}$ (and $\vec{A}$, the electromagnetic vector potential, is zero because we are dealing with a free hydrogen atom) any motion of the electron is due solely to the spin-dependent part of eqn. (2.15). Colijn analyzed hydrogen atoms for which the electron has a constant spin vector which points in the z-direction, $\vec{s} = \frac{\hbar}{2}\hat{k}$. For the real eigenstates considered by Colijn, it is easy to show that the spin-dependent term of (2.15), $\nabla\rho \times \vec{s}$, produces motion only in the ϕ-direction, i.e., circular orbits around the z-axis [11]. From the definition of the cross product the momentum associated with this term is orthogonal to both $\nabla\rho$ and $\vec{s}$. Since $\vec{s}$ points in the z-direction, the momentum lies in planes of constant z. This is true for *all wavefunctions*. Note that the directions orthogonal to $\nabla\rho$ are along level sets of ρ. For the $1s$ and $2s$ states (respective quantum numbers $(1,0,0)$ and $(2,0,0)$,) the wavefunction depends only on r and therefore the level sets of ρ are spheres centered at the origin. Thus, the trajectories are constrained to lie on the intersection of these spheres with planes of constant z, which, of course, are circles around the z-axis. For the $2p_0$ state (quantum numbers $(2,1,0)$), ρ is given by

$$\rho_{2,1,0} = |\Psi_{2,1,0}|^2 = \frac{1}{32\pi a^5} e^{-r/a} (r\cos\theta)^2, \tag{4.9}$$

where $a = \hbar^2/(m_e e^2)$ is the Bohr radius. Setting $z = r\cos\theta = C$ where C is a constant and $\rho = \textit{constant}$ and using (4.9) leads to the condition

[3]Actually when Bohm published his two seminal papers in 1952 the spin-dependent term of the guidance condition had not yet been derived. The guidance condition was originally given as $\vec{p} = \nabla S$ and so according to Bohm the ground state electron was permanently stationary until an external force caused it to move (see [5]).

$$\frac{C}{32\pi a^5} e^{-r/a} = constant. \tag{4.10}$$

Eqn. (4.10) has solution $r = constant$, which when coupled with the condition $z = constant$ yields circular trajectories around the z-axis.

Colijn also examines the eigenstates with quantum numbers $(2, 1, -1)$ and $(2, 1, 1)$. In these cases the phases of the wavefunction are non-zero and are given by $S = \pm\hbar\phi$ where the "+" corresponds to the quantum number $m = 1$ and the "−" corresponds to the quantum number $m = -1$. Thus, the first term of eqn. (2.15) has a non-zero component in the ϕ-direction equal to $\pm\phi$. Since ϕ is the polar angle this corresponds to circular motion around the z-axis. As for the $m = 0$ case, the spin-dependent term of (2.15) again yields circular motion about the z-axis.[4] Thus, the total motion for the $(2, 1, 1)$ and $(2, 1, -1)$ eigenstates are circles around the z-axis.

It is natural to assume that the trajectories for the $m = 1$ and $m = -1$ states are the same except that the direction of motion changes. Indeed, the spin-independent term, $\nabla S = \pm\phi\hat{e}_\phi$ changes sign when the sign of m is changed but the spin-dependent term, $\frac{\nabla\rho\times\vec{s}}{\rho}$, does not. This is because ρ is independent of m and this is true for any values of the quantum numbers n and l. In order to obtain the result that the trajectories reverse direction when the sign of m is changed one must also change the sign of $\vec{s}$ (which amounts to changing the direction of $\vec{s}$ by π radians). This is a reasonable result since one normally associates a state with a positive value of m with a spin "up" state and a state with a negative value of m with a spin "down" state.

The last states we wish to discuss are the real-valued $2p_x$ and $2p_y$ states, given by

$$\Psi_{2p_x} = \frac{1}{\sqrt{32\pi a^5}} r e^{-r/2a} \sin\theta\cos\phi$$
$$\Psi_{2p_y} = \frac{1}{\sqrt{32\pi a^5}} r e^{-r/2a} \sin\theta\sin\phi$$

of which each is formed from appropriate linear combinations of the wavefunctions associated with the $(2, 1, 1)$ and $(2, 1, -1)$ states. These are eigenstates

[4]We refer the reader to [11] for proof of this. The calculations are not difficult and are similar to those used to analyze the $(2, 1, 0)$ state.

of the Hamiltonian, $\hat{H}_{hyd}$, and $\hat{L}^2$ but not of $\hat{L}_z$. Since the wavefunctions are real, $S = 0$ and there is no motion associated with the spin-independent term, ∇S. The spin-dependent term has components in all three directions and the motion is given by the set of three coupled DEs,

$$\begin{aligned}
\frac{dr}{dt} &= -\frac{\hbar}{mr}\tan\phi \\
\frac{d\theta}{dt} &= -\frac{\hbar}{mr^2}\cot\theta\tan\phi \\
\frac{d\phi}{dt} &= -\frac{\hbar}{mr^2}\left(1 - \frac{r}{2a} + \cot^2\theta\right).
\end{aligned} \tag{4.11}$$

Colijn solves the system (4.11) numerically and obtains the trajectories shown in figure 4.2. Notice the similarity between these trajectories and the plots of $|\Psi|^2$ for the $2p_x$ wavefunction in figures 4.2 and 4.3.[5] The first figure in 4.3 shows the shape of the orbital and the second shows slices through some contour curves of $|\Psi|^2$. Recall that the motion of the electron in the $2p_x$ state is due entirely to the spin-dependent term. Thus, the trajectories lie along the level sets of $|\Psi|^2$ which is precisely what we see in figure 4.2. The similarity of the Bohmian trajectories with the orbitals is evidence in favor of the consistency of BM with SQM.

It is easy to show that the Bohmian trajectories of any hydrogenic eigenstate have non-zero components only in the ϕ-direction and thus, are circular orbits around the z-axis. This is due to the fact that the eigenfunctions have the form

$$\Phi_{n,l,m}(r,\theta,\phi) = F(r,\theta)e^{-im\phi}$$

where $F(r,\theta)$ is a real function. Thus, the ∇S term has a non-zero component only in the ϕ-direction. Similarly, the spin-dependent term produces motion only in the ϕ-direction for all eigenstates. This is because $\rho_{n,l,m} = |\Phi_{n,l,m}|^2$ has no ϕ-dependence. Thus, $\nabla\rho_{n,l,m}$ has a ϕ-component equal to zero. Since the ϕ-component of $\vec{s}$ is also equal to zero, $\nabla\rho \times \vec{s}$ has a non-zero component only in the ϕ-direction. Thus, the total momentum is non-zero only in the ϕ-direction and consequently all trajectories are circular orbits around the z-axis.

[5]The diagrams in figure 4.3 were taken from the website http://csi.chemie.tu-darmstadt.de/ak/immel.

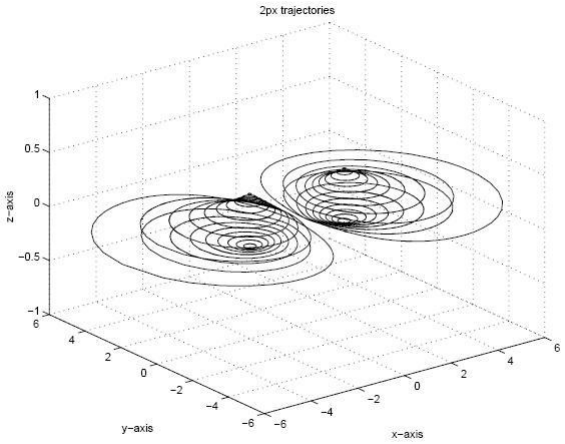

Figure 4.2: The Bohmian trajectories of a hydrogenic electron in the $2p_x$ state for a number of initial particle positions (taken from [11]).

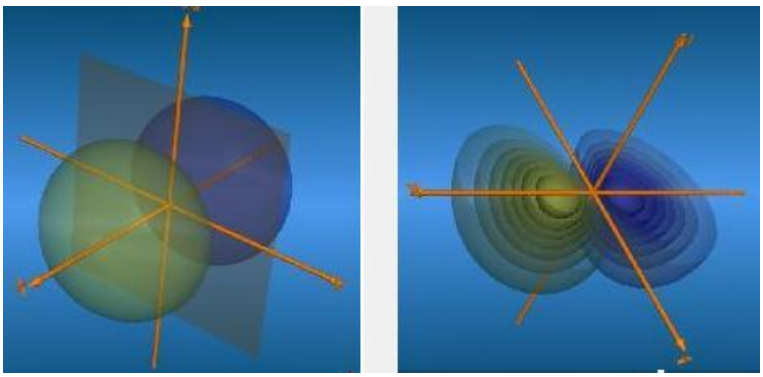

Figure 4.3: 3-D Plots of the $2p_x$ orbital. The first figure shows the shape of the orbitals while the second shows slices of constant probability.

Chapter 5

The Helium Atom

5.1 The Model

The helium atom is the simplest many-body quantum system.[1] It consists of two electrons which orbit a nucleus containing two protons and two neutrons. The neutrons are electrically neutral and for our purposes can be considered to contribute nothing to the overall dynamics of the atom. As was done for the hydrogen atom, we will approximate the nucleus to be infinitely heavy. Due to conservation of linear momentum the nucleus can then be approximated as being stationary over the course of any simulation we wish to run. Using these approximations, the Hamiltonian of the helium atom is

$$\hat{H}_{hel} = -\frac{\hbar^2}{2m_e}\nabla_1^2 - \frac{\hbar^2}{2m_e}\nabla_2^2 - \frac{Ze^2}{r_1} - \frac{Ze^2}{r_2} + \frac{e^2}{r_{12}} \tag{5.1}$$

where r_1 is the distance from electron 1 to the nucleus, r_2 is the distance from electron 2 to the nucleus and r_{12} is the distance between the two electrons. The Schrödinger equation for this Hamiltonian is not exactly solvable so approximations must be made. We will use a perturbation approach in which the $\frac{1}{r_{12}}$ term is assumed to be small enough to be treated as a perturbation. In effect, we write

$$\hat{H}_{hel} = \hat{H}_0 + \hat{H}_1 \tag{5.2}$$

[1]For our purposes, we are considering an atom to be described by the motion of its electrons around a stationary, infinitely heavy nucleus. Thus, we consider the hydrogen atom to be a single-body system.

where

$$\hat{H}_0 = -\frac{\hbar^2}{2m_e}\nabla_1^2 - \frac{\hbar^2}{2m_e}\nabla_2^2 - \frac{Ze^2}{r_1} - \frac{Ze^2}{r_2} \tag{5.3}$$

is the Hamiltonian for two independent (i.e. non-interacting) hydrogenic electrons and

$$\hat{H}_1 = \frac{e^2}{r_{12}} \tag{5.4}$$

represents the interaction between the electrons and is the perturbation. Thus, the Schrödinger equation for helium is

$$i\hbar\frac{\partial\Psi_{hel}}{\partial t} = \hat{H}_{hel}\Psi_{hel} = (\hat{H}_0 + \hat{H}_1)\Psi_{hel}. \tag{5.5}$$

As we saw in the previous chapter, the Schrödinger equation for the free hydrogen atom admits a spectrum of eigenfunctions according to the eigenvalue equation

$$\hat{H}_{hyd}\Phi_{n,l,m} = E_n^{(0)}\Phi_{n,l,m} \qquad \text{for } n \in N \tag{5.6}$$

where $\Phi_{n,l,m} = R_{n,l}Y_l^m$ and $E_n^{(0)}$ are the energy eigenvalues. The solution to the free hydrogenic Schrödinger equation can be written as (cf. eqn. (4.8))

$$\Psi_{hyd} = \sum_{n=1}^{\infty}\Phi_{n,l,m}\exp\left(\frac{-iE_n^{(0)}t}{\hbar}\right). \tag{5.7}$$

The Schrödinger equation for $\hat{H}_0$,

$$i\hbar\frac{\partial\Psi_0}{\partial t} = \hat{H}_0\Psi_0 \tag{5.8}$$

has an exact solution which is nothing more than the tensor product of two hydrogenic eigenfunctions according to the eigenvalue equation

$$\hat{H}_0\Phi_{n_i,l_i,m_i}(r_1,\theta_1,\phi_1)\Phi_{n_j,l_j,m_j}(r_2,\theta_2,\phi_2) = \left(E_{n_i}^{(0)} + E_{n_j}^{(0)}\right)\Phi_{n_i,l_i,m_i}(r_1,\theta_1,\phi_1)\Phi_{n_j,l_j,m_j}(r_2,\theta_2,\phi_2) \tag{5.9}$$

where (r_1, θ_1, ϕ_1) are the spherical coordinates of electron 1 and (r_2, θ_2, ϕ_2) are the spherical coordinates of electron 2. The time-dependent solution of (5.8) is then

$$\Psi_0 = \sum_{i=1}^{\infty} \sum_{j=1}^{\infty} \exp\left(\frac{-i\left(E_{n_i}^{(0)} + E_{n_j}^{(0)}\right) t}{\hbar} \right) \Phi_i(\vec{r}_1)\Phi_j(\vec{r}_2) \tag{5.10}$$

where the subscripts i and j refer respectively to the quantum number triplets (n_i, l_i, m_i) and (n_j, l_j, m_j).

In order to take account of the perturbation term in the Hamiltonian, we write Ψ_{hel} in the same form as Ψ_0 except that we allow arbitrary time-dependence. In effect, we write the solution of (5.5) as

$$\Psi_{hel}(r_1, \theta_1, \phi_1, r_2, \theta_2, \phi_2, t) = \sum_{i=1}^{\infty} \sum_{j=1}^{\infty} c_{ij}(t) \Phi_i(r_1, \theta_1, \phi_1) \Phi_j(r_2, \theta_2, \phi_2) \tag{5.11}$$

where each c_{ij} is an arbitrary function of the time, t.

Thus, the Schrödinger equation becomes

$$\begin{aligned} i\hbar \sum_{i=1}^{\infty} \sum_{j=1}^{\infty} \frac{dc_{ij}(t)}{dt} \Phi_i(\vec{r}_1)\Phi_j(\vec{r}_2) = & \sum_{i=1}^{\infty} \sum_{j=1}^{\infty} c_{ij}(t) \left(E_i^{(0)} + E_j^{(0)}\right) \Phi_i(\vec{r}_1)\Phi_j(\vec{r}_2) \\ & + e^2 \sum_{i=1}^{\infty} \sum_{j=1}^{\infty} c_{ij}(t) \frac{1}{r_{12}} \Phi_i(\vec{r}_1)\Phi_j(\vec{r}_2). \end{aligned} \tag{5.12}$$

To find the $\{c_{ij}(t)\}$ we use the same technique as was used for the hydrogen atom in the previous chapter. Multiplying both sides of this equation by $\Phi_g(\vec{r}_1)\Phi_h(\vec{r}_2)$, integrating over all space[2] and using the orthonormality of the hydrogenic eigenfunctions (cf. eqn. (4.6)) eqn. (5.12) becomes

[2]Note that "all space" refers to the coordinate space of both electrons, i.e., we integrate over $\Re^3$ twice.

$$i\hbar\frac{dc_{gh}(t)}{dt} = c_{gh}(t)\left(E_g^{(0)} + E_h^{(0)}\right) + \sum_{i=1}^{\infty}\sum_{j=1}^{\infty} e^2 c_{ij}(t)\int_{\Re^3}\int_{\Re^3}\Phi_g(\vec{r}_1)\Phi_h(\vec{r}_2)\frac{1}{r_{12}}\Phi_i(\vec{r}_1)\Phi_j(\vec{r}_2)\,d^3\tau_1\,d^3\tau_2 \quad (5.13)$$

where $d^3\tau_1$ is an element of volume in the coordinate space of electron 1 and $d^3\tau_2$ is an element of volume in the coordinate space of electron 2.

This can be written as the matrix equation

$$i\hbar\frac{dC(t)}{dt} = EC(t) + RC(t)$$

where $C(t)$ is the infinite-dimensional column vector

$$C(t) = \begin{pmatrix} c_{11}(t) \\ \vdots \\ c_{1n}(t) \\ \vdots \\ c_{21}(t) \\ \vdots \\ c_{nn}(t) \\ \vdots \end{pmatrix},$$

E is the infinite-dimensional square matrix

$$E = \begin{pmatrix} E_{11}^{(0)} & 0 & 0 & & & \dots & & 0 & \dots \\ 0 & E_{12}^{(0)} & 0 & \ddots & & & 0 & 0 & 0 \\ 0 & 0 & \ddots & 0 & & & 0 & 0 & \\ & \ddots & 0 & E_{1n}^{(0)} & 0 & & & & \ddots \\ & & & 0 & \ddots & 0 & & & \\ \vdots & & & & 0 & E_{21}^{(0)} & 0 & \ddots & \\ & 0 & 0 & & & 0 & \ddots & 0 & \\ 0 & 0 & 0 & & & \ddots & 0 & E_{nn}^{(0)} & \ddots \\ \vdots & 0 & & \ddots & & & & \ddots & \ddots \end{pmatrix},$$

and

$$R = \begin{pmatrix} R_{11,11} & \dots & R_{11,1n} & \dots & R_{11,21} & \dots & R_{11,nn} & \dots \\ \vdots & \ddots & & & & & & \\ R_{1n,11} & & R_{1n,1n} & \ddots & & & \ddots & \\ \vdots & & \ddots & \ddots & \ddots & & & \ddots \\ R_{12,11} & & & \ddots & \ddots & \ddots & & \\ \vdots & \ddots & & & \ddots & \ddots & & \\ R_{nn,11} & & & & & \ddots & R_{nn,nn} & \\ \vdots & & & \ddots & & & & \ddots \end{pmatrix}.$$

where $E_{ij}^{(0)} = E_i^{(0)} + E_j^{(0)}$ and

$$\begin{aligned} R_{gh,ij} &= \int_{\Re^3}\int_{\Re^3} \Phi_g \Phi_h \frac{e^2}{r_{12}} \Phi_i \Phi_j \, d^3\vec{r}_1 \, d^3\vec{r}_2 \\ &= \left\langle \Phi_g(\vec{r_1})\Phi_h(\vec{r_2}) \left| \frac{e^2}{r_{12}} \right| \Phi_i(\vec{r_1})\Phi_j(\vec{r_2}) \right\rangle \end{aligned} \tag{5.14}$$

The vector C contains all the time-dependent coefficients, $c_{ij}(t)$ for $i, j \in N$, the matrix E represents the contribution of $\hat{H}_0$ and the matrix R represents the contribution of the perturbation,[3] $\hat{H}_1$. Note that the matrix E is diagonal and maintains the independence of each $c_{ij}(t)$ while the matrix R is non-diagonal and is responsible for breaking this independence and coupling each $c_{ij}(t)$ to the others.

In order that we only have to deal with real-valued functions, we will separate the coefficients into real and imaginary parts, i.e., $c_{ij}(t) = a_{ij}(t) + ib_{ij}(t)$. Eqn. (5.13) then becomes the two equations

$$\frac{da_{gh}(t)}{dt} = \frac{E^{(0)}_{gh}}{\hbar} b_{gh}(t) + \frac{1}{\hbar} \sum_{i=1}^{\infty} \sum_{j=1}^{\infty} b_{ij}(t) R_{gh,ij}, \qquad \text{for } 1 \leq i, j, < \infty, \quad (5.15)$$

$$\frac{db_{gh}(t)}{dt} = -\frac{E^{(0)}_{gh}}{\hbar} a_{gh}(t) - \frac{1}{\hbar} \sum_{i=1}^{\infty} \sum_{j=1}^{\infty} a_{ij}(t) R_{gh,ij}, \qquad \text{for } 1 \leq i, j, < \infty. \quad (5.16)$$

For simplicity we will work in atomic units. The atomic unit of length is defined by

$$1\, a.u. = \frac{\hbar^2}{m_e e^2} = 0.52917 \cdot 10^{-10}\, m$$

and the atomic unit of energy is defined by

$$1\, a.u. = \frac{m_e e^4}{\hbar^2} = 27.21\, eV.$$

These definitions imply that $m_e = e = \hbar = 1$. We will use "a.u." to denote both the unit of length and energy. It will always be clear from the context which quantity we are referring to.

Using atomic units, eqns. (5.15) and (5.16) become

[3] See appendix A for the explicit calculation of each of the components of R.

$$\frac{da_{gh}(t)}{dt} = \frac{Z}{2}\left(\frac{1}{n_g^2} + \frac{1}{n_h^2}\right) b_{gh}(t) + Z\sum_{i=1}^{\infty}\sum_{j=1}^{\infty} b_{ij}(t) R_{gh,ij}, \qquad \text{for } 1 \leq i,j < \infty,$$

$$\frac{db_{gh}(t)}{dt} = -\frac{Z}{2}\left(\frac{1}{n_g^2} + \frac{1}{n_h^2}\right) a_{gh}(t) - Z\sum_{i=1}^{\infty}\sum_{j=1}^{\infty} a_{ij}(t) R_{gh,ij}, \quad \text{for } 1 \leq i,j < \infty.$$

We now have a model of the helium atom in which the wavefunction is represented as a time-dependent linear combination of the vectors $\Phi_i(\vec{r}_1)\Phi_j(\vec{r}_2)$, each of which are eigenfunctions[4] of the Hamiltonian, $\hat{H}_0$. The Hamiltonian term, $\hat{H}_1$ which represents the electrical interaction between the two electrons is treated as a perturbation which influences the time-dependence of the wavefunction. Thus, our job is to determine the evolution of the coefficients, $c_{ij}(t)$, via the solution of the Schrödinger equation for some set of initial conditions, $c_{ij}(0)$.

As it stands, we need to solve for the infinite number of coefficients, $c_{ij}(t)$. To make the problem tractable, we will truncate each infinite series at three terms. This restricts each term in the wavefuction to being a product of hydrogenic eigenstates corresponding to the hydrogenic orbitals $1s$, $2s$ and $2p_0$. These eigenstates have corresponding quantum numbers $(1,0,0)$, $(2,0,0)$ and $(2,1,0)$. This approximation reduces the column vector C to nine components and the matrices E and R to a size of 9×9, i.e.,

$$C(t) = \begin{pmatrix} c_{11}(t) \\ c_{12}(t) \\ c_{13}(t) \\ c_{21}(t) \\ c_{22}(t) \\ c_{23}(t) \\ c_{31}(t) \\ c_{32}(t) \\ c_{33}(t) \end{pmatrix},$$

[4]These vectors are not basis vectors of the general helium wavefunction since the helium wavefunction is an element of the Hilbert space $\mathcal{L}^2(\Re^6)$. The set of vectors $\{\Phi_i(\vec{r}_1)\Phi_j(\vec{r}_2)\}$ form a basis for the Hilbert space $\mathcal{L}^2(\Re^3) \otimes \mathcal{L}^2(\Re^3)$ since $\{\Phi_i\}$ is a basis of $\mathcal{L}^2(\Re^3)$ but not of $\mathcal{L}^2(\Re^6)$. However, we will refer to the set $\{\Phi_i(\vec{r}_1)\Phi_j(\vec{r}_2)\}$ as basis vectors (or basis functions), for lack of a better term.

$$E = \begin{pmatrix} E_{11}^{(0)} & 0 & 0 & & & \dots & & 0 & 0 \\ 0 & E_{12}^{(0)} & 0 & \ddots & & & & & 0 \\ 0 & 0 & E_{13}^{(0)} & 0 & & & 0 & & \\ & \ddots & 0 & E_{21}^{(0)} & 0 & & & & \vdots \\ & & & 0 & E_{22}^{(0)} & 0 & & & \\ \vdots & & & & 0 & E_{23}^{(0)} & 0 & \ddots & \\ & & 0 & & & 0 & E_{31}^{(0)} & 0 & 0 \\ 0 & & & & & \ddots & 0 & E_{32}^{(0)} & 0 \\ 0 & 0 & & \dots & & & 0 & 0 & E_{33}^{(0)} \end{pmatrix}, \tag{5.17}$$

and

$$R = \begin{pmatrix} R_{11,11} & R_{11,12} & R_{11,13} & & & \dots & & R_{11,32} & R_{11,33} \\ R_{12,11} & R_{12,12} & R_{12,13} & & & & & & R_{12,33} \\ R_{13,11} & R_{13,12} & R_{13,13} & \ddots & & & \ddots & & \\ & & R_{21,13} & \ddots & \ddots & & & & \vdots \\ & \ddots & & \ddots & \ddots & \ddots & & \ddots & \\ \vdots & & & & \ddots & \ddots & R_{23,31} & & \\ & & & & & \ddots & R_{31,31} & R_{31,32} & R_{31,33} \\ R_{32,11} & & & \ddots & & & R_{32,31} & R_{32,32} & R_{32,33} \\ R_{33,11} & R_{33,12} & & \dots & & & R_{33,31} & R_{33,32} & R_{33,33} \end{pmatrix}. \tag{5.18}$$

Finally, we arrive at the two sets of ordinary differential equations (each set containing nine ODEs)

$$\frac{da_{gh}(t)}{dt} = \frac{Z}{2}\left(\frac{1}{n_g^2} + \frac{1}{n_h^2}\right) b_{gh} + Z\sum_{i=1}^{3}\sum_{j=1}^{3} b_{ij}(t) R_{gh,ij} \tag{5.19}$$

$$\frac{db_{gh}(t)}{dt} = -\frac{Z}{2}\left(\frac{1}{n_g^2} + \frac{1}{n_h^2}\right) a_{gh} - Z\sum_{i=1}^{3}\sum_{j=1}^{3} a_{ij}(t) R_{gh,ij} \tag{5.20}$$

These can be solved numerically to yield the time-evolution of the wavefunction which is now given by

$$\Psi_{hel}(r_1, \theta_1, \phi_1, r_2, \theta_2, \phi_2, t) = \sum_{i=1}^{3}\sum_{j=1}^{3} c_{ij}(t)\Phi_i(r_1, \theta_1, \phi_1)\Phi_j(r_2, \theta_2, \phi_2) \tag{5.21}$$

5.2 Energy Expectation

The energy expectation of our model is given by the standard formula[5]

$$\begin{aligned}\langle E\rangle &= \left\langle \Psi_{hel}^* \middle| \hat{H}_{hel} \middle| \Psi_{hel} \right\rangle \\ &= \sum_{i=1}^{3}\sum_{j=1}^{3} |c_{ij}|^2 \left(E_{n_i} + E_{n_j}\right) + \sum_{g=1}^{3}\sum_{h=1}^{3}\sum_{i=1}^{3}\sum_{j=1}^{3} (a_{gh}a_{ij} + b_{gh}b_{ij}) R_{gh,ij}\end{aligned} \tag{5.22}$$

where the $R_{gh,ij}$ are given by eqn. (5.14). The first term represents the energy associated with the first term in the Hamiltonian, $\hat{H}_0$. Recall that this represents the energy of two independent hydrogenic electrons. The second term is the energy associated with the perturbation term, $\hat{H}_1$. This represents the effect of the interaction between the electrons. Since this interaction arises from a potential energy between the electrons, it has the net result of increasing the total energy of the system, thus increasing the energy expectation. In section 5.4 we will approximate the ground state of the helium atom by the wavefunction

[5]See Appendix B for this calculation.

$$\Psi(\vec{r}_1, \vec{r}_2)\big|_{t=0} = \Phi_1(\vec{r}_1)\Phi_1(\vec{r}_2)$$

which represents each electron being in the hydrogenic ground state. Since this is an eigenstate of $\hat{H}_0$, it must have an energy expectation which is lower than the energy of the true helium ground state. Thus, we can establish a lower bound for the ground state energy expectation based purely on the fact that $\hat{H}_1$ represents a source of positive energy in the atom.

5.3 Inclusion of Spin in the Wavefunction – Symmetry Properties

5.3.1 Discussion of Spin

Thus far we have not made any mention of spin with respect to the wavefunction. However, as discussed in the introduction, the guidance condition for a system in which there is a non-zero spin vector is quite different from that in which the spin is zero. As we saw for the case of hydrogen, the addition of the spin-dependent term, $\nabla(\log\rho) \times \vec{s}$ where $\vec{s}$ is the spin vector of the electron, to the guidance condition has the effect of introducing an additional circulating motion to the electron. In the case of real eigenstates, the spin-dependent term is responsible for the entire motion of the electron and provides a model of the atom in which the electron is not stationary. This is a much more intuitive picture of the atom since a motionless electron, while not forbidden by quantum mechanics, is nonetheless a strange and potentially troublesome result. Thus, it is clear that spin must also be taken into account in the case of the helium atom, lest we forfeit a major source of the underlying dynamics.

To represent spin in our model, we will make the assumption that the spin vector of each electron does not change in time. This assumption is reasonable since the spin part of the wavefunction couples only to a magnetic field and we are dealing with a free atom. Thus, it is acceptable to write the total, spin-dependent wavefunction as the tensor product of a term which depends only on space and time and a term which depends only on the spin coordinates of each electron. For this spin-dependent term we will use eigenfunctions of the spin operator in the z-direction where the spin operators are given by

$$\hat{s}_{i_j} = \left(\frac{\hbar}{2\rho}\right)\sigma_{i_j} \tag{5.23}$$

where $i = 1, 2$ represents electron number and $j = 1, 2, 3$ refers respectively to the x-direction, y-direction and z-direction and σ_{i_j} is the j^{th} Pauli spin matrix for electron i (cf. (2.9)). Following the discussion in section 2.2, we will represent these spin eigenfunctions as scalar functions of a suitable set of spin coordinates. This may be troublesome to the reader as Ψ_{hel} and $\Psi^{\dagger}_{hel}$ must be 2-component objects for eqn. (5.23) to make sense. We will address this issue in appendix C where we explicitly compute the spin vectors. However, for the time being it is beneficial to treat Ψ_{hel} like a scalar function (cf. section 2.2). We will represent the spin functions as

$$\Omega_{spin}(s_1, s_2)$$

where s_1 represents the spin coordinates of electron 1 and s_2 represents the spin coordinates of electron 2. The form of s_1, s_2 are unimportant both to the evolution of the wavefunction and to the trajectories of the electrons since the spin vector of each electron is constant in time. Denoting the spin "up" state by α and the spin "down" state as β the general spin eigenfunction can be represented by the linear combination[6]

$$\Omega_{spin}(s_1, s_2) = d_{11}\alpha(s_1)\alpha(s_2) + d_{12}\alpha(s_1)\beta(s_2) + d_{21}\beta(s_1)\alpha(s_2) + d_{22}\beta(s_1)\beta(s_2) \tag{5.24}$$

where d_{11}, d_{12}, d_{21} and d_{21} are arbitrary constants. Putting this all together the total wavefunction for the helium atom is

$$\Psi_{total}(\vec{r_1}, \vec{r_2}, s_1, s_2, t) = \Psi_{hel}(\vec{r_1}, \vec{r_2}, t)\Omega_{spin}(s_1, s_2), \tag{5.25}$$

where Ψ_{hel} is given by eqn. (5.11) and Ω_{spin} is given by eqn. (5.24).[7] The only

[6]By spin "up" we mean that the spin function obeys the eigenvalue equation $\sigma_{i_3}\alpha = \alpha$ for $i = 1, 2$ and by spin "down" we mean that the spin function obeys the eigenvalue equation $\sigma_{i_3}\beta = -\beta$ for $i = 1, 2$.

[7]The expectation value of any spin-independent operator is not affected by the inclusion of the spin-dependent term in the total wavefunction [36]. In particular, the energy expectation is not changed by the inclusion of spin because $\hat{H}_{hel}$ is spin-independent. However, in a more complete treatment of the helium atom the spin of the electron would interact with the magnetic properties of the nucleus and $\hat{H}_{hel}$ would depend on spin.

ambiguity in our wavefunction arises from our choice of the time-dependent constants, $\{c_{ij}(t)\}$, which determine the spatial dependence of the wavefunction and the time-independent constants, $\{d_{kl}\}$, which determine the spin-dependence of the wavefunction. By examining the symmetry of the system one can remove the majority of this ambiguity. It is to this topic that we now turn.

5.3.2 Symmetry Considerations

The basic symmetry principle in quantum mechanics is embodied in the *Symmetrization Postulate* [33] which states:

In a system containing indistinguishable particles, the only possible states of the system are the ones described by wavefunctions that are, with respect to permutations of the labels of those particles, either completely symmetrical – in which case the particles are called bosons, or completely antisymmetrical – in which case the particles are called fermions.

For a two-particle system, a symmetric wavefunction (which we label Ψ_s) has the property that

$$\Psi_s(\vec{r}_1, \vec{r}_2, s_1, s_2, t) = \Psi_s(\vec{r}_2, \vec{r}_1, s_2, s_1, t)$$

and an antisymmetric wavefunction (which we label Ψ_a) has the property that

$$\Psi_a(\vec{r}_1, \vec{r}_2, s_1, s_2, t) = -\Psi_a(\vec{r}_2, \vec{r}_1, s_2, s_1, t).$$

Since our system consists of two (indistinguishable) electrons, which are fermions,[8] the total wavefunction must be completely antisymmetric with

[8]There is a strong, yet not well-understood, connection between the spin of a particle and its classification as fermion or boson. This connection is embodied in the *Spin-Statistics Theorem* (see [33] for a statement and discussion of the *Spin-Statistics Theorem* and [35] for a general discussion of quantum statistics and spin) which states that particles with integer spin are bosons while particles with half-integer spin are fermions. There have been various attempts at a proof of this theorem, but none are free of controversy. To date there is no experimental evidence to contradict the *Spin-Statistics Theorem*. We also wish to point out that, in general, the particles that make up the material world (electrons, protons, etc.) are fermions while the force-mediating particles (photons, W^+ bosons, gluons, etc.) are bosons.

respect to interchange of all particle coordinates. Since the helium wavefunction is (cf. eqn. (5.25))

$$\Psi_{total}(\vec{r_1}, \vec{r_2}, s_1, s_2, t) = \Psi_{hel}(\vec{r_1}, \vec{r_2}, t)\Omega_{spin}(s_1, s_2),$$

Ψ_{total} will be antisymmetric only if Ψ_{hel} is symmetric and Ω_{spin} is antisymmetric or vice versa.

Consider first the case where Ψ_{hel} is symmetric. There are many different forms Ψ_{hel} can take and be symmetric. Two of these forms which will be important in our analysis are[9]

$$\Psi_{hel}^{(sym_{gr})}(\vec{r_1}, \vec{r_2}) = \phi_j(\vec{r_1})\phi_j(\vec{r_2}) \qquad \text{for } j = 1, 2, 3 \tag{5.26a}$$

and

$$\Psi_{hel}^{(sym_{ex})}(\vec{r_1}, \vec{r_2}) = \frac{1}{\sqrt{2}}\left(\phi_1(\vec{r_1})\phi_j(\vec{r_2}) + \phi_j(\vec{r_1})\phi_1(\vec{r_2})\right) \qquad \text{for } j = 2, 3. \tag{5.26b}$$

The possible normalized forms of Ω_{spin} are

$$\frac{1}{\sqrt{2}}(\alpha(s_1)\beta(s_2) + \beta(s_1)\alpha(s_2)), \tag{5.27a}$$

$$\alpha(s_1)\alpha(s_2), \tag{5.27b}$$

$$\beta(s_1)\beta(s_2), \tag{5.27c}$$

and

$$\frac{1}{\sqrt{2}}(\alpha(s_1)\beta(s_2) - \beta(s_1)\alpha(s_2)). \tag{5.27d}$$

The first three are symmetric with respect to interchange of the spin coordinates while the last is antisymmetric.[10] In the language of quantum mechanics, one says that (5.27a), (5.27b) and (5.27c) form a *spin triplet* while

[9] We use the labels $\Psi_{hel}^{(sym_{gr})}$ and $\Psi_{hel}^{(sym_{ex})}$ because one of the ways we will represent the ground state of the helium atom is using a wavefunction of the form $\Psi_{hel}^{(sym_{gr})}$ and we will represent an excited state using a wavefunction of the form $\Psi_{hel}^{(sym_{ex})}$.

[10] Using eqn. (5.23) it is easy to show that the spin functions (5.27a) and (5.27d) have associated spin vectors $\vec{s}_1 = \vec{s}_2 = \vec{0}$ while (5.27b) and (5.27c) have associated spin vectors $\vec{s}_1 = \vec{s}_2 = (0, 0, \frac{\hbar}{2})$ and $\vec{s}_1 = \vec{s}_2 = (0, 0, -\frac{\hbar}{2})$, respectively. See appendix C for these calculations.

(5.27d) forms a *spin singlet*. Thus, for any spatial wavefunction having either of the two symmetric forms, $\Psi_{hel}^{(sym_{gr})}$ or $\Psi_{hel}^{(sym_{ex})}$, the only possible total spin-dependent wavefunctions are

$$\Psi_{total} = \frac{1}{\sqrt{2}}(\alpha(s_1)\beta(s_2) - \beta(s_1)\alpha(s_2))\Psi_{hel}^{(sym_{gr})} \tag{5.28}$$

and

$$\Psi_{total} = \frac{1}{\sqrt{2}}(\alpha(s_1)\beta(s_2) - \beta(s_1)\alpha(s_2))\Psi_{hel}^{(sym_{ex})}. \tag{5.28}$$

Now consider the case where Ψ_{hel} is antisymmetric with respect to interchange of coordinates. As with the symmetric case there are many antisymmetric forms of Ψ_{hel}. We highlight one of these which will prove useful in our analysis and label it $\Psi_{hel}^{(anti_{ex})}$. It is given by

$$\Psi_{hel}^{(anti_{ex})} = \frac{1}{\sqrt{2}}\left(\phi_1(\vec{r_1})\phi_j(\vec{r_2}) - \phi_j(\vec{r_1})\phi_1(\vec{r_2})\right) \qquad \text{for } j = 2, 3. \tag{5.29}$$

Thus, there are three different forms of an antisymmetric total spin-dependent wavefunction which contain $\Psi_{hel}^{(anti_{ex})}$, given by

$$\Psi_{total} = \frac{1}{\sqrt{2}}(\alpha(s_1)\beta(s_2) + \beta(1)\alpha(2))\Psi_{hel}^{(anti_{ex})}$$

$$\Psi_{total} = \alpha(s_1)\alpha(s_2)\Psi_{hel}^{(anti_{ex})}$$

and

$$\Psi_{total} = \beta(s_1)\beta(s_2)\Psi_{hel}^{(anti_{ex})}. \tag{5.30}$$

The first represents the spin vectors $\vec{s}_1 = \vec{s}_2 = \vec{0}$, the second represents the spin vectors $\vec{s}_1 = \vec{s}_2 = (0, 0, \frac{\hbar}{2})$ and the third, the spin vectors $\vec{s}_1 = \vec{s}_2 = (0, 0, -\frac{\hbar}{2})$.

To summarize, the *Symmetrization Postulate* requires the helium atom to have an antisymmetric wavefunction. We have assumed a constant spin vector for each electron and our wavefunction is correspondingly the product of a term which depends only of the spatial coordinates and the time and a term which depends only on the spin coordinates. As a result, the total helium wavefunction must be composed of either a symmetric spatial part and an antisymmetric spin part or vice versa.

5.4 The Ritz Variational Method

At this point one may ask how we are to represent a specific state of the helium atom, for instance, the ground state, using our model. The obvious thought is to set $c_{11}(0) = 1$ and all other $c_{ij}(0) = 0$, i.e., use $\Psi_{hel}^{(sym_{gr})}$ with $j = 1$ (cf. eqn. (5.26a)). Since this is a symmetric function we must multiply it by an antisymmetric spin function in accordance with the *Symmetrization Postulate*. Thus, the total wavefunction is

$$\begin{aligned}\Psi_{total}(\vec{r_1}, \vec{r_2}, s_1, s_2, 0) &= \frac{1}{\sqrt{2}}\phi_1(\vec{r_1})\phi_1(\vec{r_2})\big(\alpha(s_1)\beta(s_2) - \beta(s_1)\alpha(s_2)\big) \\ &= \frac{1}{\sqrt{2}}\left[4\left(\frac{Z}{a_\mu}\right)^3\right] e^{-\frac{Zr_1}{a_\mu}} e^{-\frac{Zr_2}{a_\mu}} \big(\alpha(s_1)\beta(s_2) - \beta(s_1)\alpha(s_2)\big).\end{aligned} \tag{5.31}$$

This amounts to representing each electron as a hydrogenic ground state electron. Using (5.22), the energy expectation of this state is -2.75 a.u.. Compare this to the best theoretical value of -2.9034 a.u. [45] and the best experimental value of -2.905 a.u. [36]. The differential equations given by (5.19), (5.20) and (2.15) have been implemented in *Matlab* using the differential equations solver, *ode45*. This implementation has been used to generate the following plots for a helium atom with initial wavefunction (5.31) and initial electron positions $(\frac{1}{2}, \frac{4\pi}{11}, \frac{6\pi}{5})$ for electron 1 and $(\frac{1}{2}, \frac{7\pi}{11}, \frac{\pi}{5})$ for electron 2 (the positions are given in spherical coordinates).[11]

It is not obvious from the trajectories that the motion of both electrons is almost entirely in the radial direction. Electron 1 moves from its initial position away from the nucleus and back while electron 2 moves from its initial position towards the nucleus and back. From the left side of figure 5.2 we see that each electron oscillates in the radial direction with an amplitude of approximately 0.08 a.u.. This purely radial motion is expected once one considers the guidance condition. Since the spatial wavefunction is symmetric, the spin is represented by the antisymmetric spin function and the spin vectors are $\vec{s}_1 = \vec{s}_2 = \vec{0}$. Consequently, the motion is due entirely to the

[11] These initial electron positions were specifically chosen since they are representative of positions where the electrons are most likely to be found according to $|\Psi|^2$. We will discuss this in more detail in section 5.6.1. For now, the important result is the trajectories.

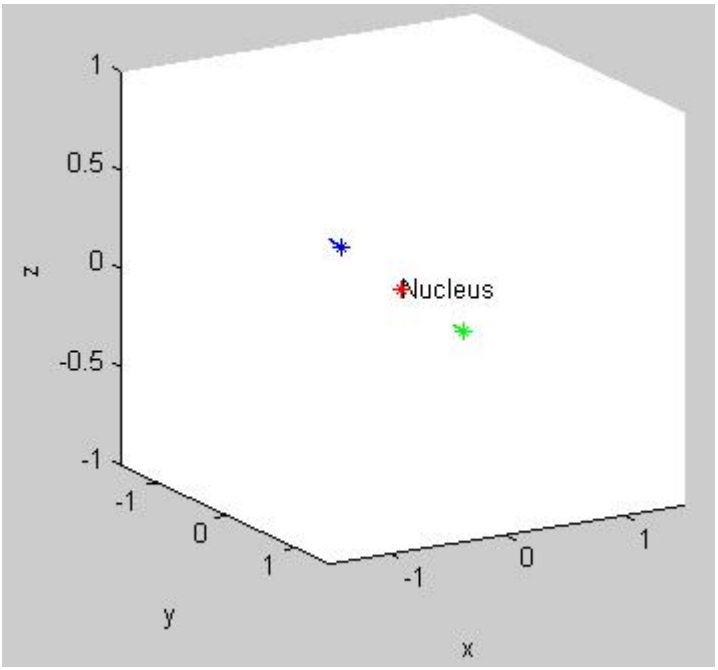

Figure 5.1: The trajectories for the initial state (5.31). The initial particle positions are marked with an asterisk.

spin-independent term, $\vec{p}_i = \nabla_i S$, where $i = 1$ refers to electron 1 and $i = 2$ refers to electron 2. Since the wavefunction is almost entirely composed of terms involving only the hydrogenic eigenfunctions Φ_1 and Φ_2 for all time, S is only a function of the radial coordinates, r_1 and r_2 and $\nabla_i S$ has a non-zero component only in the r-direction.[12]

We can see from figure 5.2 that some of the coefficients which were initially set equal to zero immediately become non-zero under the action of eqns. (5.19) and (5.20). This is an indication that the initial state (5.31) is not

[12]This is not entirely true. According to figure 5.2 the coefficient c_{33} becomes non-zero after $t = 0$ and this introduces θ_i-dependence into the wavefunction. Consequently, $\frac{\partial S}{\partial \theta_i} \neq 0$ and there is motion in the θ-direction for each electron. However, since $|c_{33}(t)|$ remains small for all t this motion is negligible when compared to the radial motion. To be specific, the amplitude of the motion in the θ-direction is approximately $5 \times 10^{-4}\, rad$ for electron 1 and $6 \times 10^{-4}\, rad$ for electron 2. Since each electron is a distance of approximately 0.5 a.u. from the nucleus, this corresponds to an amplitude of approximately $(0.5)(6 \times 10^{-4}) = 3 \times 10^{-4}$ a.u. which is clearly negligible compared to the amplitude of the radial motion.

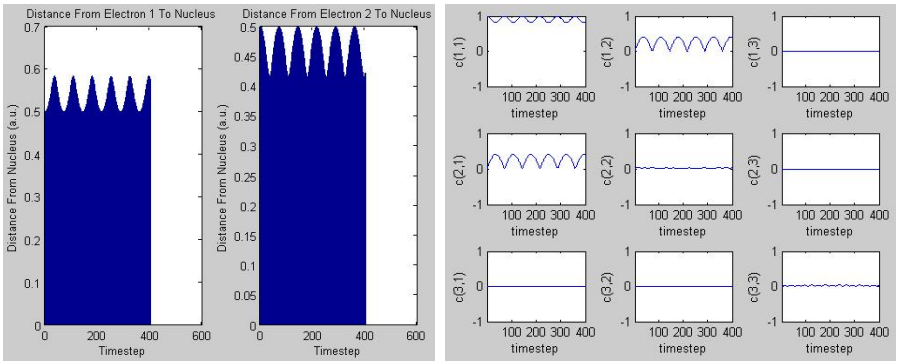

Figure 5.2: Left: The radial coordinate of each electron in time for the initial state (5.31) Right: The coefficients $\{c_{ij}(t)\}$.

an eigenstate and does not correspond to the ground state as we might have hoped. The question then arises as to whether we can find values of the $\{c_{ij}\}$ for which (5.21) would represent the ground state or at least represent a better approximation to the ground state. Luckily for us, the response to this question is a resounding yes and the method we use to find the $\{c_{ij}\}$ is called the *Ritz Variational Method*.[13]

The *Ritz Variational Method* is a procedure commonly used in quantum mechanics to estimate the lowest eigenvalue of the eigenvalue equation

$$\hat{H} f_i = E_i f_i \tag{5.32}$$

when the eigenfunctions, $\{f_i\}$, are not known. It is based on Schrödinger's variational principle and only applies when the Hamiltonian, $\hat{H}$, has a discrete set of eigenvalues, E_i. The procedure goes as follows. Let g be an arbitrary function having the same number of dimensions as f_i. If g is an exact eigenfunction of $\hat{H}$, (if $g = f_j$ where $f_j \in \{f_i\}$), then the functional

$$E[g] = \frac{\int g^* \hat{H} g \, d\tau}{\int g^* g \, d\tau}, \tag{5.33}$$

where the integration is taken over the configuration space of the system, is equal to the energy eigenvalue, E_j, corresponding to $g = f_j$. Schrödinger's variational principle states that any function g for which the expression (5.33)

[13]The following discussion is adapted from [4].

is stationary is a solution of (5.32).

Now suppose g is close to the eigenfunction f_1 which belongs to the *lowest* eigenvalue, E_1, of $\hat{H}$. Since we know that every Hamiltonian possesses a complete set of eigenfunctions, we can write g as a linear combination of the eigenfunctions of $\hat{H}$, i.e.,

$$g = N_1 f_1 + \sum_{n \neq 1} \epsilon_n f_n \tag{5.34}$$

where N_1 is a constant and $\{\epsilon_n\}$ is a set of small expansion coefficients (they are small because we assumed g was close to f_1). Substituting (5.34) into (5.33) gives

$$E[g] = E_1 + \frac{\sum\limits_{n \neq 1} |\epsilon_n|^2 (E_n - E_1)}{|N_1|^2 + \sum\limits_{n \neq 1} |\epsilon_n|^2}. \tag{5.35}$$

Since E_1 is the smallest of the eigenvalues, $E_n - E_1 \geq 0$ for all n and the numerator is clearly non-negative. Similarly, the denominator is non-negative and can only equal zero if $g = 0$. Since $g = 0$ leads to the eigenvalue equation $\hat{H}0 = 0$, which gives us no information, we require that $g \neq 0$. Thus, the denominator is positive and we arrive at the result

$$E[g] \geq E_1. \tag{5.36}$$

Thus, if g is not equal to f_1 then $E[g]$ will be larger than E_1. Similarly, the closer g is to f_1, the closer $E[g]$ will be to E_1. This is due to the fact that the closer g is to f_1, the smaller are the coefficients $\{\epsilon_n\}$. Since g is assumed to be close to f_1 $N_1 \gg \epsilon_n$ for each n, hence the denominator is dominated by the $|N_1|^2$ term. Thus, the numerator will shrink faster than the denominator as the size of the $\{\epsilon_n\}$ decrease and E_1 will be closer to $E[g]$.

The Ritz variational method is then to choose a trial form of the function g which involves a set of undetermined coefficients, $\{C_m\}$. The functional $E[g]$ then depends on the $\{C_m\}$. Minimizing $E[g]$ with respect to the C_m gives an *upper* bound for E_1. Note that this method only works for the lowest eigenvalue: if E_1 is not the lowest eigenvalue, then there will exist at least one value of $n \neq 1$ for which the numerator, $|\epsilon_n|^2(E_n - E_1)$, will be negative so that the result (5.36) does not necessarily follow.

As an example of using the method to find the ground state energy of the

helium atom, consider the trial function

$$g(\vec{r_1}, \vec{r_2}) = 4\left(\frac{Z}{a_\mu}\right)^3 e^{-\frac{(Z-\sigma)r_1}{a_\mu}} e^{-\frac{(Z-\sigma)r_2}{a_\mu}} \tag{5.37}$$

where Z is the nuclear charge and σ is the minimizing parameter. Note the resemblance between this wavefunction and (5.31). Recall that (5.31) is the product of two hydrogenic ground state wavefunctions. The only difference between the two is that (5.37) contains the factor $(Z-\sigma)$ in the exponential while (5.31) contains the factor Z. Thus, one could look at (5.37) as representing two hydrogenic electrons that are attracted to a nucleus of charge $Z-\sigma$. This is the common way of interpreting the wavefunction (5.37) and σ is usually referred to as a "screening factor". The screening factor represents in a very approximate way the effect of each electron's repulsion on the other. This repulsion is thought of, according to this model, as screening the effect of the nucleus on the electrons, thus reducing the effective charge from Z to $Z-\sigma$.

The details of the calculation are unimportant (see [4, 31]) , but minimizing the functional (5.33) with respect to σ leads to the value $\sigma = \frac{5}{16}$ and the ground state energy is given by[14]

$$E_g = -(Z-\sigma)^2 \approx -2.848$$

upon substitution of the nuclear charge of the helium atom, $Z = 2$. This result is an improvement over our previous result of -2.75 which we obtained using the trial function (5.31).[15]

Now we are ready to analyze our wavefunction, (5.25), using the Ritz variational method. Since the Hamiltonian does not act on the spin coordinates the spin function Ω_{spin} will drop out of the functional (5.33) and we can use (5.21) instead of (5.25). Notice that (5.21) is already written in the form of a trial function where there are 9 complex parameters, $\{c_{ij}\}$, or equivalently, 18 real parameters, $\{a_{ij}\}$ and $\{b_{ij}\}$. So, in summary, the problem is to minimize the functional

[14]We use the notation E_g to denote the energy given by the Ritz variational method with respect to the trial function g.

[15]Recall that the best experimental result for the ground state energy of the helium atom is -2.905 a.u..

$$E[\Psi_{hel}] = \frac{\int \Psi^*_{hel} \hat{H}_{hel} \Psi_{hel} \, d\vec{r_1} \, d\vec{r_2}}{\int \Psi^*_{hel} \Psi_{hel} \, d\vec{r_1} \, d\vec{r_2}} \tag{5.38}$$

with respect to the $\{a_{ij}\}$ and $\{b_{ij}\}$, where

$$\Psi_{hel}(r_1, \theta_1, \phi_1, r_2, \theta_2, \phi_2, t) = \sum_{i=1}^{3} \sum_{j=1}^{3} c_{ij}(t) \Phi_i(r_1, \theta_1, \phi_1) \Phi_j(r_2, \theta_2, \phi_2)$$

(cf. eqn. (5.21)) and $\hat{H}_{hel}$ is given by eqn. (5.1).

To minimize (5.38) we must solve

$$\frac{\partial E[\Psi_{hel}]}{\partial c^*_{ij}} = 0 \text{ for } 1 \leq i, j \leq 3. \tag{5.39}$$

Eqns. (5.39) are equivalent to the nine coupled equations[16]

$$\begin{aligned} &\sum_{i,j=1}^{3} c_{ij} \left[(E_i + E_j) I_{ghij} + R_{ghij} \right] \sum_{k,l,m,n=1}^{3} c^*_{kl} c_{mn} I_{klmn} \\ &= \sum_{i,j=1}^{3} c_{ij} I_{ghij} \sum_{k,l,m,n=1}^{3} c^*_{kl} c_{mn} \left[(E_m + E_n) I_{klmn} + R_{klmn} \right] \text{ for } 1 \leq g, h \leq 3, \end{aligned} \tag{5.40}$$

where

$$I_{ghij} \equiv \int d\vec{r_1} \, d\vec{r_2} \, \Phi_g(\vec{r_1}) \Phi_h(\vec{r_2}) \Phi_i(\vec{r_1}) \Phi_j(\vec{r_2})$$

and R_{ghij} is defined in eqn. (5.14).

Once we have the solutions of eqns. (5.40) we can normalize them to yield the best approximation to the ground state of the helium atom available to us using our model. To normalize the coefficients really means to normalize the initial wavefunction, Ψ, which is determined by the coefficients but due to the orthogonality of the hydrogenic eigenfunctions this amounts to nothing more than the condition

[16] See Appendix D for the derivation of these equations.

$$\sum_{i,j=1}^{3} |c_{ij}(0)|^2 = 1.$$

Alternatively, recall that if the function Ψ_{hel} used in the variational integral, (5.38), is an exact eigenfunction of $\hat{H}_{hel}$ then $E[\Psi_{hel}]$ will be an exact eigenvalue of $\hat{H}_{hel}$. Thus, solving eqns. (5.40) is equivalent to finding the lowest eigenfunction of $\hat{H}_{hel}$. The nine eigenfunctions and corresponding eigenvalues of $\hat{H}_{hel}$ have been found using *Maple*. The lowest energy obtained was

$$E_{hel}^{(0)} = -2.8318$$

for the coefficients

$c_{11}^{(0)} = 0.9526$, $c_{12}^{(0)} = -0.2143$, $c_{21}^{(0)} = -0.2143$, $c_{22}^{(0)} = -0.0156$, $c_{33}^{(0)} = -0.0192$ and all other $c_{ij}^{(0)} = 0$.

The wavefunction formed by the above coefficients corresponds to the "ground state" of the helium atom. We use quotes because it is important to realize that the wavefunction formed by the $\{c_{ij}\}$ above is nothing more than the eigenfunction of $\hat{H}_{hel}$ with the lowest eigenvalue *for wavefunctions of the form* (5.21). And of course we know that (5.21) is an approximation to the real helium wavefunction.

The "ground state" solution along with the other eight sets of solutions are given in Table 5.4. Denoting $\Psi_{hel}^{(\alpha)}$ as the wavefunction formed by the set of coefficients corresponding to $E_{hel}^{(\alpha)}$, $\Psi_{hel}^{(\alpha)}$ can be thought of as an "excited state" of the helium atom with the same caveat given above for the "ground state". It is very interesting to note that the Ritz variational principle has yielded spatial wavefunctions which have the proper symmetry. $\Psi_{hel}^{(0)}$, $\Psi_{hel}^{(3)}$, $\Psi_{hel}^{(4)}$, $\Psi_{hel}^{(6)}$, $\Psi_{hel}^{(7)}$ and $\Psi_{hel}^{(8)}$ are symmetric while $\Psi_{hel}^{(1)}$, $\Psi_{hel}^{(2)}$ and $\Psi_{hel}^{(5)}$ are antisymmetric. Thus, we can make antisymmetric total wavefunctions for each of the nine spatial wavefunctions given above by multiplying them by spin functions of the appropriate symmetry.

To summarize, the following nine eigenvalue equations hold:

$$\hat{H}_{hel}\Psi_{hel}^{(\alpha)} = E_{hel}^{(\alpha)}\Psi_{hel}^{(\alpha)}$$

where $\alpha \in \{0, \ldots, 8\}$. We approximate the ground state of the helium atom

by $\Psi_{hel}^{(0)}$ and the first eight excited states by $\Psi_{hel}^{(\alpha)}$ for $\alpha \in \{1, \ldots, 8\}$. Recall that according to the Ritz Variational Method only the "ground state" energy, $E_{hel}^{(0)}$, is guaranteed to be an upper bound for the actual ground state energy of the helium atom. We cannot make analogous conclusions for the "excited state" energies, $E_{hel}^{(\alpha)}, \alpha \in \{1, \ldots, 8\}$ since for $E_{hel}^{(\alpha)}$, α terms in the numerator of the sum in eqn. (5.35) will be negative and the desired conclusion does not hold. However, note that the lower the value of α, the closer $E_{hel}^{(\alpha)}$ will be to an upper bound for the corresponding exact energy level in the helium atom.

When the initial wavefunction is one of $\{\Psi_{hel}^{(\alpha)}\}$ the real and imaginary parts of the coefficients are periodic in time and the magnitudes of the coefficients are constant in time as well, i.e.,

$$a_{ij}(t) = C_{ij} \cos(\omega^{(\alpha)} t) \tag{5.41a}$$

and

$$b_{ij}(t) = -C_{ij} \sin(\omega^{(\alpha)} t), \tag{5.41b}$$

where $C_{ij} = |c_{ij}(0)|$ for $1 \leq i, j \leq 3$.[17] We prove eqns. (5.41a) and (5.41b) in Appendix E as well as show that each $C_{ij} = a_{ij}(0)$. Eqns. (5.41a) and (5.41b) will have a very particular effect on the trajectories associated with the initial wavefunctions $\{\Psi_{hel}^{(\alpha)}\}$ as we will see in the next section.

[17]Naturally, as a consequence, $|c_{ij}(t)| = \sqrt{a_{ij}(t)^2 + b_{ij}(t)^2} = |C_{ij}| = |c_{ij}(0)|$ so the $\{|c_{ij}(t)|\}$ are constant in time.

α	Energy ($E_{hel}^{(\alpha)}$)	c_{11}	c_{12}	c_{13}	c_{21}	c_{22}	c_{23}	c_{31}	c_{32}	c_{33}	Symmetry
0	-2.83181	0.95265	-0.21431	0	-0.21431	-0.01563	0	0	0	-0.01918	symmetric
1	-2.12414	0	-0.70711	0	0.70711	0	0	0	0	0	antisymmetric
2	-2.04994	0	0	0.70673	0	0	-0.02305	-0.70673	0.02305	0	antisymmetric
3	-1.98031	0	0	0.70709	0	0	0.00445	0.70709	0.00445	0	symmetric
4	-1.95747	-0.30289	-0.67342	0	-0.67342	0.02984	0	0	0	-0.01934	symmetric
5	-0.73297	0	0	0.02305	0	0	0.70673	-0.02305	-0.70673	0	antisymmetric
6	-0.72637	0.01601	0.02260	0	0.02260	0.89684	0	0	0	-0.44091	symmetric
7	-0.61713	0	0	0.00445	0	0	-0.70709	0.00445	-0.70709	0	symmetric
8	-0.57850	0.02171	-0.00799	0	-0.00799	0.44107	0	0	0	0.89714	symmetric

Table 5.1: The coefficients and energy expectations of the "eigenstates".

5.5 Analysis of the Trajectories

Before presenting plots of the trajectories and coefficients we will analyze the motion of the electrons algebraically. Recall that according to the guidance condition, each electron has a momentum given by

$$\vec{p_i} = \frac{\hbar}{2iR^2}\left[\Psi^*\nabla_i\Psi - (\nabla_i\Psi^*)\Psi\right] + \frac{\nabla_i(R^2)\times\vec{s_i}}{R^2} \tag{5.42}$$

where $i = 1$ refers to electron 1 and $i = 2$ refers to electron 2 (cf. eqn. (2.15)). We will examine each of the two terms on the right-hand side separately.

The first term is

$$\frac{\hbar}{2iR^2}\left[\Psi^*\nabla_i\Psi - (\nabla_i\Psi^*)\Psi\right],$$

which, using our helium wavefunction, (5.21), is easily shown to be equal to[18]

$$\frac{\hbar}{R^2}\sum_{g,h,j,k=1}^{3}\left(a_{gh}b_{jk} - a_{jk}b_{gh}\right)\phi_g(\vec{r_1})\phi_h(\vec{r_2}) \times\left\{A^i_{jk}(\vec{r_1},\vec{r_2})\hat{e}_r + B^i_{jk}(\vec{r_1},\vec{r_2})\hat{e}_\phi + C^i_{jk}(\vec{r_1},\vec{r_2})\hat{e}_\theta\right\},$$

where

$$A^i_{jk}(\vec{r_1},\vec{r_2}) = \begin{cases}\frac{\partial R_{n_j,l_j}(r_1)}{\partial r_1}Y_{l_j}(\theta_1,\phi_1)R_{n_k,l_k}(r_2)Y_{l_k}(\theta_2,\phi_2) & \text{if } i=1;\\ R_{n_j,l_j}(r_1)Y_{l_j}(\theta_1,\phi_1)\frac{\partial R_{n_k,l_k}(r_2)}{\partial r_2}Y_{l_k}(\theta_2,\phi_2) & \text{if } i=2,\end{cases}$$

$$B^i_{jk}(\vec{r_1},\vec{r_2}) = 0 \text{ for } i = 1,2$$

because each Φ_i has no ϕ-dependence and

$$C^i_{jk}(\vec{r_1},\vec{r_2}) = \begin{cases}R_{n_j,l_j}(r_1)\frac{\partial Y_{l_j}(\theta_1,\phi_1)}{\partial\theta_1}R_{n_k,l_k}(r_2)Y_{l_k}(\theta_2,\phi_2) & \text{if } i=1;\\ R_{n_j,l_j}(r_1)Y_{l_j}(\theta_1,\phi_1)R_{n_k,l_k}(r_2)\frac{\partial Y_{l_k}(\theta_2,\phi_2)}{\partial\theta_2} & \text{if } i=2.\end{cases}$$

[18] See Appendix F for these calculations.

Here $n_\alpha = \begin{cases} 1, & \text{if } \alpha = 1 \\ 2, & \text{if } \alpha = 2 \\ 2, & \text{if } \alpha = 3 \end{cases}$ and $l_\alpha = \begin{cases} 0, & \text{if } \alpha = 1 \\ 0, & \text{if } \alpha = 2. \\ 1, & \text{if } \alpha = 3 \end{cases}$

For the nine eigenstates given in the previous section $\nabla S = 0$ and the first term in (5.42) vanishes. This is a consequence of eqns. (5.41a) and (5.41b) and a proof is given in Appendix G. Thus, all of the motion for eigenstates comes from the spin-dependent momentum (the second term in (5.42)). Recall that of our nine eigenstates, six are symmetric and three are antisymmetric. The six symmetric states must be multiplied by the antisymmetric spin function, eqn. (5.27d), which represents the spin vectors $\vec{s}_1 = \vec{s}_2 = \vec{0}$. Thus, the term $\nabla_i(R^2) \times \vec{s}_i$ is identically zero for $i = 1, 2$ and the spin-dependent momentum vanishes. Therefore, we arrive at the somewhat strange conclusion that *both electrons are stationary when the helium atom is in one of the symmetric eigenstates given in section 5.4.*

When the system is in one of the antisymmetric eigenstates it must be multiplied by one of the symmetric spin functions (eqns. (5.27a), (5.27b) and (5.27c)). The function (5.27a) represents the spin vectors $\vec{s}_1 = \vec{s}_2 = \vec{0}$, (5.27b) represents the spin vectors $\vec{s}_1 = \vec{s}_2 = (0, 0, \frac{\hbar}{2})$ and (5.27c) represents the spin vectors $\vec{s}_1 = \vec{s}_2 = (0, 0, -\frac{\hbar}{2})$.[19] Clearly, (5.27a) leads to the same conclusion as for the symmetric eigenstates – no spin-dependent momentum and consequently, stationary electrons. (5.27b) and (5.27c) will lead to different dynamics as we will now see.

Consider the total wavefunction formed by multiplying one of the antisymmetric eigenstates by the spin function (5.27b). Since our basis functions are products of the three hydrogenic eigenfunctions corresponding to the $1s$, $2s$ and $2p_0$ hydrogenic eigenstates, Ψ_{total} does not depend on the azimuthal angles, ϕ_1 and ϕ_2. As such, the term $\nabla_i \rho$ has non-zero components only in the r- and θ-directions for both $i = 1, 2$, i.e.,

$$\nabla_i \rho = P_i \hat{e}_r + Q_i \hat{e}_\theta,$$

where $P_i = P_i(r_1, \theta_1, r_2, \theta_2)$ and $Q_i = Q_i(r_1, \theta_1, r_2, \theta_2)$ are functions whose form is unimportant to our desired result. Taking the cross product of $\nabla_i \rho$ and $\vec{s}_i$ gives

[19] These vectors are given in Cartesian coordinates. In spherical coordinates (i.e. $\vec{A} = (A_r, A_\theta, A_\phi)$) (5.27b) represents the spin vectors $\vec{s}_i = \left(\frac{\hbar}{2}\cos(\theta), -\frac{\hbar}{2}\sin(\theta), 0\right)$ and (5.27c) represents the spin vectors $\vec{s}_i = \left(\frac{\hbar}{2}\cos(\theta), \frac{\hbar}{2}\left(\pi - \sin(\theta)\right), 0\right)$.

$$\nabla_i \rho \times \vec{s}_i = \begin{vmatrix} \hat{e}_r & \hat{e}_\theta & \hat{e}_\phi \\ P_i & Q_i & 0 \\ \cos(\theta) & -\sin(\theta) & 0 \end{vmatrix}$$
$$= -\big[P_i \sin(\theta) + Q_i \cos(\theta)\big]\hat{e}_\phi.$$

Thus, we see that the spin-dependent term gives motion only in the ϕ-direction and consequently the total motion of each electron is given by the momentum field

$$\vec{p}_i = -\frac{[P_i \sin(\theta) - Q_i \cos(\theta)]}{R^2}\hat{e}_\phi. \tag{5.43}$$

Now let us examine this motion more carefully. Since the total momentum comes entirely from the term $\nabla_i \rho \times \vec{s}_i$, it lies in a plane orthogonal to $\vec{s}_i$. Thus, $z = r\cos(\theta)$ is constant. Since the motion is only in the ϕ-direction, r and θ are constant as well. Consequently, the trajectories are circles in planes of constant z, i.e., circles around the spin axis. This is the same result as that obtained by Colijn [11] for the hydrogen atom – when the wavefunction is an eigenstate of $\hat{H}_{hyd}$ and the spin vector is non-zero, the electron follows a circular orbit around the spin axis (cf. chapter 4).

The velocity of each electron is given by

$$\frac{d\phi_i}{dt} = \frac{p_{\phi_i}}{mr_i \sin(\theta_i)}.$$

where m is the electron mass, (r_i, θ_i, ϕ_i) are the spherical coordinates of electron i and p_{ϕ_i} is the ϕ-component of the momentum of electron i given by eqn. (5.43). Since r_i and θ_i are constant over all eigenstate trajectories for both electrons, the functions P_i, Q_i and $R^2 = \rho$ in (5.43) are constant and consequently, we arrive at the result

$$\frac{d\phi_i}{dt} = C_i \text{ for } i = 1, 2,$$

where C_1 and C_2 are constants. Since the other two antisymmetric eigenstates, $\Phi^{(2)}_{hel}$ and $\Psi^{(6)}_{hel}$, do not depend on the azimuthal angles, ϕ_1 and ϕ_2, the cross product $\nabla_i \rho \times \vec{s}_i$ has a non-zero component only in the ϕ-direction and the same conclusions hold as for $\Psi^{(3)}_{hel}$. Similarly, if we put the electrons in the "spin down" state (if we use the symmetric spin function (5.27c) instead

of (5.27b)), the spin vector changes direction and the motion is the same except the direction is reversed.[20]

We have analyzed the Bohmian trajectories associated with eigenstates of $\hat{H}_{hel}$ and found they fall into two classes:

1. stationary electrons for symmetric eigenstates or states with a zero spin vector

2. circular orbits around the spin axis for antisymmetric eigenstates with a non-zero spin vector.

In the second case we have shown that both electrons move with constant velocity. We have also shown that the coefficients of the wavefunction oscillate sinusoidally in time for all eigenstates. To gain a better perspective on these results, we will now analyze the motion of some non-eigenstate wavefunctions.

5.6 A More Detailed Look At the Trajectories

5.6.1 A Comparison of Eigenstate Trajectories With Non-Eigenstate Trajectories

In section 5.3.2 we gave some particular forms of Ψ_{hel} which are either symmetric or antisymmetric. We will now examine the Bohmian trajectories and time-evolution of the wavefunction for certain initial states having these forms. We present these results only as a comparison to the eigenstates and as such, we will not be concerned with analysing them. Before proceeding, we wish to remark on the choice of initial electron positions.

Recall that the wavefunction has the property that $|\Psi(\vec{r},t)|^2 d\vec{r}$ gives a measure of the relative probability of finding the system within the volume element $\vec{r} + d\vec{r}$ if a corresponding measurement is made at time t. Thus, it makes the most physical sense to start each electron where the initial

[20]Note that this only holds for states where $\nabla_i S = 0$. Changing the direction of the spin vector has no bearing on the term $\nabla_i S$ and consequently only the motion due to the spin-dependent term is effected. Thus, if $\nabla_i S \neq 0$, we cannot say that reversing the spin vector reverses the direction of motion.

wavefunction is the largest. In practice it is difficult to determine where these points are since the wavefunction is a function of the six spatial coordinates, $(r_1, \theta_1, \phi_1, r_2, \theta_2, \phi_2)$. Thus, for simplicity we will start each electron at a radial distance from the nucleus dictated by the hydrogenic eigenstates of which the wavefunction is composed.

Consider the basis functions $\Phi_j(\vec{r}_1)\Phi_k(\vec{r}_2)$ where $1 \leq j \leq 3$ and $1 \leq k \leq 3$. Here, electron 1 is in the hydrogenic eigenstate Φ_j and electron 2 is in the hydrogenic eigenstate Φ_k. Both Φ_1 (the $1s$-state) and Φ_2 (the $2s$-state) are functions only of the radial coordinate while Φ_3 (the $2p_0$-state) is a function of r and θ. Using the fact that $d\vec{r} = r^2 dr sin(\theta) d\theta d\phi$, the most likely radial distances that the electron in the hydrogenic eigenstate, Φ_j, will be found is given by the maxima of the radial distribution function

$$D_{n_j,L_j}(r) = r^2 R_{n_j,l_j}(r),$$

where $R_{n_j,l_j}(r)$ is the radial part of Φ_{n_j,l_j} (cf. eqns. (4.2) and (4.3)). For $j = 1$ (i.e., quantum numbers $(n, l) = (1, 0)$),

$$\begin{aligned} D_{1,0}(r) &= r^2 R_{1,0}(r) \\ &= r \left(\frac{Z}{a_0}\right)^3 r^2 \exp\left(-\frac{2Zr}{a_0}\right) \end{aligned}$$

and has one maximum at

$$r_{1,0} = \frac{a_0}{Z} = 0.5\, a.u.,$$

since $Z = 2$ for helium. Consequently, we will give a ground state electron the initial radial coordinate $r(0) = 0.5\, a.u.$. Similarly, for $j = 2$ (i.e., quantum numbers $(n, l) = (2, 0)$),

$$\begin{aligned} D_{2,0}(r) &= r^2 R_{2,0}(r) \\ &= 4 \left(\frac{Z}{2a_0}\right)^3 \left(1 - \frac{Zr}{2a_0}\right)^2 r^2 \exp\left(-\frac{Zr}{a_0}\right) \end{aligned}$$

and has two maxima at

$$r_{2,0} = 3 \pm \sqrt{5}\, a.u..$$

We will use the smaller of these two values, $3 - \sqrt{5} \approx 0.764\, a.u.$ for the initial radial position of an electron in the $(2,0)$-eigenstate (this corresponds to the global maximum of $D_{2,0}(r)$). For $j = 3$ (i.e., quantum numbers $(n,l) = (2,1)$),

$$\begin{aligned} D_{2,1}(r) &= r^2 R_{2,1}(r) \\ &= \frac{4}{3}\left(\frac{Z}{2a_0}\right)^5 r^4 \exp\left(-\frac{Zr}{a_0}\right) \end{aligned}$$

and has a maximum at

$$r_{2,1} = \frac{4a_0}{Z} = 2\, a.u..$$

Thus, we will give an electron in the $(2,1)$-eigenstate the initial radial coordinate $r(0) = 2\, a.u.$.

Although the $2p_0$ hydrogenic eigenfunction Φ_3 is a function of θ we will not situate an electron in this state at a particular value of θ. The reason for this is that the θ-dependence of Φ_3 is due to the $\cos(\theta)$ term. Thus, $|\Psi|^2$ is maximized when $\theta = 0, \pi$ which are points on the z-axis. However, starting the electrons on the z-axis would lead to no spin-dependent motion because the electronic motion for eigenstates with non-zero spin consists of circles around the z-axis, as we have previously shown. Thus, for each simulation we run we choose to assign electron 1 the initial angular coordinates $(\theta, \phi) = (\frac{4\pi}{11}, \frac{6\pi}{5})$ and electron 2 the angular coordinates $(\frac{7\pi}{11}, \frac{\pi}{5})$. This keeps the initial positions of the electrons on a line which goes through the origin, and thus, preserves a sense of symmetry over the angular directions. Let us now turn to an examination of some non-eigenstate trajectories.

Without a knowledge of the eigenstates of $\hat{H}_{hel}$ one may be tempted to represent an excited state of the helium atom by keeping one electron in the hydrogenic ground state and raising the other to a hydrogenic excited state. There are two ways to do this – using the symmetric spatial function, (5.26b), or the antisymmetric spatial function, (5.29). We will examine the symmetric case first. Since the total wavefunction must be antisymmetric we must represent spin using the antisymmetric spin function, (5.27d). Recall

that this has no effect on the motion since the spin vectors associated with (5.27d) are $\vec{s}_1 = \vec{s}_2 = \vec{0}$. The total wavefunction is

$$\Psi_{hel}^{(sym_{ex})}(\vec{r_1}, \vec{r_2}) = \frac{1}{2}\left[\phi_1(\vec{r_1})\phi_j(\vec{r_2}) + \phi_j(\vec{r_1})\phi_1(\vec{r_2})\right]\left[\alpha(s_1)\beta(s_2) - \beta(s_1)\alpha(s_2)\right], \quad \text{for } j = 2, 3. \tag{5.44}$$

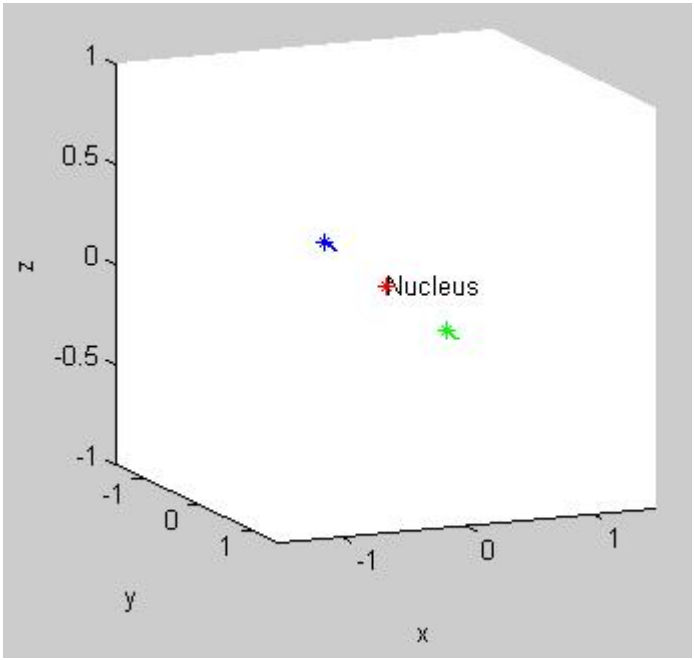

Figure 5.3: The trajectories for the initial state $\Psi_{hel}^{(sym_{ex})}$ with $j = 2$.

Simulations were run for $j = 2$ with initial electron positions $\vec{r}_1 = (\frac{1}{2}, \frac{4\pi}{11}, \frac{6\pi}{5})$ and $\vec{r}_2 = (0.764, \frac{7\pi}{11}, \frac{\pi}{5})$ and for $j = 3$ with initial electron positions $\vec{r}_1 = (\frac{1}{2}, \frac{4\pi}{11}, \frac{6\pi}{5})$ and $\vec{r}_2 = (2, \frac{7\pi}{11}, \frac{\pi}{5})$. The trajectories for the $j = 2$ state are very similar to those for $\Psi_{hel}^{(sym_{gr})}$ – motion almost exclusively along the radial direction. For the $j = 3$ state, the motion is similar except that the amplitude of the radial motion is very small – on the order of $10^{-2}\, a.u.$. Also, the angular motion of the electrons is more pronounced in the $j = 3$ state because the wavefunction has more θ-dependence. The amplitude of the θ-motion is approximately $4 \cdot 10^{-3}\, rad$ for electron 1 and $10^{-3}\, rad$ for

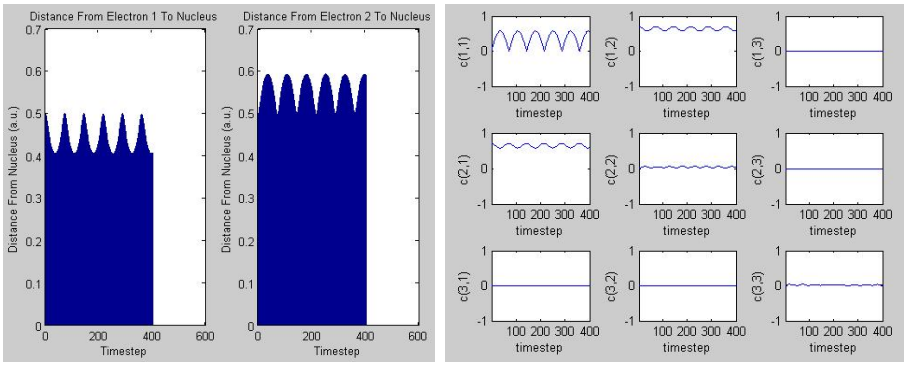

Figure 5.4: Left: The radial coordinate of each electron in $a.u.$ for the initial state $\Psi_{hel}^{(sym_{ex})}$ with $j = 2$. Right: The time-dependence of the coefficients.

electron 2. This corresponds to an amplitude of approximately $2 \cdot 10^{-3}\, a.u.$ for each electron. We show the trajectories and coefficients for the $j = 2$ state in figures 5.3 and 5.4.

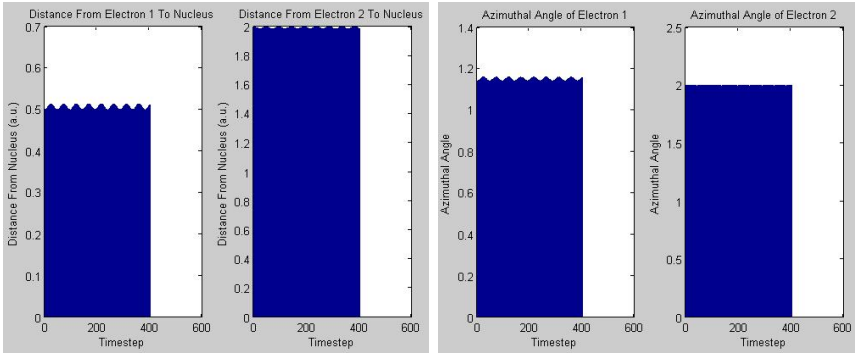

Figure 5.5: Results for the initial state $\Psi_{hel}^{(anti_{ex})}$ with $j = 3$ and no spin. Left: The radial coordinate of each electron in time in a.u.. Right: The azimuthal coordinate of each electron in time in radians.

Similarly, one may also attempt to construct an excited state using a wavefunction of the form $\Psi_{hel}^{(anti_{ex})}$ which has the form (cf. eqn. (5.29)),

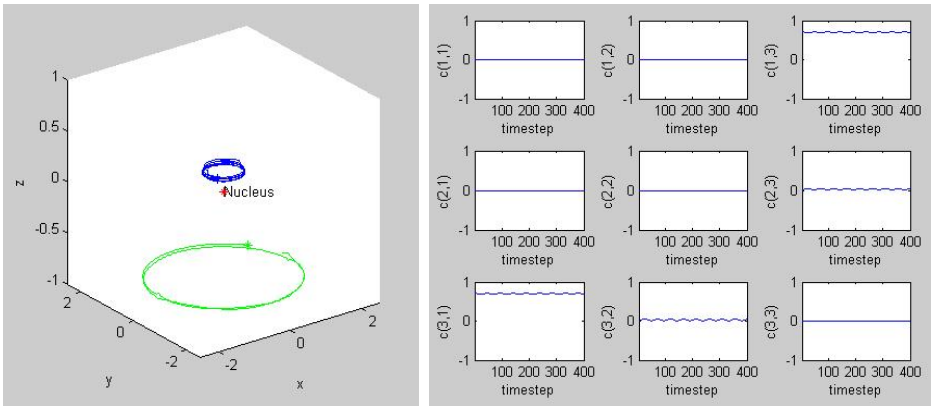

Figure 5.6: Left: The trajectories for initial state $\Psi_{hel}^{(anti_{ex})}$ with $j = 3$ and spin "up". Right: The coefficients of the wavefunction for initial state $\Psi_{hel}^{(anti_{ex})}$ with $j = 3$.

$$\Psi_{hel}^{(anti_{ex})} = \frac{1}{\sqrt{2}} \left(\phi_1(\vec{r_1})\phi_j(\vec{r_2}) - \phi_j(\vec{r_1})\phi_1(\vec{r_2})\right) \qquad \text{for } j = 2, 3.$$

In this case, we see that the $j = 2$ state is actually (the negative of) the eigenstate $\Psi_{hel}^{(2)}$ (cf. section 5.4). Therefore, we will only analyze the $j = 3$ state. However, the $j = 3$ state is also very close to the eigenstate $\Psi_{hel}^{(3)}$. Thus, we expect the trajectories and coefficients to be somewhat close to those of $\Psi_{hel}^{(3)}$. Since we are dealing with an antisymmetric spatial function, we must represent spin using a symmetric spin function. Thus, we can put the system in the "spin up" state, the "spin down" state, or the spinless state. We will look at both the "spin up" state and the spinless state and in this way we will see the effect of the spin-dependent term of the guidance condition on the trajectories. For the spinless state we give the time-dependence of the radial and azimuthal coordinates for each electron in figure 5.5. Since the amplitude of the motion in each component direction is very small for both electrons, the trajectories are virtually undetectable to the human eye unless we magnify them and consequently, we refrain from displaying them. In the "spin up" state each electron experiences the expected circular motion around the spin axis. The trajectories and the time-dependence of the coefficients in

figure 5.6. Naturally, since the coefficients do not depend on spin, they are the same for the spinless state and the "spin up" state.

Notice how similar the trajectories of figure 5.6 are to those of the eigenstate $\Psi_{hel}^{(3)}$. This is a very reasonable result since the initial wavefunctions are so close to each other. However, it begs the question as to whether there is a "continuity of trajectories", i.e., do the trajectories continuously morph as the initial wavefunction is continuously changed? It is to this question we now turn.

5.6.2 Continuity of the Trajectories

We will close our discussion of the helium atom by showing how the trajectories of the electrons depend continuously on the initial wavefunction. To do this we will construct a wavefunction which depends on a parameter, γ, where $0 \leq \gamma \leq 1$. We will denote this wavefunction Ψ_γ. When $\gamma = 0$ Ψ_γ will represent a state for which the trajectories are well known and the same goes for the wavefunction obtained from setting $\gamma = 1$. When $0 < \gamma < 1$ the wavefunction will be a linear combination of Ψ_0 and Ψ_1. Our aim will be to show that as γ is continuously changed from 0 to 1, the trajectories of the associated state will continuously change from those of Ψ_0 to those of Ψ_1.

Since Ψ_0 and Ψ_1 should be states with well-known trajectories, it is natural to choose them to be eigenstates. We will set $\Psi_0 = \Psi_{hel}^{(3)}$ and $\Psi_1 = \Psi_{hel}^{(6)}$ because both $\Psi_{hel}^{(3)}$ and $\Psi_{hel}^{(6)}$ have symmetric spin functions and therefore, have circular trajectories when multiplied by the appropriate spin function. This will make the trajectories easy to compare with others.

To construct Ψ_γ we will use a convex combination of Ψ_0 and Ψ_1. First we define the non-normalized coefficients,

$$g_{ij}(\gamma) = \gamma c_{ij}^{(3)} + (1-\gamma)c_{ij}^{(6)}, \qquad 0 \leq \gamma \leq 1,$$

where $\{c_{ij}^{(3)}\}$ are the initial coefficients of $\Psi_{hel}^{(3)}$ and $\{c_{ij}^{(6)}\}$ are the initial coefficients of $\Psi_{hel}^{(6)}$ (cf. section 5.4). Normalization yields

$$h_{ij}(\gamma) = \frac{g_{ij}(\gamma)}{\sqrt{\sum_{p,q=1}^{3} \left[g_{pq}(\gamma)\right]^2}} \tag{5.45}$$

and Ψ_γ is given by

$$\Psi_\gamma(\vec{r}_1, \vec{r}_2, s_1, s_2, t) = \sum_{i,j=1}^{3} h_{ij}(\gamma; t)\Phi_i(\vec{r}_1)\Phi_j(\vec{r}_2)\Big[\alpha(s_1)\alpha(s_2)\Big]$$

where $h_{ij}(\gamma; 0) = h_{ij}(\gamma)$ as given in eqn. (5.45).

Before giving the trajectories for various values of γ, consider the initial energy expectation for Ψ_α. When $\gamma = 0$ the initial energy expectation is $E^{(6)}_{hel}$ and when $\gamma = 1$ the initial energy expectation is $E^{(3)}_{hel}$. Since the energy expectation is a continuous function which depends on the coefficients of the wavefunction, continuously varying γ from 0 to 1 should continuously vary the initial energy expectation from $E^{(6)}_{hel}$ to $E^{(3)}_{hel}$. In addition, since the coefficients of Ψ_γ are formed from a nonlinear combination of the $\{c^{(3)}_{ij}\}$ and $\{c^{(6)}_{ij}\}$, the variation of initial energy expectation with respect to γ should also be nonlinear. This is what we see in figure 5.7.

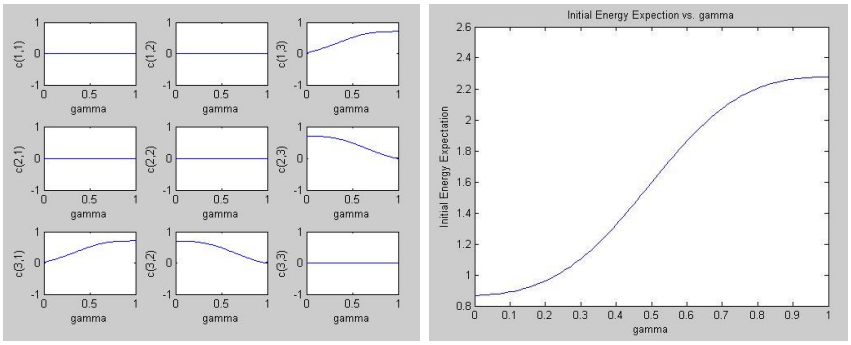

Figure 5.7: Left: The dependence of the initial coefficients on γ. Right: The dependence of the initial energy expectation on γ.

Now let us examine the trajectories of Ψ_γ for different values of γ. Since we are investigating how the trajectories change with respect to changing the initial wavefunction we will always give the electrons the same initial positions; $\vec{r}_1 = (1.1, \frac{4\pi}{11}, \frac{5\pi}{6})$ and $\vec{r}_2 = (1.1, \frac{7\pi}{11}, \frac{\pi}{6})$ irregardless of the value of γ. The initial radial distances were chosen out of convenience – they produced simulations in which the electrons move at a reasonable speed.

Some trajectories for various values of γ are given in figure 5.8. Each simulation covers $2.28 \cdot 10^{-14}$ seconds in real time. Clearly, the trajectories continuously (and very quickly) deviate from the circular orbits of $\Psi^{(6)}_{hel}$ to

trajectories which appear to have no connection at all to those of $\Psi_{hel}^{(6)}$ as γ is slowly increased from 0. Similarly, as γ is increased towards 1 the trajectories appear to continuously morph to the circular trajectories of $\Psi_{hel}^{(3)}$. Note that although the paths the electrons follow are the same for both eigenstates, their speed is different. For $\Psi_0 = \Psi_{hel}^{(6)}$ the period is $3.24 \cdot 10^{-16}\, s$ while the period of $\Psi_1 = \Psi_{hel}^{(3)}$ is $7.98 \cdot 10^{-17}\, s$. This corresponds to approximately 6 revolutions for Ψ_0 and 1.5 revolutions for Ψ_1 over the course of the simulation. This behaviour is seen in the plots.

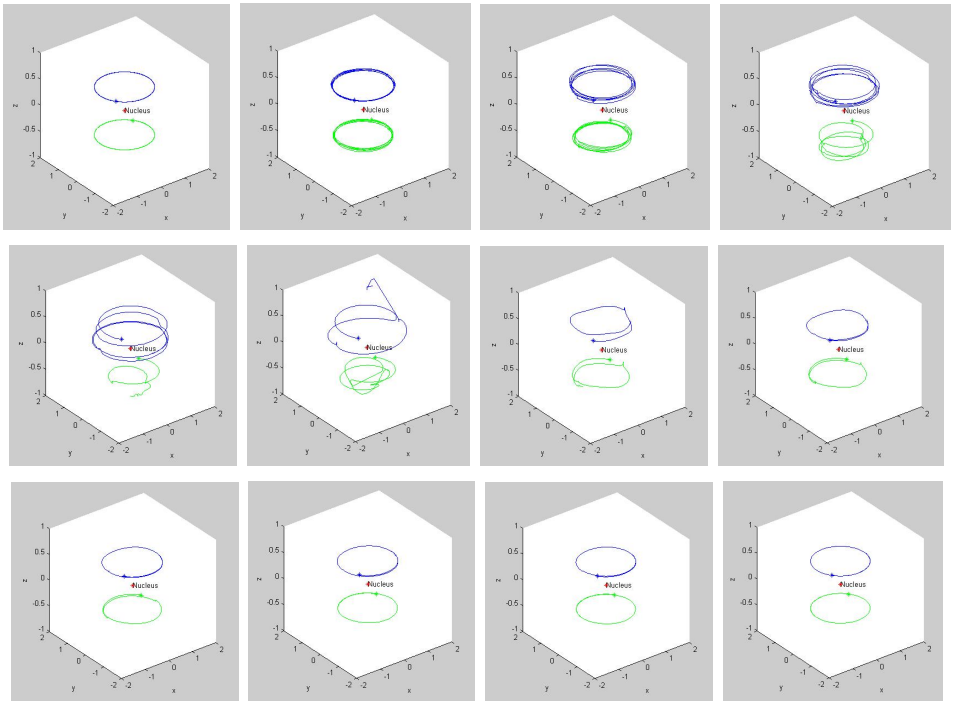

Figure 5.8: The trajectories for the following values of γ: 0 , 0.001 , 0.002 , 0.003 , 0.004 , 0.005 , 0.006 , 0.7 , 0.8 , 0.9 , 0.95 , 0.97 , 0.99 , 1.

We wish to point out some technical difficulties encountered with the *Matlab* implementation. First of all, it was found that the ODE solver *ode45* is somewhat fickle in that it can not compute the solutions to the differential equations (5.42), (5.19) and (5.20) for long periods of time for a wide variety of initial wavefunctions. Changing the error tolerances had no observable effect on the performance. *Matlab* has other built-in ODE solvers; these

were tried, but similar problems were encountered.

Secondly, for many values of γ the trajectories are jagged with sharp points where the particles appear to instantaneously change direction. This is due to the size of the timestep used in the simulations. The trajectories are determined by the positions of the particles at a finite number of times. The trajectories are interpolated between these times by connecting the positions of successive times by straight lines. Thus, if a particle undergoes a strong acceleration during any particular timestep and travels a large distance the trajectory can acquire a "corner" which appears in the corresponding plot as a discontinuous change in velocity. These corners are not representative of the true, continuously differentiable paths generated from the continuously differentiable Hamiltonian, $\hat{H}_{hel}$.[21]

Due to these two difficulties, trajectories for values of γ above 0.006 and below 0.7 are unobtainable. If *ode45* is able to find a solution, the trajectories are so jagged so as to be virtually useless. However, the trajectories given above, at the very least, provide evidence that the Bohmian trajectories associated with Ψ_γ change continuously with γ. We wish to point out that this is not intended to be a general proof that Bohmian trajectories depend continuously on the initial wavefunction. Although "continuity of trajectories" is a physically intuitive idea and seemingly "should" be correct, our purpose is not to prove it to be so. Our intention is merely to show that for one particular pair of states we can establish "continuity of trajectories" and show the consistency of BM in this way.

[21] Actually, $\hat{H}_{hel}$ is not continuously differentiable everywhere because there are singularities at $\vec{r}_1 = \vec{0}$, $\vec{r}_2 = \vec{0}$ and $\vec{r}_1 = \vec{r}_2$. However, $\hat{H}_{hel}$ is continuously differentiable everywhere else. Since the above three conditions correspond either to one of the electrons occupying the same position as the nucleus or both electrons occupying the same position, we can ignore them on physical grounds. Thus, when we say "$\hat{H}_{hel}$ is continuously differentiable everywhere" we mean that it is continuously differentiable in our restricted domain, $\{\Re^3 \times \Re^3 \,|\, \vec{r}_1 \neq \vec{0}, \vec{r}_2 \neq \vec{0}, \vec{r}_1 \neq \vec{r}_2\}$.

Chapter 6

Summary and Conclusions

6.1 Results on the Helium Atom

In this thesis we have attempted to find certain Bohmian trajectories of the electrons in the helium atom. Since there is no closed-form solution to the Schrödinger equation for $\hat{H}_{hel}$, we had to make use of an approximation method. Recall that we represented the wavefunction as a linear combination of the basis functions, $\{\Phi_i(\vec{r}_1)\Phi_j(\vec{r}_2)\}$ which are themselves products of hydrogenic eigenfunctions. This choice of basis functions was motivated by breaking $\hat{H}_{hel}$ into two pieces, $\hat{H}_{hel} = \hat{H}_0 + \hat{H}_1$ and treating $\hat{H}_1$ as a perturbation (cf. eqns. (5.2)-(5.11)). An arbitrarily good approximation to the true helium wavefunction can be represented by such a linear combination, but it would necessarily be composed of an arbitrarily large number of terms. In order to make the problem tractable we truncated the linear combination at nine terms, involving three different hydrogenic eigenfunctions – the $1s$-state, the $2s$-state and the $2p_0$-state. Solving for the eigenfunctions of $\hat{H}_{hel}$ in this finite basis led to nine "eigenstates" of the helium atom. It is very important to keep in mind that these are not true eigenstates because we truncated our basis to nine terms. However, our representation of the ground state, while not exact in any respect, is still a fairly good approximation. This is because the majority of the ground state wavefunction is composed of the basis functions representing the lowest hydrogenic eigenstates. Since we kept nine of the least energetic basis functions, we are able to represent the helium ground state wavefunction fairly accurately. We can also see this by the energy expectation of our ground state which is -2.8318 a.u.. This has a

relative error of 2.52% compared to the experimental value of -2.905 a.u..

We have also analyzed the trajectories of the "eigenstates" and found that the spin-independent motion disappears for each of them. Thus, all motion is due to the spin-dependent term of the guidance condition. As such, the eigenstates fall into two categories. The first consists of eigenstates with zero spin vectors (note that all eigenstates with a symmetric spatial function fall into this group). Eigenstates in this category have no spin-dependent motion and consequently, the Bohmian trajectories are stationary electrons. The second category consists of eigenstates which have an antisymmetric spatial function and non-zero spin vectors. For eigenstates in this category, the electrons follow circular orbits around the spin axis, which for our purposes was assumed to be constant and in the z-direction.

Lastly, we constructed a wavefunction, Ψ_γ, which depends on a parameter, $\gamma,\ 0 \leq \gamma \leq 1$ that produces an initial wavefunction that continuously changes from the eigenstate $\Psi^{(6)}_{hel}$ to the eigenstate $\Psi^{(3)}_{hel}$ as γ is continually increased from 0 to 1. We saw that the initial energy expectation increases from $E^{(6)}_{hel}$ to $E^{(3)}_{hel}$ in a continuous, nonlinear fashion, and more importantly, that the trajectories appear to continuously morph from those of $\Psi_0 = \Psi^{(6)}_{hel}$ to those of $\Psi_1 = \Psi^{(3)}_{hel}$. The point of this exercise was to show that BM provides a consistent model of the helium atom, and in general, we hope to leave the impression that BM is, at the very least, a consistent interpretation of non-relativistic quantum mechanics.

6.2 Additional Discussion of Bohmian Mechanics

We have also examined BM in light of some pressing issues in quantum mechanics. In chapter 2 we looked at the Bohmian descriptions of the EPR paradox and the measurement problem and found that BM is able to provide a consistent and reasonable resolution to both of these difficulties. According to the EPR experiment the measurement of the spin along any direction of one particle in a correlated pair, call it particle A, reveals the value of the spin of the other particle (particle B) in that direction with certainty. Since the direction along which the spin is measured is arbitrary, it seems that measurement of particle A immediately forces particle B into a particular spin state. However, according to the Bohmian description, particles travel

along trajectories through space and time and have well-defined spin vectors along these trajectories. Thus, measurement of the spin of particle A does not force particle B to take on the corresponding value, but merely reveals the pre-existing value of particle B. In this way, the EPR paradox is explained in a reasonable fashion.

Similarly, the continuous trajectories of BM provide a completely continuous description of a quantum measurement. According to Von Neumann, the wavefunction of the relevant apparatus particles splits into non-overlapping packets after a finite time, δt, each packet corresponding to a different eigenstate of the measured system. Thus, measurement is described through the one-to-one correspondence of the apparatus packets and the eigenstates of the measured system – if the apparatus packet A triggers the apparatus to "fire", then the eigenstate corresponding to the packet A is ascribed to the measured system. According to SQM, the wavefunction "collapses" to the state corresponding to the eigenvalue A and this "collapse" is discontinuous. Hence, it cannot be described by the Schrödinger equation. BM addresses this problem very easily. Since the apparatus particles follow trajectories through space and time, they will inevitably enter **one and only one** packet, thus producing a distinct measurement according to Von Neumann, but in a completely continuous way. The "collapse" of the wavefunction is consequently explained because the packets into which the apparatus particles do not enter become ineffective to the dynamics of the overall system and can be dropped from the wavefunction.

In addition to this, we have discussed some other benefits that BM has over SQM. First of all, there is potential for BM to be experimentally tested. In chapter 3 we outlined a number of experiments from multiple sources that propose to be able to differentiate between BM and SQM. Many of these experiments are based on variations of the classic double-slit experiment, one is based on the concept of ergodicity and one is based on BM's ability to distinguish between a "large" particle and a "small" one. Thus, there are multiple methods and as such, it seems promising that experiment will one day tell us whether BM is a true candidate for an accurate picture of matter on the quantum level. To our best knowledge, no experiment has yet made this determination.

Secondly, we examined three different attempts to connect the "wavy" quantum world with the classical world of experience. Each of these attempts relies specifically on the concept of particle trajectories and consequently, cannot be made in the context of SQM. The first paper derives the conditions

necessary under which the motion of the center of mass of a macroscopic object obeys the classical equation of motion, $M\ddot{x}_{CM} = F^{ext}$, where M is the mass of the object, x_{CM} is the position of the center of mass of the object and F^{ext} is the external force on the object. In order to arrive at their conclusion, the authors show that under the proper conditions the quantum forces become negligible and the object is guided purely by the classical forces acting on it.

The second paper is similar to the first, in that it endeavors to show that under certain conditions the quantum forces on a macroscopic object are negligible and the center of mass of the object moves classically. They approach this problem in a different way and start with the condition

$$\lambda \ll L \tag{3.37}$$

where λ is the deBroglie wavelength of the object and L is the scale of variation of the potential. Eqn. (3.37) is analogous to the condition

$$\hbar \ll A_0 \tag{3.38}$$

where A_0 is a characteristic action of the corresponding classical motion. This is commonly used as the condition to ensure classical behaviour. The authors find appropriate conditions on the potential so that eqn. (3.37) holds.

The third paper is an attempt to construct a single theory that describes both the classical and quantum domains. This theory is formulated in terms of a wave equation, similar in form to the Schrödinger equation, and particles are supposed to move along trajectories given by the Bohmian guidance condition, eqn. (2.7). It describes a continuous transition from classical mechanics to quantum mechanics using a continuous parameter λ. For $\lambda = 0$ the theory is equivalent to quantum mechanics and the system moves along its Bohmian trajectories. For $\lambda = 1$ the theory is equivalent to classical mechanics and the system moves along its classical trajectories. For $0 < \lambda < 1$ the system is in a "mixture" of classical and quantum mechanics which the authors call a "mesoscopic system". By making λ a time-dependent parameter, $\lambda = \lambda(t)$, and giving it appropriate time-dependence the theory describes a system which begins as completely quantum and continuously morphs into a completely classical system. In this way, the authors propose a model of decoherence in which the particles of the system move along continuous trajectories, thus giving a very intuitive picture of the process of decoherence.

6.3 Recommendations For Future Research

We were careful in Chapter 5 to point out all of the approximations used in constructing our model and in computing the trajectories. Recall that we truncated the infinite sum, eqn. (5.11), at nine terms. As mentioned in the previous section, this had little effect on our ability to accurately represent the ground state wavefunction. This is due to the fact that the nine terms we kept dominate the composition of the true ground state. This provides a method to represent an arbitrary helium eigenstate using a small number of terms in eqn. (5.11) – all one has to do is choose the terms of which the desired eigenstate is mostly composed. It is not obvious how to do this, but in general, eigenstates of higher energy will be composed of terms which represent hydrogenic eigenstates of higher energy. Table 5.4 provides examples of this principle. Similarly, the number of terms used increases the accuracy of the wavefunction. However, the tradeoff is that the matrices (5.17) and (5.18) are of size $n \times n$ where n is the number of terms retained in the sum (5.11). Thus, the computation requirements grow very fast with the number of terms in the wavefunction.

In addition, recall that our treatment of spin is somewhat artificial. Since we used the Schrödinger equation we had to assume that each electron had a constant spin vector. Since the spin-dependent motion of the eigenstates is either no motion, or circular orbits around the spin axis, the trajectories for the eigenstates are somewhat "unexciting". However, in the presence of magnetic field, (i.e., changing spin vectors), this term can be responsible for some interesting dynamics. As such, a natural extension of this work is to compute the Bohmian trajectories of the electrons in the helium atom under the Pauli equation and in the presence of a magnetic field. Although giving a full relativistic treatment would certainly give even more accurate results, we anticipate that the relativistic corrections supplied by the Dirac equation would be outweighed by the intrinsic error in the model due to the truncation of the sum (5.11). Although our model can be made increasingly accurate by using an appropriate number of terms in the wavefunction, we anticipate that in order to achieve the accuracy necessary so that relativistic corrections are at least of the order of the error in the overall wavefunction a large number of terms must be used. This fact, coupled with the complexity of the Dirac equation would amount to a problem that is computationally massive. As such, it is not recommended that one compute Bohmian trajectories under the Dirac equation unless a different model is used – one that is simpler

computationally.[1] However, we feel that our model should be satisfactory to compute trajectories under the Pauli equation.

Lastly, we propose that BM be used to analyze other systems. Although our study of the helium atom gave some fairly idealized results that most likely do not represent a true helium atom very accurately, BM can be used to give useable results about certain systems of interest. For example, Bohmian trajectories are currently being calculated for electrons traveling through a carbon nanotube. This allows one to analyze the conductance of a carbon nanotube quantum mechanically, something that would be much more difficult to do without the concept of particle trajectories.[2] Since technology is becoming increasingly smaller, quantum effects will become more and more prominent in various devices and we will need tools to analyze these effects. We propose that BM be added to the toolbox as the concept of particle trajectories may be very instructive to our understanding of our future hardware.

6.4 Concluding Remarks

We have attempted to show in this thesis that BM gives a consistent and reasonable description of quantum systems. It is our hope that anyone who reads this will walk away with not only an understanding of the Bohmian interpretation of non-relativistic quantum mechanics, but with an appreciation for the simple and intuitive picture of the quantum world that BM provides.

[1] *Quantum Mechanics of One- and Two-Electron Atoms* by Bethe and Selpeter is an excellent reference for different models of the helium wavefunction and may be a good starting point for this endeavour.

[2] The work of the author with D. Borka et. al. on this topic is not reported in this thesis. We expect our results to be published within a year.

Appendix A

Calculation of $R_{gh,ij}$

Recall from section 5.1 that

$$R_{gh,ij} = \int_{\Re^3}\int_{\Re^3} \Phi_g \Phi_h \frac{1}{r_{12}} \Phi_i \Phi_j \, d^3\tau_1 \, d^3\tau_2$$

where $1 \leq g, h, i, j \leq 3$ (we have set $e = 1$ because we are using atomic units). To calculate these terms, we expand $\frac{1}{r_{12}}$ in terms of the spherical harmonics, i.e.,

$$\frac{1}{r_{12}} = \sum_{l=0}^{\infty} \sum_{m=-l}^{l} \frac{4\pi}{2l+1} \frac{r_<^l}{r_>^{l+1}} Y_l^m\big(\theta_1, \phi_1\big)^* Y_l^m\big(\theta_2, \phi_2\big), \tag{A.1}$$

where $r_<$ is the smaller of r_1 and r_2, $r_>$ is the larger of r_1 and r_2 and Y_l^m is defined in eqn. (4.4). Using (A.1)

$$R_{gh,ij} = \sum_{l=0}^{\infty} \sum_{m=-l}^{l} \frac{4\pi}{2l+1} \big[RAD\big]\big[ANG\ 1\big]\big[ANG\ 2\big]$$

where

$$RAD = \int_0^{\infty}\int_0^{\infty} R_{n_g,l_g}(r_1) R_{n_h,l_h}(r_2) \frac{r_<^l}{r_>^{l+1}} R_{n_i,l_i}(r_1) R_{n_j,l_j}(r_2) r_1^2 r_2^2 \, dr_1 \, dr_2,$$

$$ANG\ 1 = \int_0^{2\pi} \int_0^{\pi} Y_{l_g}^{m_g}(\theta_1,\phi_1)^* Y_l^m(\theta_1,\phi_1)^* Y_{l_h}^{m_h}(\theta_1,\phi_1) \sin(\theta_1)\, d\theta_1\, d\phi_1$$

and

$$ANG\ 2 = \int_0^{2\pi} \int_0^{\pi} Y_{l_i}^{m_i}(\theta_2,\phi_2)^* Y_l^m(\theta_2,\phi_2) Y_{l_j}^{m_j}(\theta_2,\phi_2) \sin(\theta_2)\, d\theta_2\, d\phi_2.$$

We will examine each of these three terms in turn. First of all,

$$\begin{aligned} RAD = \int_0^{\infty} R_{n_h,l_h}(r_1) R_{n_j,l_j}(r_2) \Bigg[\int_0^{r_2} R_{n_g,l_g}(r_1) R_{n_i,l_i}(r_2) \frac{r_1^l}{r_2^{(l+1)}} r_1^2\, dr_1 \\ + \int_{r_2}^{\infty} R_{n_g,l_g}(r_1) R_{n_i,l_i}(r_1) \frac{r_2^l}{r_1^{(l+1)}} r_1^2\, dr_1 \Bigg] dr_2 \\ = \int_0^{\infty} R_{n_h,l_h}(r_2) R_{n_j,l_j}(r_2) r_2^{(-l+1)} \left[\int_0^{r_2} R_{n_g.l_g}(r_1) R_{n_i,l_i}(r_1) r_1^{(l+2)}\, dr_1 \right] dr_2 \\ + \int_0^{\infty} R_{n_h,l_h}(r_2) R_{n_j,l_j}(r_2) r_2^{(l+2)} \left[\int_{r_2}^{\infty} R_{n_g,l_g}(r_1) R_{n_i,l_i}(r_1) r_1^{(-l+1)}\, dr_1 \right] dr_2. \end{aligned}$$

Secondly,

$$\begin{aligned} ANG\ 1 = \int_0^{2\pi} \exp\left(\frac{i(-m_g - m + m_i)\phi_1}{\hbar} \right) d\phi_1 \\ \times \int_0^{\pi} C \mathcal{P}_{l_g}^{m_g}(cos\theta_1) \mathcal{P}_l^m(cos\theta_1) \mathcal{P}_{l_i}^{m_i}(cos\theta_1)\, d\theta_1. \end{aligned}$$

The ϕ_1-integral is zero unless $m = m_i - m_g$. When $m = m_i - m_g$ the ϕ_1-integral is equal to 2π and

$$ANG\ 1 = 2\pi C \int_0^{\pi} \mathcal{P}_{l_g}^{m_g}(cos\theta_1) \mathcal{P}_l^m(cos\theta_1) \mathcal{P}_{l_i}^{m_i}(cos\theta_1)\, d\theta_1.$$

Here, C is a constant that depends on l_g, m_g, l, m, l_i and m_i.

Similarly,

$$ANG\ 2 = \int_0^{2\pi} \exp\left(\frac{i(-m_h + m + m_j)\phi_2}{\hbar}\right) d\phi_2$$
$$\times \int_0^{\pi} D\mathcal{P}_{l_h}^{m_h}(cos\theta_2)\mathcal{P}_l^m(cos\theta_2)\mathcal{P}_{l_j}^{m_j}(cos\theta_2)\, d\theta_2$$

and the ϕ_2-integral is zero unless $m = m_h - m_j$. When $m = m_h - m_j$

$$ANG\ 2 = 2\pi D \int_0^{\pi} \mathcal{P}_{l_h}^{m_h}(cos\theta_2)\mathcal{P}_l^m(cos\theta_2)\mathcal{P}_{l_j}^{m_j}(cos\theta_2)\, d\theta_2,$$

where D is a constant that depends on l_h, m_h, l, m. l_j and m_j.

Thus, $R_{gh,ij} = 0$ unless $m = m_i - m_g = m_h - m_j$. In addition, integrals of the form $ANG\ 1$ vanish unless $|l_g - l_i| \leq l \leq l_g + l_i$ **and** $m_g + m + m_i + L_g + L + L_i = 0$ (and similarly, for $ANG\ 2$) [2].

$R_{gh,ij}$ has been evaluated for $1 \leq g, h, i, j \leq 3$ using *Maple*. The results are displayed in the following table.

(g,h)\(i,j)	(1,1)	(1,2)	(1,3)	(2,1)	(2,2)	(2,3)	(3,1)	(3,2)	(3,3)
(1,1)	$\frac{5}{8}$	$\frac{4096\sqrt{2}}{64827}$	0	$\frac{4096\sqrt{2}}{64827}$	$\frac{16}{729}$	0	0	0	$\frac{112}{6561}$
(1,2)	$\frac{4096\sqrt{2}}{64827}$	$\frac{17}{81}$	0	$\frac{16}{729}$	$\frac{512\sqrt{2}}{84375}$	0	0	0	$-\frac{256\sqrt{2}}{28125}$
(1,3)	0	0	$\frac{59}{243}$	0	0	$\frac{512\sqrt{2}}{84375}$	$\frac{112}{6561}$	$-\frac{256\sqrt{2}}{28125}$	0
(2,1)	$\frac{4096\sqrt{2}}{64827}$	$\frac{16}{729}$	0	$\frac{17}{81}$	$\frac{512\sqrt{2}}{84375}$	0	0	0	$-\frac{256\sqrt{2}}{28125}$
(2,2)	$\frac{16}{729}$	$\frac{512\sqrt{2}}{84375}$	0	$\frac{512\sqrt{2}}{84375}$	$\frac{77}{512}$	0	0	0	$\frac{15}{512}$
(2,3)	0	0	$\frac{512\sqrt{2}}{84375}$	0	0	$\frac{83}{512}$	$-\frac{256\sqrt{2}}{28125}$	$\frac{15}{512}$	0
(3,1)	0	0	$\frac{112}{6561}$	0	0	$-\frac{256\sqrt{2}}{28125}$	$\frac{59}{243}$	$\frac{512\sqrt{2}}{84375}$	0
(3,2)	0	0	$-\frac{256\sqrt{2}}{28125}$	0	0	$\frac{15}{512}$	$\frac{512\sqrt{2}}{84375}$	$\frac{83}{512}$	0
(3,3)	$\frac{112}{6561}$	$-\frac{256\sqrt{2}}{28125}$	0	$-\frac{256\sqrt{2}}{28125}$	$\frac{15}{512}$	0	0	0	$\frac{501}{2560}$

Table A.1: The $R_{gh,ij}$.

Appendix B

Energy Expectation

The energy expectation is given by the standard formula

$$\langle E \rangle = \left\langle \Psi^*_{hel} \left| \hat{H}_{hel} \right| \Psi_{hel} \right\rangle, \tag{B.1}$$

where

$$\hat{H}_{hel} = -\frac{\hbar^2}{2m}\nabla_1^2 - \frac{\hbar^2}{2m}\nabla_2^2 - \frac{Ze^2}{r_1} - \frac{Ze^2}{r_2} + \frac{e^2}{r_{12}}$$

and

$$\Psi_{hel}(r_1, \theta_1, \phi_1, r_2, \theta_2, \phi_2, t) = \sum_{i=1}^{3}\sum_{j=1}^{3} c_{ij}(t)\Phi_i(r_1, \theta_1, \phi_1)\Phi_j(r_2, \theta_2, \phi_2).$$

Recall that the Hamiltonian is the sum of two terms. The first, $\hat{H}_0$, represents two independent hydrogenic electrons and the second, $\hat{H}_1$, represents the interaction between them (cf. eqns. (5.2), (5.3) and (5.4)). Thus, we can expand (B.1) as

$$\left\langle \Psi^*_{hel} \left| \hat{H}_{hel} \right| \Psi_{hel} \right\rangle = \left\langle \Psi^*_{hel} \left| \hat{H}_0 \right| \Psi_{hel} \right\rangle + \left\langle \Psi^*_{hel} \left| \hat{H}_1 \right| \Psi_{hel} \right\rangle.$$

The first term is

$$\left\langle \Psi^*_{hel} \left| \hat{H}_0 \right| \Psi_{hel} \right\rangle = \sum_{g,h=1}^{3} \sum_{i,j=1}^{3} c^*_{gh} c_{ij} \times \left\langle \Phi_{n_g,l_g}(\vec{r}_1)\Phi_{n_h,l_h}(\vec{r}_2) \left| \hat{H}_0^{(1)} + \hat{H}_0^{(2)} \right| \Phi_{n_i,l_i}(\vec{r}_1)\Phi_{n_j,l_j}(\vec{r}_2) \right\rangle \quad \text{(B.2)}$$

where $\hat{H}_0^{(1)}$ is a hydrogenic Hamiltonian acting on electron 1 and $\hat{H}_0^{(2)}$ is a hydrogenic Hamiltonian acting on electron 2.
Using the hydrogenic eigenvalue equation

$$\hat{H}_0^{(i)} \Phi_{n_\alpha,l_\alpha}(\vec{r_i}) = E^{(0)}_{n_\alpha} \Phi_{n_\alpha,l_\alpha}(\vec{r_i}),$$

(B.2) becomes

$$\begin{aligned}
\left\langle \Psi^*_{hel} \left| \hat{H}_0 \right| \Psi_{hel} \right\rangle &= \sum_{g,h=1}^{3} \sum_{i,j=1}^{3} c^*_{gh} c_{ij} \big(E^{(0)}_{n_i} + E^{(0)}_{n_j} \big) \\
&\qquad \times \left\langle \Phi_{n_g,l_g}(\vec{r}_1)\Phi_{n_h,l_h}(\vec{r}_2) | \Phi_{n_i,l_i}(\vec{r}_1)\Phi_{n_j,l_j}(\vec{r}_2) \right\rangle \\
&= \sum_{g,h=1}^{3} \sum_{i,j=1}^{3} c^*_{gh} c_{ij} \big(E^{(0)}_{n_i} + E^{(0)}_{n_j} \big) \delta_{g,i} \delta_{h,j} \\
&= \sum_{i,j=1}^{3} |c_{ij}|^2 \big(E^{(0)}_{n_i} + E^{(0)}_{n_j} \big)
\end{aligned}$$

where $\delta_{\alpha,\beta}$ is the Kronecker delta and the orthogonality of the hydrogenic eigenfunctions was used in the above calculations (cf. eqn. (4.6)).

The second term is

$$\begin{aligned}
\left\langle \Psi^*_{hel} \left| \hat{H}_1 \right| \Psi_{hel} \right\rangle &= \sum_{g,h=1}^{3} \sum_{i,j=1}^{3} c^*_{gh} c_{ij} \left\langle \Phi_g(\vec{r_1})\Phi_h(\vec{r_2}) \left| \frac{e^2}{r_{12}} \right| \Phi_i(\vec{r_1})\Phi_j(\vec{r_2}) \right\rangle \\
&= \sum_{g,h=1}^{3} \sum_{i,j=1}^{3} c^*_{gh} c_{ij} R_{gh,ij}
\end{aligned}$$

Putting this together, the energy expectation is given by

$$\begin{aligned}\langle E\rangle &= \sum_{i,j=1}^{3} |c_{ij}|^2\big(E^{(0)}_{n_i} + E^{(0)}_{n_j}\big) + \sum_{g,h=1}^{3}\sum_{i,j=1}^{3} c^*_{gh}c_{ij}R_{gh,ij} \\ &= \sum_{i,j=1}^{3} |c_{ij}|^2\big(E^{(0)}_{n_i} + E^{(0)}_{n_j}\big) + \sum_{g,h=1}^{3}\sum_{i,j=1}^{3} \big(a_{gh}a_{ij} + b_{gh}b_{ij}\big)R_{gh,ij}.\end{aligned}$$

Appendix C

Calculation of Spin Vectors

The components of the spin vectors are given by the Pauli spin operators:

$$\hat{s}_{i_j} = \left(\frac{\hbar}{2\rho} \Psi^{\dagger}_{hel} \sigma_{i_j} \Psi_{hel} \right) \tag{C.1}$$

where $i = 1, 2$ represents electron number and $j = 1, 2, 3$ refers respectively to the x-direction, y-direction and z-direction and σ_{i_j} is the j^{th} Pauli spin matrix for electron i. Recall that the Pauli spin matrices are given by

$$\sigma_{i_x} = \begin{pmatrix} 0 & 1 \\ 1 & 0 \end{pmatrix}_i, \quad \sigma_{i_y} = \begin{pmatrix} 0 & -i \\ i & 0 \end{pmatrix}_i \quad \text{and} \quad \sigma_{i_z} = \begin{pmatrix} 1 & 0 \\ 0 & -1 \end{pmatrix}_i \tag{2.9}$$

.

where $i = 1$ refers to electron 1 and $i = 2$ refers to electron 2. Pauli matrices with subscript i act only on the parts of the wavefunction that refer to electron i. Since the wavefunction factors into a spatial part multiplied by a spin part, eqn. (C.1) becomes

$$\begin{aligned}\hat{s}_{i_j} &= \left(\frac{\hbar}{2\rho}\Psi^{\dagger}_{hel}\sigma_{i_j}\Psi_{hel}\right) \\ &= \frac{\hbar}{2\rho}\left(\Psi^{*}_{hel}\Omega^{\dagger}_{spin}\sigma_{i_j}\Psi_{hel}\Omega_{spin}\right) \\ &= \left(\frac{\hbar}{2\rho}\right)\left(\Psi^{*}_{hel}\Psi_{hel}\right)\left(\Omega^{\dagger}_{spin}\sigma_{i_j}\Omega_{spin}\right) \\ &= \frac{\hbar}{2}\left(\Omega^{\dagger}_{spin}\sigma_{i_j}\Omega_{spin}\right). \end{aligned} \tag{C.2}$$

It is clear from (C.2) that Ω_{spin} and $\Omega^{\dagger}_{spin}$ must be 2-component entities. Recall from section 5.3 that Ω_{spin} has the general form

$$\Omega_{spin} = d_{11}\alpha(s_1)\alpha(s_2)+d_{12}\alpha(s_1)\beta(s_2)+d_{21}\beta(s_1)\alpha(s_2)+d_{22}\beta(s_1)\beta(s_2), \tag{5.24}$$

where d_{11}, d_{12}, d_{21} and d_{22} are constants. Thus, we need to represent $\alpha(s_i)$ and $\beta(s_i)$ as 2-component spinors. To do this we make use of the eigenvalue equations

$$\hat{s}_{i_3}\alpha(s_i) = \alpha(s_i) \tag{C.3}$$

and

$$\hat{s}_{i_3}\beta(s_i) = -\beta(s_i). \tag{C.4}$$

Solving (C.3) and (C.4) gives

$$\alpha(s_i) = \begin{pmatrix}1\\0\end{pmatrix}_i \qquad \text{and} \qquad \beta(s_i) = \begin{pmatrix}0\\1\end{pmatrix}_i.$$

Since Ω_{spin} is composed of real 2-component spinors, $\Omega^{\dagger}_{spin}$ becomes Ω^{T}_{spin} and (C.2) becomes

$$\hat{s}_{i_j} = \frac{\hbar}{2}\left(\Omega^{T}_{spin}\sigma_{i_j}\Omega_{spin}\right).$$

Now let us calculate the spin vectors for each electron. We will examine each of the four spin states separately. First consider the antisymmetric spin state

given by

$$\begin{aligned}\Omega_{anti} &= \frac{1}{\sqrt{2}}\big(\alpha(s_1)\beta(s_2) - \alpha(s_2)\beta(s_1)\big) \\ &= \frac{1}{\sqrt{2}}\left[\begin{pmatrix}1\\0\end{pmatrix}_1\begin{pmatrix}0\\1\end{pmatrix}_2 - \begin{pmatrix}0\\1\end{pmatrix}_1\begin{pmatrix}1\\0\end{pmatrix}_2\right].\end{aligned}$$

The spin vector for electron 1 is $\vec{s}_1 = (s_{1_1}, s_{1_2}, s_{1_3})$ where

$$\begin{aligned}s_{1_1} &= \left(\frac{\hbar}{2}\right)\Omega_{anti}^T\sigma_{1_1}\Omega_{anti} \\ &= \frac{\hbar}{4}\left[\begin{pmatrix}1 & 0\end{pmatrix}_1\begin{pmatrix}0 & 1\end{pmatrix}_2 - \begin{pmatrix}0 & 1\end{pmatrix}_1\begin{pmatrix}1 & 0\end{pmatrix}_2\right]\begin{bmatrix}0 & 1\\1 & 0\end{bmatrix}_1\left[\begin{pmatrix}1\\0\end{pmatrix}_1\begin{pmatrix}0\\1\end{pmatrix}_2 - \begin{pmatrix}0\\1\end{pmatrix}_1\begin{pmatrix}1\\0\end{pmatrix}_2\right] \\ &= \frac{\hbar}{4}\left[\begin{pmatrix}1 & 0\end{pmatrix}_1\begin{pmatrix}0 & 1\end{pmatrix}_2 - \begin{pmatrix}0 & 1\end{pmatrix}_1\begin{pmatrix}1 & 0\end{pmatrix}_2\right]\left[\begin{pmatrix}0\\1\end{pmatrix}_1\begin{pmatrix}0\\1\end{pmatrix}_2 - \begin{pmatrix}1\\0\end{pmatrix}_1\begin{pmatrix}1\\0\end{pmatrix}_2\right] \\ &= \frac{\hbar}{4}\big[(0)(1) - (1)(0) - (1)(0) + (0)(1)\big] \\ &= 0,\end{aligned}$$

$$\begin{aligned}s_{1_2} &= \left(\frac{\hbar}{2}\right)\Omega_{anti}^T\sigma_{1_2}\Omega_{anti} \\ &= \frac{\hbar}{4}\left[\begin{pmatrix}1 & 0\end{pmatrix}_1\begin{pmatrix}0 & 1\end{pmatrix}_2 - \begin{pmatrix}0 & 1\end{pmatrix}_1\begin{pmatrix}1 & 0\end{pmatrix}_2\right]\begin{bmatrix}0 & -i\\i & 0\end{bmatrix}_1\left[\begin{pmatrix}1\\0\end{pmatrix}_1\begin{pmatrix}0\\1\end{pmatrix}_2 - \begin{pmatrix}0\\1\end{pmatrix}_1\begin{pmatrix}1\\0\end{pmatrix}_2\right] \\ &= \frac{\hbar}{4}\left[\begin{pmatrix}1 & 0\end{pmatrix}_1\begin{pmatrix}0 & 1\end{pmatrix}_2 - \begin{pmatrix}0 & 1\end{pmatrix}_1\begin{pmatrix}1 & 0\end{pmatrix}_2\right]\left[\begin{pmatrix}0\\i\end{pmatrix}_1\begin{pmatrix}0\\1\end{pmatrix}_2 - \begin{pmatrix}-i\\0\end{pmatrix}_1\begin{pmatrix}1\\0\end{pmatrix}_2\right] \\ &= \frac{\hbar}{4}\big[(0)(1) - (-i)(0) - (i)(0) + (0)(1)\big] \\ &= 0\end{aligned}$$

and

$$
\begin{aligned}
s_{1_3} &= \left(\frac{\hbar}{2}\right)\Omega_{anti}^{T}\sigma_{1_3}\Omega_{anti} \\
&= \frac{\hbar}{4}\Big[\,(1\ \ 0)_1\,(0\ \ 1)_2 - (0\ \ 1)_1\,(1\ \ 0)_2\,\Big]\begin{bmatrix}1 & 0\\ 0 & -1\end{bmatrix}_1\left[\binom{1}{0}_1\binom{0}{1}_2 - \binom{0}{1}_1\binom{1}{0}_2\right] \\
&= \frac{\hbar}{4}\Big[\,(1\ \ 0)_1\,(0\ \ 1)_2 - (0\ \ 1)_1\,(1\ \ 0)_2\,\Big]\left[\binom{1}{0}_1\binom{0}{1}_2 - \binom{0}{-1}_1\binom{1}{0}_2\right] \\
&= \frac{\hbar}{4}\big[(1)(1) - (0)(0) - (0)(0) + (-1)(1)\big] \\
&= 0.
\end{aligned}
$$

Thus, the spin vector of electron 1 is $\vec{s}_1 = (0, 0, 0)$. Similarly, the spin vector for electron 2 is $\vec{s}_2 = (s_{2_1}, s_{2_2}, s_{2_3})$ where

$$
\begin{aligned}
s_{2_1} &= \left(\frac{\hbar}{2}\right)\Omega_{anti}^{T}\sigma_{2_1}\Omega_{anti} \\
&= \frac{\hbar}{4}\Big[\,(1\ \ 0)_1\,(0\ \ 1)_2 - (0\ \ 1)_1\,(1\ \ 0)_2\,\Big]\begin{bmatrix}0 & 1\\ 1 & 0\end{bmatrix}_2\left[\binom{1}{0}_1\binom{0}{1}_2 - \binom{0}{1}_1\binom{1}{0}_2\right] \\
&= \frac{\hbar}{4}\Big[\,(1\ \ 0)_1\,(0\ \ 1)_2 - (0\ \ 1)_1\,(1\ \ 0)_2\,\Big]\left[\binom{1}{0}_1\binom{1}{0}_2 - \binom{0}{1}_1\binom{0}{1}_2\right] \\
&= \frac{\hbar}{4}\big[(1)(0) - (0)(1) - (0)(1) + (1)(0)\big] \\
&= 0,
\end{aligned}
$$

$$
\begin{aligned}
s_{2_2} &= \left(\frac{\hbar}{2}\right)\Omega_{anti}^{T}\sigma_{2_2}\Omega_{anti} \\
&= \frac{\hbar}{4}\Big[\,(1\ \ 0)_1\,(0\ \ 1)_2 - (0\ \ 1)_1\,(1\ \ 0)_2\,\Big]\begin{bmatrix}0 & -i\\ i & 0\end{bmatrix}_2\left[\binom{1}{0}_1\binom{0}{1}_2 - \binom{0}{1}_1\binom{1}{0}_2\right] \\
&= \frac{\hbar}{4}\Big[\,(1\ \ 0)_1\,(0\ \ 1)_2 - (0\ \ 1)_1\,(1\ \ 0)_2\,\Big]\left[\binom{1}{0}_1\binom{i}{0}_2 - \binom{0}{1}_1\binom{0}{-i}_2\right] \\
&= \frac{\hbar}{4}\big[(1)(0) - (0)(i) - (0)(-i) + (1)(0)\big] \\
&= 0
\end{aligned}
$$

and

$$
\begin{aligned}
s_{2_3} &= \left(\frac{\hbar}{2}\right)\Omega_{anti}^{T}\sigma_{2_3}\Omega_{anti} \\
&= \frac{\hbar}{4}\Big[\,(1\ \ 0)_1\,(0\ \ 1)_2 - (0\ \ 1)_1\,(1\ \ 0)_2\,\Big]\begin{bmatrix}1 & 0\\ 0 & -1\end{bmatrix}_2\left[\begin{pmatrix}1\\0\end{pmatrix}_1\begin{pmatrix}0\\1\end{pmatrix}_2 - \begin{pmatrix}0\\1\end{pmatrix}_1\begin{pmatrix}1\\0\end{pmatrix}_2\right] \\
&= \frac{\hbar}{4}\Big[\,(1\ \ 0)_1\,(0\ \ 1)_2 - (0\ \ 1)_1\,(1\ \ 0)_2\,\Big]\left[\begin{pmatrix}1\\0\end{pmatrix}_1\begin{pmatrix}0\\-1\end{pmatrix}_2 - \begin{pmatrix}0\\1\end{pmatrix}_1\begin{pmatrix}1\\0\end{pmatrix}_2\right] \\
&= \frac{\hbar}{4}\big[(1)(-1) - (0)(0) - (0)(0) + (1)(1)\big] \\
&= 0.
\end{aligned}
$$

Thus, the spin vector of electron 2 is $\vec{s}_2 = (0, 0, 0)$. The calculations are very similar for the symmetric spin function

$$
\begin{aligned}
\Omega_{sym} &= \frac{1}{\sqrt{2}}\big(\alpha(s_1)\beta(s_2) + \alpha(s_2)\beta(s_1)\big) \\
&= \frac{1}{\sqrt{2}}\left[\begin{pmatrix}1\\0\end{pmatrix}_1\begin{pmatrix}0\\1\end{pmatrix}_2 + \begin{pmatrix}0\\1\end{pmatrix}_1\begin{pmatrix}1\\0\end{pmatrix}_2\right]
\end{aligned}
$$

and the result is $\vec{s}_1 = \vec{s}_2 = (0, 0, 0)$.

Now consider the symmetric "spin up" function

$$
\begin{aligned}
\Omega_{up} &= \alpha(s_1)\alpha(s_2) \\
&= \begin{pmatrix}1\\0\end{pmatrix}_1\begin{pmatrix}1\\0\end{pmatrix}_2.
\end{aligned}
$$

The spin vector for electron 1 is $\vec{s}_1 = (s_{1_1}, s_{1_2}, s_{1_3})$ where

$$
\begin{aligned}
s_{1_1} &= \left(\frac{\hbar}{2}\right) \Omega_{up}^T \sigma_{1_1} \Omega_{up} \\
&= \frac{\hbar}{2}\left[\begin{pmatrix} 1 & 0 \end{pmatrix}_1 \begin{pmatrix} 1 & 0 \end{pmatrix}_2 \right] \begin{bmatrix} 0 & 1 \\ 1 & 0 \end{bmatrix}_1 \left[\begin{pmatrix} 1 \\ 0 \end{pmatrix}_1 \begin{pmatrix} 1 \\ 0 \end{pmatrix}_2 \right] \\
&= \frac{\hbar}{2}\left[\begin{pmatrix} 1 & 0 \end{pmatrix}_1 \begin{pmatrix} 1 & 0 \end{pmatrix}_2 \right] \left[\begin{pmatrix} 0 \\ 1 \end{pmatrix}_1 \begin{pmatrix} 1 \\ 0 \end{pmatrix}_2 \right] \\
&= \frac{\hbar}{2}\big[(0)(1)\big] \\
&= 0,
\end{aligned}
$$

$$
\begin{aligned}
s_{1_2} &= \left(\frac{\hbar}{2}\right) \Omega_{up}^T \sigma_{1_2} \Omega_{up} \\
&= \frac{\hbar}{2}\left[\begin{pmatrix} 1 & 0 \end{pmatrix}_1 \begin{pmatrix} 1 & 0 \end{pmatrix}_2 \right] \begin{bmatrix} 0 & -i \\ i & 0 \end{bmatrix}_1 \left[\begin{pmatrix} 1 \\ 0 \end{pmatrix}_1 \begin{pmatrix} 1 \\ 0 \end{pmatrix}_2 \right] \\
&= \frac{\hbar}{2}\left[\begin{pmatrix} 1 & 0 \end{pmatrix}_1 \begin{pmatrix} 1 & 0 \end{pmatrix}_2 \right] \left[\begin{pmatrix} 0 \\ i \end{pmatrix}_1 \begin{pmatrix} 1 \\ 0 \end{pmatrix}_2 \right] \\
&= \frac{\hbar}{2}\big[(0)(1)\big] \\
&= 0
\end{aligned}
$$

and

$$
\begin{aligned}
s_{1_3} &= \left(\frac{\hbar}{2}\right) \Omega_{up}^T \sigma_{1_1} \Omega_{up} \\
&= \frac{\hbar}{2}\left[\begin{pmatrix} 1 & 0 \end{pmatrix}_1 \begin{pmatrix} 1 & 0 \end{pmatrix}_2 \right] \begin{bmatrix} 1 & 0 \\ 0 & -1 \end{bmatrix}_1 \left[\begin{pmatrix} 1 \\ 0 \end{pmatrix}_1 \begin{pmatrix} 1 \\ 0 \end{pmatrix}_2 \right] \\
&= \frac{\hbar}{2}\left[\begin{pmatrix} 1 & 0 \end{pmatrix}_1 \begin{pmatrix} 1 & 0 \end{pmatrix}_2 \right] \left[\begin{pmatrix} 1 \\ 0 \end{pmatrix}_1 \begin{pmatrix} 1 \\ 0 \end{pmatrix}_2 \right] \\
&= \frac{\hbar}{2}\big[(1)(1)\big] \\
&= \frac{\hbar}{2}.
\end{aligned}
$$

Thus, the spin vector for electron 1 is $\vec{s}_1 = (0, 0, \frac{\hbar}{2})$. Similarly, the spin vector for electron 2 is $\vec{s}_2 = (s_{2_1}, s_{2_2}, s_{2_3})$ where

$$\begin{aligned}
s_{2_1} &= \left(\frac{\hbar}{2}\right) \Omega_{up}^T \sigma_{2_1} \Omega_{up} \\
&= \frac{\hbar}{2}\left[\begin{pmatrix} 1 & 0 \end{pmatrix}_1 \begin{pmatrix} 1 & 0 \end{pmatrix}_2 \right] \begin{bmatrix} 0 & 1 \\ 1 & 0 \end{bmatrix}_2 \left[\begin{pmatrix} 1 \\ 0 \end{pmatrix}_1 \begin{pmatrix} 1 \\ 0 \end{pmatrix}_2 \right] \\
&= \frac{\hbar}{2}\left[\begin{pmatrix} 1 & 0 \end{pmatrix}_1 \begin{pmatrix} 1 & 0 \end{pmatrix}_2 \right] \left[\begin{pmatrix} 1 \\ 0 \end{pmatrix}_1 \begin{pmatrix} 0 \\ 1 \end{pmatrix}_2 \right] \\
&= \frac{\hbar}{2}\big[(1)(0)\big] \\
&= 0,
\end{aligned}$$

$$\begin{aligned}
s_{2_2} &= \left(\frac{\hbar}{2}\right) \Omega_{up}^T \sigma_{2_2} \Omega_{up} \\
&= \frac{\hbar}{2}\left[\begin{pmatrix} 1 & 0 \end{pmatrix}_1 \begin{pmatrix} 1 & 0 \end{pmatrix}_2 \right] \begin{bmatrix} 0 & -i \\ i & 0 \end{bmatrix}_2 \left[\begin{pmatrix} 1 \\ 0 \end{pmatrix}_1 \begin{pmatrix} 1 \\ 0 \end{pmatrix}_2 \right] \\
&= \frac{\hbar}{2}\left[\begin{pmatrix} 1 & 0 \end{pmatrix}_1 \begin{pmatrix} 1 & 0 \end{pmatrix}_2 \right] \left[\begin{pmatrix} 1 \\ 0 \end{pmatrix}_1 \begin{pmatrix} 0 \\ i \end{pmatrix}_2 \right] \\
&= \frac{\hbar}{2}\big[(1)(0)\big] \\
&= 0
\end{aligned}$$

and

$$
\begin{aligned}
s_{2_3} &= \left(\frac{\hbar}{2}\right)\Omega_{up}^{T}\sigma_{2_3}\Omega_{up} \\
&= \frac{\hbar}{2}\begin{bmatrix} (1 \quad 0)_1 (1 \quad 0)_2 \end{bmatrix}\begin{bmatrix} 1 & 0 \\ 0 & -1 \end{bmatrix}_2 \left[\binom{1}{0}_1 \binom{1}{0}_2\right] \\
&= \frac{\hbar}{2}\begin{bmatrix} (1 \quad 0)_1 (1 \quad 0)_2 \end{bmatrix}\left[\binom{1}{0}_1 \binom{1}{0}_2\right] \\
&= \frac{\hbar}{2}\big[(1)(1)\big] \\
&= \frac{\hbar}{2}.
\end{aligned}
$$

Thus, the spin vector of electron 2 is $\vec{s}_2 = (0, 0, \frac{\hbar}{2})$. The calculations are similar for the "spin down" function

$$
\begin{aligned}
\Omega_{down} &= \beta(s_1)\beta(s_2) \\
&= \left[\binom{0}{1}_1 \binom{0}{1}_2\right]
\end{aligned}
$$

and the result is $\vec{s}_1 = \vec{s}_2 = (0, 0, -\frac{\hbar}{2})$.

Appendix D

The Ritz Variational Method For Helium

Substituting Ψ_{hel} into (5.33) yields

$$E[\Psi_{hel}] = \frac{\int \Psi^*_{hel} \hat{H}_{hel} \Psi_{hel} \, d\vec{r}_1 \, d\vec{r}_2}{\Psi^*_{hel} \Psi_{hel} \, d\vec{r}_1 \, d\vec{r}_2}.$$

The numerator is

$$\int \Psi^*_{hel} \hat{H}_0 \Psi_{hel} \, d\vec{r}_1 \, d\vec{r}_2 + \int \Psi^*_{hel} \hat{H}_1 \Psi_{hel} \, d\vec{r}_1 \, d\vec{r}_2 \tag{D.1}$$

which is the sum of two terms. We will examine each term in turn. Using the fact that $\hat{H}_0$ is the Hamiltonian for two independent hydrogenic electrons and substituting for Ψ_{hel} the first term becomes

$$\int d\vec{r}_1 \, d\vec{r}_2 \left(\sum_{g,h=1}^{3} c^*_{gh} \Phi_g(\vec{r}_1) \Phi_h(\vec{r}_2) \right) \left(\sum_{i,j=1}^{3} (E_i + E_j) c_{ij} \Phi_i(\vec{r}_1) \Phi_j(\vec{r}_2) \right).$$

Similarly, the second term is

$$\int d\vec{r}_1 \, d\vec{r}_2 \left(\sum_{g,h=1}^{3} c^*_{gh} \Phi_g(\vec{r}_1) \Phi_h(\vec{r}_2) \right) \left(e^2 \sum_{i,j=1}^{3} \frac{c_{ij} \Phi_i(\vec{r}_1) \Phi_j(\vec{r}_2)}{r_{12}} \right).$$

Let I_{ghij} be defined by

$$I_{ghij} \equiv \int d\vec{r}_1\, d\vec{r}_2\, \Phi_g(\vec{r}_1)\Phi_h(\vec{r}_2)\Phi_i(\vec{r}_1)\Phi_j(\vec{r}_2)$$

and let R_{ghij} be defined by

$$R_{ghij} \equiv e^2 \int \frac{d\vec{r}_1\, d\vec{r}_2\, \Phi_g(\vec{r}_1)\Phi_h(\vec{r}_2)\Phi_i(\vec{r}_1)\Phi_j(\vec{r}_2)}{r_{12}}.$$

Then (D.1) can be written as

$$\sum_{g,h,i,j=1}^{3} c^*_{gh} c_{ij} \left[(E_i + E_j) I_{ghij} + R_{ghij}\right]. \tag{D.2}$$

Now we will examine the denominator. The denominator is

$$\sum_{g,h,i,j=1}^{3} c^*_{gh} c_{ij} \int d\vec{r}_1\, d\vec{r}_2\, \Phi_g(\vec{r}_1)\Phi_h(\vec{r}_2)\Phi_i(\vec{r}_1)\Phi_j(\vec{r}_2)$$

$$= \sum_{g,h,i,j=1}^{3} c^*_{gh} c_{ij} I_{ghij}. \tag{D.3}$$

Putting (D.2) and (D.3) together gives

$$E[\Psi_{hel}] = \frac{\sum_{g,h,i,j=1}^{3} c^*_{gh} c_{ij} \left[(E_i + E_j) I_{ghij} + R_{ghij}\right]}{\sum_{g,h,i,j=1}^{3} c^*_{gh} c_{ij} I_{ghij}}. \tag{D.4}$$

The variational method is to minimize (D.4) with respect to each of the c_{ij}. To do this we set

$$\frac{\partial E[\psi_{hel}]}{\partial c^*_{ij}} = 0 \text{ for } 1 \le i, j \le 3.$$

This yields 9 coupled equations which can be solved simultaneously to give the $\{c_{ij}\}$. Taking the derivative of $E[\Psi_{hel}]$ with respect to c^*_{ij} gives

$$\frac{\partial E[\psi_{hel}]}{\partial c^*_{gh}} = \frac{\sum_{i,j=1}^{3} c_{ij}\left[(E_i+E_j)I_{ghij}+R_{ghij}\right]}{\sum_{k,l,m,n=1}^{3} c^*_{kl}c_{mn}I_{klmn}} - \frac{\sum_{i,j=1}^{3} c_{ij}I_{ghij}\sum_{k,l,m,n=1}^{3} c^*_{kl}c_{mn}\left[(E_m+E_n)I_{klmn}+R_{klmn}\right]}{\left[\sum_{k,l,m,n=1}^{3} c^*_{kl}c_{mn}I_{klmn}\right]^2}. \quad \text{(D.5)}$$

and setting the right-hand side of (D.5) equal to zero gives the nine equations we desire. These equations are

$$\sum_{i,j=1}^{3} c_{ij}\left[(E_i+E_j)I_{ghij}+R_{ghij}\right]\sum_{k,l,m,n=1}^{3} c^*_{kl}c_{mn}I_{klmn} = \sum_{i,j=1}^{3} c_{ij}I_{ghij}\sum_{k,l,m,n=1}^{3} c^*_{kl}c_{mn}\left[(E_m+E_n)I_{klmn}+R_{klmn}\right] \text{ for } 1\le g,h\le 3. \quad \text{(D.6)}$$

These equations can be solved simultaneously for the nine complex coefficients, $\{c_{ij}\}$. Alternatively, we can break (D.6) into real and imaginary parts which leads to the following 18 coupled equations for the $\{a_{ij}\}$ and $\{b_{ij}\}$:

$$\sum_{i,j=1}^{3} a_{ij}\left[(E_i+E_j)I_{ghij}+R_{ghij}\right]\sum_{k,l,m,n=1}^{3}\left(a_{kl}a_{mn}+b_{kl}b_{mn}\right)I_{klmn} = \sum_{i,j=1}^{3} a_{ij}I_{ghij}\sum_{k,l,m,n=1}^{3}\left(a_{kl}a_{mn}+b_{kl}b_{mn}\right)\left[(E_m+E_n)I_{klmn}+R_{klmn}\right] \quad \text{(D.7)}$$

and

$$\sum_{i,j=1}^{3} b_{ij}\left[(E_i+E_j)I_{ghij}+R_{ghij}\right]\sum_{k,l,m,n=1}^{3}\left(a_{kl}a_{mn}+b_{kl}b_{mn}\right)I_{klmn}$$
$$=\sum_{i,j=1}^{3} b_{ij}I_{ghij}\sum_{k,l,m,n=1}^{3}\left(a_{kl}a_{mn}+b_{kl}b_{mn}\right)\left[(E_m+E_n)I_{klmn}+R_{klmn}\right]. \quad \text{(D.8)}$$

Eqn. (D.7) gives nine equations and eqn. (D.8) gives nine equations (one for each $1 \leq g, h \leq 3$). These can be simultaneously solved to yield the $\{a_{ij}\}$ and $\{b_{ij}\}$.

Appendix E

Coefficients For Eigenstates of $\hat{H}_{hel}$

For each of the eigenstates of $\hat{H}_{hel}$ the following eigenvalue equation holds:

$$\hat{H}_{hel}\Psi_{hel}^{(\alpha)} = E_{hel}^{(\alpha)}\Psi_{hel}^{(\alpha)}. \tag{E.1}$$

Substituting (E.1) into the Schrödinger equation gives

$$i\hbar\frac{\partial\Psi_{hel}^{(\alpha)}}{\partial t} = E_{hel}^{(\alpha)}\Psi_{hel}^{(\alpha)}.$$

Expanding $\Psi_{hel}^{(\alpha)}$ using eqn. (5.21) and separating $\Psi_{hel}^{(\alpha)}$ into real and imaginary parts, i.e., writing $c_{ij}(t) = a_{ij}(t) + ib_{ij}(t)$, leads to the 18 coupled ODEs

$$\frac{da_{ij}}{dt} = \frac{E_{hel}^{(\alpha)}}{\hbar}b_{ij} \tag{E.2a}$$

and

$$\frac{db_{ij}}{dt} = -\frac{E_{hel}^{(\alpha)}}{\hbar}a_{ij} \tag{E.2b}$$

where $1 \leq i, j \leq 3$. Taking the derivative of eqn. (E.2a) with respect to t and using eqn. (E.2b) we get

$$\frac{d^2a_{ij}}{\partial t^2} = -\left(\frac{E_{hel}^{(\alpha)}}{\hbar}\right)^2 a_{ij}$$

which has the two solutions

$$a_{ij}(t) = \begin{cases} a_{ij}(0)\cos\left(\frac{E_{hel}^{(\alpha)}}{\hbar}t\right) \\ C\sin\left(\frac{E_{hel}^{(\alpha)}}{\hbar}t\right) \end{cases} \tag{E.3}$$

where C is a constant to be determined.

We will examine the first solution in (E.3) first. Using (E.2a) we get

$$\begin{aligned} b_{ij}(t) &= \frac{\hbar}{E_{hel}^{(\alpha)}}\frac{\partial a_{ij}(t)}{\partial t} \\ &= -a_{ij}(0)\sin\left(\frac{E_{hel}^{(\alpha)}}{\hbar}t\right). \end{aligned}$$

Since this is consistent with eqn. (E.2b) one solution for the coefficients is

$$a_{ij}(t) = a_{ij}(0)\cos\left(\frac{E_{hel}^{(\alpha)}}{\hbar}t\right) \tag{E.4a}$$

and

$$b_{ij}(t) = -a_{ij}(0)\sin\left(\frac{E_{hel}^{(\alpha)}}{\hbar}t\right). \tag{E.4b}$$

Now consider the second solution in (E.3). Once again, using (E.2a) we get

$$\begin{aligned} b_{ij}(t) &= \frac{\hbar}{E_{hel}^{(\alpha)}}\frac{\partial a_{ij}(t)}{\partial t} \\ &= C\cos\left(\frac{E_{hel}^{(\alpha)}}{\hbar}t\right). \end{aligned}$$

Evaluating $b_{ij}(t)$ at $t = 0$ implies that $C = b_{ij}(0)$ and the solution for $b_{ij}(t)$ is

$$b_{ij}(t) = b_{ij}(0)\cos\left(\frac{E_{hel}^{(\alpha)}}{\hbar}t\right).$$

Since this is consistent with eqn. (E.2b) the other solution for the coefficients is

$$a_{ij}(t) = b_{ij}(0) \sin\left(\frac{E_{hel}^{(\alpha)}}{\hbar} t\right) \tag{E.5}$$

and

$$b_{ij}(t) = b_{ij}(0) \cos\left(\frac{E_{hel}^{(\alpha)}}{\hbar} t\right). \tag{E.5}$$

Since all of the $b_{ij}(0)$ are zero for each of the eigenstates of $\hat{H}_{hel}$, we see that the eigenstates of $\hat{H}_{hel}$ fall under the category of eqns. (E.4a) and (E.4b). Thus, for each of the eigenstates the coefficients are given by

$$a_{ij}(t) = a_{ij}(0) \cos\left(\omega^{(\alpha)} t\right) \tag{E.4a}$$

and

$$b_{ij}(t) = -a_{ij}(0) \sin\left(\omega^{(\alpha)} t\right), \tag{E.4b}$$

where $\omega^{(\alpha)} = \frac{E_{hel}^{(\alpha)}}{\hbar}$.

Appendix F

Calculation of ∇S For Helium Trajectories

We want to calculate the spin-independent term of the guidance condition. This term is given by

$$\nabla_i S = \frac{\hbar}{2iR^2}\left[\Psi^*\nabla_i\Psi - (\nabla_i\Psi^*)\Psi\right] \tag{F.1}$$

which can equivalently be written as

$$\nabla_i S = \frac{\hbar}{R^2} Im(\Psi^*\nabla_i\Psi). \tag{F.2}$$

We will use (F.2) as it is easier in practice to evaluate than (F.1).

First, the $\nabla_i\Psi$ term is given by

$$\nabla_i\Psi = \begin{cases} \sum_{j,k=1}^{3} c_{jk}\left[\nabla\phi_j(\vec{r}_1)\right]\phi_k(\vec{r}_2) & \text{if } i=1; \\ \sum_{j,k=1}^{3} c_{jk}\phi_j(\vec{r}_1)\left[\nabla\phi_k(\vec{r}_2)\right] & \text{if } i=2. \end{cases} \tag{F.3}$$

Substituting this into (F.2), writing

$$\Psi(\vec{r}_1,\vec{r}_2) = \sum_{i,j=1}^{3} c_{ij}\phi_i(\vec{r}_1)\phi_j(\vec{r}_2), \tag{F.4}$$

and expanding each hydrogenic eigenfunction as

$$\phi_\alpha(\vec{r}_i) = R_{n_\alpha,l_\alpha}(r_i)Y_{l_\alpha}(\theta_i,\phi_i),$$

where $n_\alpha = \begin{cases} 1, & \text{if } \alpha = 1 \\ 2, & \text{if } \alpha = 2 \\ 2, & \text{if } \alpha = 3 \end{cases}$ and $l_\alpha = \begin{cases} 0, & \text{if } \alpha = 1 \\ 0, & \text{if } \alpha = 2 \\ 1, & \text{if } \alpha = 3 \end{cases}$,

yields

$$\nabla_1 S = \sum_{g,h=1}^{3}\sum_{i,j=1}^{3}\big(a_{gh}b_{ij} - a_{ij}b_{gh}\big)R_{n_g,l_g}(r_1)Y_{l_g}(\theta_1,\phi_1)R_{n_h,l_h}(r_2)Y_{l_h}(\theta_2,\phi_2)$$
$$\times\left(\frac{\partial R_{n_i,l_i}(r_1)}{\partial r_1}Y_{l_i}(\theta_1,\phi_1)\ ,\ 0\ ,\ R_{n_i,l_i}\frac{\partial Y_{l_i}(\theta_1,\phi_1)}{\partial\theta_1}\right)R_{n_j,l_j}(r_2)Y_{l_j}(\theta_2,\phi_2) \quad \text{(F.5)}$$

and

$$\nabla_2 S = \sum_{g,h=1}^{3}\sum_{i,j=1}^{3}\big(a_{gh}b_{ij} - a_{ij}b_{gh}\big)R_{n_g,l_g}(r_1)Y_{l_g}(\theta_1,\phi_1)R_{n_h,l_h}(r_2)Y_{l_h}(\theta_2,\phi_2)$$
$$\times R_{n_i,l_i}(r_1)Y_{l_i}(\theta_1,\phi_1)\left(\frac{\partial R_{n_j,l_j}(r_2)}{\partial r_2}Y_{l_j}(\theta_2,\phi_2)\ ,\ 0\ ,\ R_{n_j,l_j}\frac{\partial Y_{l_j}(\theta_2,\phi_2)}{\partial\theta_2}\right). \quad \text{(F.6)}$$

Note that the third component of $\nabla_i S = 0$ for $i = 1, 2$ because the wavefunction does not depend on the polar angle, ϕ. Eqns. (F.5) and (F.6) can be written more succinctly as

$$\nabla_i S = \frac{\hbar}{R^2}\sum_{g,h,j,k=1}^{3}\big(a_{gh}b_{jk} - a_{jk}b_{gh}\big)\phi_g(\vec{r_1})\phi_h(\vec{r_2})$$
$$\times\left\{A^i_{jk}(\vec{r}_1,\vec{r}_2)\hat{e}_r + B^i_{jk}(\vec{r}_1,\vec{r}_2)\hat{e}_\phi + C^i_{jk}(\vec{r}_1,\vec{r}_2)\hat{e}_\theta\right\},$$

where

$$A^i_{jk}(\vec{r}_1,\vec{r}_2)=\begin{cases}\frac{\partial R_{n_j,l_j}(r_1)}{\partial r_1}Y_{l_j}(\theta_1,\phi_1)R_{n_k,l_k}(r_2)Y_{l_k}(\theta_2,\phi_2) & \text{if } i=1;\\ R_{n_j,l_j}(r_1)Y_{l_j}(\theta_1,\phi_1)\frac{\partial R_{n_k,l_k}(r_2)}{\partial r_2}Y_{l_k}(\theta_2,\phi_2) & \text{if } i=2,\end{cases}$$

$$B^i_{jk}(\vec{r}_1,\vec{r}_2)=0 \text{ for } i=1,2$$

because each Φ_i has no ϕ-dependence and

$$C^i_{jk}(\vec{r}_1,\vec{r}_2)=\begin{cases}R_{n_j,l_j}(r_1)\frac{\partial Y_{l_j}(\theta_1,\phi_1)}{\partial\theta_1}R_{n_k,l_k}(r_2)Y_{l_k}(\theta_2,\phi_2) & \text{if } i=1;\\ R_{n_j,l_j}(r_1)Y_{l_j}(\theta_1,\phi_1)R_{n_k,l_k}(r_2)\frac{\partial Y_{l_k}(\theta_2,\phi_2)}{\partial\theta_2} & \text{if } i=2.\end{cases}$$

Appendix G

Proof That $\nabla S = 0$ For Helium Eigenstates

Beginning with eqn. (F.2), expanding $\nabla_i \Psi$ using eqn. (F.3) and expanding Ψ using eqn. (F.4) we get the equations

$$\nabla_1 S = \frac{\hbar}{R^2} \sum_{g,h=1}^{3} \sum_{i,j=1}^{3} \big(a_{gh}(t) b_{ij}(t) - a_{ij}(t) b_{gh}(t)\big) \phi_g(\vec{r}_1) \phi_h(\vec{r}_2) \left[\nabla \phi_i(\vec{r}_1)\right] \phi_j(\vec{r}_2)$$

and

$$\nabla_2 S = \frac{\hbar}{R^2} \sum_{g,h=1}^{3} \sum_{i,j=1}^{3} \big(a_{gh}(t) b_{ij}(t) - a_{ij}(t) b_{gh}(t)\big) \phi_g(\vec{r}_1) \phi_h(\vec{r}_2) \phi_i(\vec{r}_1) \left[\nabla \phi_j(\vec{r}_2)\right].$$

We will set $i = 1$ and examine the r-component on its own. This term is given by

$$\frac{\hbar}{R^2} \sum_{g,h=1}^{3} \sum_{i,j=1}^{3} \big(a_{gh}(t) b_{ij}(t) - a_{ij}(t) b_{gh}(t)\big) \phi_g(\vec{r}_1) \phi_h(\vec{r}_2) \left[\frac{\partial \phi_i(\vec{r}_1)}{\partial r_1}\right] \phi_j(\vec{r}_2).$$

Thus, if we can show that the sum

$$\sum_{g,h=1}^{3}\sum_{i,j=1}^{3}\big(a_{gh}(t)b_{ij}(t)-a_{ij}(t)b_{gh}(t)\big)\phi_g(\vec{r}_1)\phi_h(\vec{r}_2)\left[\frac{\partial\phi_i(\vec{r}_1)}{\partial r_1}\right]\phi_j(\vec{r}_2) \quad \text{(G.1)}$$

is identically zero, then the r-component of ∇S_1 is equal to zero and electron 1 has no spin-independent motion in the r-direction.

Recall from Appendix E that when the spatial part of the initial wavefunction is in an eigenstate of $\hat{H}_{hel}$ (i.e. one of $\{\Psi_{hel}^{(\alpha)}\}$for $\alpha \in \{0,\ldots,8\}$) the coefficients are given by

$$a_{ij}(t) = C_{ij}\cos\left(\omega^{(\alpha)}t\right) \quad \text{(5.41a)}$$

and

$$b_{ij}(t) = C_{ij}\sin\left(\omega^{(\alpha)}t\right) \quad \text{(5.41b)}$$

where $C_{ij} = |c_{ij}(0)|$ are constants and

$$\omega^{(\alpha)} = \frac{E_{hel}^{(\alpha)}}{\hbar}$$

is the frequency associated with the wavefunction $\Psi_{hel}^{(\alpha)}$.[1]

Now consider a general term in the sum (G.1), which we will call (g,h,i,j). This term is given by

$$(g,h,i,j) = \big(a_{gh}(t)b_{ij}(t)-a_{ij}(t)b_{gh}(t)\big)\phi_g(\vec{r_1})\phi_h(\vec{r_2})\left[\frac{\partial\phi_i(\vec{r_1})}{\partial r_1}\right]\phi_j(\vec{r_2}) \quad \text{(G.3)}$$

Substituting (5.41a) and (5.41b) into (G.3) yields

[1]Recall that the coefficients of the wavefunction are given by $c_{ij}(t) = a_{ij}(t) + ib_{ij}(t)$ for $1 \le i,j \le 3$.

$$
\begin{aligned}
(g,h,i,j) = &\left[C_{gh}\cos\left(\omega^{(\alpha)}t\right)C_{ij}\sin\left(\omega^{(\alpha)}t\right) - C_{ij}\cos\left(\omega^{(\alpha)}t\right)C_{gh}\sin\left(\omega^{(\alpha)}t\right)\right] \\
&\qquad \times \phi_g(\vec{r_1})\phi_h(\vec{r_2})\left[\frac{\partial\phi_i(\vec{r_1})}{\partial r_1}\right]\phi_j(\vec{r_2}) \\
= &\, C_{gh}C_{ij}\left[\cos\left(\omega^{(\alpha)}t\right)\sin\left(\omega^{(\alpha)}t\right) - \cos\left(\omega^{(\alpha)}t\right)\sin\left(\omega^{(\alpha)}t\right)\right] \\
&\qquad \times \phi_g(\vec{r_1})\phi_h(\vec{r_2})\left[\frac{\partial\phi_i(\vec{r_1})}{\partial r_1}\right]\phi_j(\vec{r_2}) \\
= &\, 0. \qquad \text{(G.4)}
\end{aligned}
$$

Thus, the (g,h,i,j) term equals zero. Since the calculations used in (G.4) do not depend on the indices $g, h, i,$ or j, each term in (G.1) is identically zero. Therefore, the sum (G.1) is equal to zero and the corresponding component of $\nabla_1 S$ is zero. The above argument holds for each of the components of $\nabla_1 S$ and similarly for each component $\nabla_2 S$. Thus, $\nabla_i S = 0$ for $i = 1, 2$ and there is no spin-independent contribution to the trajectory of either electron when the initial wavefunction is an eigenstate of $\hat{H}_{hel}$.

Bibliography

[1] V. Allori, D. Dürr, S. Goldstein and N. Zanghi, *Seven Steps Towards the Classical World*, Found on the website arXiv.org, Ref. arXiv:quant-ph/0112005v1. Submitted (2001).

[2] G. Arfken, *Mathematical Methods For Physicists* 2^{nd} *Ed.*, Academic Press Inc., New York, 1971.

[3] V. I. Arnold and A. Avez, *Ergodic Problems of Classical Mechanics*, W. A. Benjamin, Inc., Menlo Park, CA., 1968.

[4] H. Bethe and E. Selpeter, *Quantum Mechanics of One- and Two-Electrons Atoms*, Plenum Publishing, New York, 1977 (reprinted from 1957 version).

[5] D. Bohm, *A Suggested Interpretation of the Quantum Theory in Terms of "Hidden" Variables. I*, Physical Review **85** (1952), 166–179.

[6] D. Bohm, *A Suggested Interpretation of the Quantum Theory in Terms of "Hidden" Variables. II*, Physical Review **85** (1952), 180–193.

[7] D. Bohm, *Quantum Theory*, Dover Publications , Mineola, N.Y., 1989 (reprint).

[8] D. Bohm, *The Undivided Universe*, Routledge, New York, 1993.

[9] N. Bohr, *Can Quantum-Mechanical Description of Physical Reality Be Considered Complete?*, Physical Review **48** (1935), 696–702.

[10] B. H. Bransden and C. J. Joachain, *Quantum Mechanics Second Edition*, Prentice Hall, Essex, U.K., 2000.

[11] C. Colijn, *The De Broglie-Bohm Causal Interpretation of Quantum Mechanics and its Application to Some Simple Systems*, Ph. D. thesis, University of Waterloo, 2003.

[12] C. Colijn and E. R. Vrscay, *Spin-dependent Bohm trajectories for hydrogen eigenstates*, Physical Letters A, **300** (2002), 334–340.

[13] C. Colijn and E. R. Vrscay, *Spin-dependent Bohm trajectories for Pauli and Dirac eigenstates of hydrogen*, Found. Phys. Lett., **300(4)** (2003), 303–323.

[14] J. Cushing, *Quantum Mechanics Historical Contingency and the Copenhagen Interpretation*, University of Chicago Press, Chicago, 1994.

[15] A. Einstein, B. Podolsky and N. Rosen, *Can Quantum-Mechanical Description of Physical Reality Be Considered Complete?*, Physical Review **47** (1935), 777–780.

[16] D. E. Evans, Comm. Math. Phys. **54** (1976), 293.

[17] A. Frigerio, Comm. Math. Phys. **63** (1978), 269.

[18] H. Geiger, G. Obermair and C. Helm, *Classical behaviour of many-body systems in Bohmian Quantum Mechanics*, Found on the website arXiv.org, Ref. arXiv:quant-ph/9906082. Submitted to Phys. Letters A in (1999).

[19] P. Ghose, *An Experiment to Distinguish Between de Broglie-Bohm and Standard Quantum Mechanics*, Found on the website arXiv.org, Ref. arXiv:quant-ph/0003037v3. Submitted (2000).

[20] P. Ghose, *On the Incompatibility of Standard Quantum Mechanics and the de Broglie-Bohm Theory*, Found on the website arXiv.org, Ref. arXiv:quant-ph/0103126v8. Submitted (2001).

[21] P. Ghose, *Comments on Struyve and Baere's paper on experiments to distinguish Bohmian mechanics from quantum mechanics*, Found on the website arXiv.org, Ref. arXiv:quant-ph/0208192v1. Submitted (2002).

[22] P. Ghose, *A Continuous Transition Between Quantum and Classical Mechanics (I)*, Found on the website arXiv.org, Ref. arXiv:quant-ph/0104104. Submitted (2002). To appear in Found. of Physics.

[23] P. Ghose and M. Samal, *A Continuous Transition Between Quantum and Classical Mechanics (II)*, Found on the website arXiv.org, Ref. arXiv:quant-ph/0104105. Submitted (2002). To appear in Found. of Physics.

[24] M. Golshani and O. Akhavan, *A two-slit experiment which distinguishes between standard and Bohmian quantum mechanics*, Found on the website arXiv.org, Ref. arXiv:quant-ph/0009040v4. Submitted (2000).

[25] M. Golshani and O. Akhavan, *Experiment can decide between standard and Bohmian quantum mechanics*, Found on the website arXiv.org, Ref. arXiv:quant-ph/0103100v2. Submitted (2001).

[26] M. Golshani and O. Akhavan, *Bohmian prediction about a two double-slit experiment and its disagreement with standard quantum mechanics*, J. Phys. A **34** (2001) 5259–5268.

[27] M. Golshani and O. Akhavan, *On the Experimental Incompatibility Between Standard and Bohmian Quantum Mechanics*, Found on the website arXiv.org, Ref. arXiv:quant-ph/0110123v1. Submitted (2001).

[28] M. Golshani and O. Akhavan, *Reply to : Comment on "Bohmian prediction about a two double-slit experiment and its disagreement with SQM"*, Found on the website arXiv.org, Ref. arXiv:quant-ph/0305020v1. Submitted (2003).

[29] M. Gondran and A. Gondran, *A Crucial Experiment to Test The Broglie-Bohm Trajectories For Indistinguishable Particles*, Found on the website arXiv.org, Ref. arXiv:quant-ph/0603200v2. Submitted (2006).

[30] P. Holland, *The Quantum Theory of Motion*, Cambridge University Press, Cambridge, 1993.

[31] I. Levine, *Quantum Chemistry Volume 1: Quantum Mechanics and Molecular Electronic Structure*, Allyn and Bacon Inc., Boston, MA, 1970.

[32] A. Messiah, *Quantum Mechanics*, Dover Publications, Mineola, N.Y., 1999 (reprint).

[33] Y. Omar, *Indistinguishable Particles in Quantum Mechanics: An Introduction*, Contemporary Physics **46** (2005), 437–448.

[34] W. Parry, *Topics in Ergodic Theory*, Cambridge University Press, Cambridge, 1981.

[35] E. Prugovečki, *Quantum Mechanics in Hilbert Space*, Academic Press, N.Y., 1981.

[36] F. Pilar, *Elementary Quantum Chemistry*, McGraw-Hill Inc., New York, 1968.

[37] E. Schrödinger, *Quantization as an eigenvalue problem*, Anallen Der Physik **79** (1926), 361-376.

[38] E. Schrödinger, *Quantification of the eigenvalue problem*, Annalen Der Physik **79** (1926), 489-527.

[39] E. Schrödinger, *On the connection of Heisenberg-Born-Jordan's quantum mechanics with mine*, Anallen Der Physik **79** (1926), 734-756.

[40] E. Schrödinger, *Quantification of the eigenvalue problem*, Annalen Der Physik **80** (1926), 437-490.

[41] E. Schrödinger, *Four Lectures on Wave Mechanics*, Blackie, London, 1929.

[42] W. Struyve and W. De Baere, *Comments on some recently proposed experiments that should distinguish Bohmian mechanics from quantum mechanics*, Found on the website arXiv.org, Ref. arXiv:quant-ph/0108038v1. Submitted (2001). To be published in "Proceedings of the Vaxjo conference", June 16-21, 2001.

[43] M. Toda, R. Kubo and N. Saitô, *Statistical Physics I, Second Edition*, Springer, N.Y., 1995.

[44] J. von Neumann, *Mathematical Foundations of Quantum Mechanics*, Princeton University Press, Princeton, N.J., 1995 (translated from German).

[45] D. Yi-Shi, L. Yu-Xiao and Z. Li-Jie, *Corrections to the Nonrelativistic Energy of the Helium Atom*, Chinese Phys. Lett. **21** (2004), 1714–1716.